uOttawa

L'Université canadienne
Canada's university

FACULTÉ DES ÉTUDES SUPÉRIEURES ET POSTOCTORALES

uOttawa

L'Université canadienne
Canada's university

FACULTY OF GRADUATE AND POSDOCTORAL STUDIES

Pawel Czechura
AUTEUR DE LA THÈSE / AUTHOR OF THESIS

M.Sc. (Chemistry)
GRADE / DEGREE

Department of Chemistry
FACULTÉ, ÉCOLE, DÉPARTEMENT / FACULTY, SCHOOL, DEPARTMENT

Saturated Neoglycopolymers for Tissue Engineering

TITRE DE LA THÈSE / TITLE OF THESIS

D. Fogg
DIRECTEUR (DIRECTRICE) DE LA THÈSE / THESIS SUPERVISOR

CO-DIRECTEUR (CO-DIRECTRICE) DE LA THÈSE / THESIS CO-SUPERVISOR

EXAMINATEURS (EXAMINATRICES) DE LA THÈSE / THESIS EXAMINERS

R. Ben

P. Sundararajan

Gary W. Slater
LE DOYEN DE LA FACULTÉ DES ÉTUDES SUPÉRIEURES ET POSTDOCTORALES /
DEAN OF THE FACULTY OF GRADUATE AND POSTDOCORAL STUDIES

SATURATED NEOGLYCOPOLYMERS FOR TISSUE ENGINEERING

By

PAWEL CZECHURA

Thesis submitted to the
Faculty of Graduate and Postdoctoral Studies
University of Ottawa
In partial fulfillment of the requirements for the degree of

Master of Science in Chemistry

Ottawa-Carleton Chemistry Institute
University of Ottawa
Ottawa, Ontario
Canada

© Pawel Czechura, Ottawa, Canada, 2005

Library and Archives Canada

Published Heritage Branch

395 Wellington Street
Ottawa ON K1A 0N4
Canada

Bibliothèque et Archives Canada

Direction du Patrimoine de l'édition

395, rue Wellington
Ottawa ON K1A 0N4
Canada

Your file Votre référence
ISBN: 0-494-14894-2
Our file Notre référence
ISBN: 0-494-14894-2

NOTICE:
The author has granted a non-exclusive license allowing Library and Archives Canada to reproduce, publish, archive, preserve, conserve, communicate to the public by telecommunication or on the Internet, loan, distribute and sell theses worldwide, for commercial or non-commercial purposes, in microform, paper, electronic and/or any other formats.

The author retains copyright ownership and moral rights in this thesis. Neither the thesis nor substantial extracts from it may be printed or otherwise reproduced without the author's permission.

AVIS:
L'auteur a accordé une licence non exclusive permettant à la Bibliothèque et Archives Canada de reproduire, publier, archiver, sauvegarder, conserver, transmettre au public par télécommunication ou par l'Internet, prêter, distribuer et vendre des thèses partout dans le monde, à des fins commerciales ou autres, sur support microforme, papier, électronique et/ou autres formats.

L'auteur conserve la propriété du droit d'auteur et des droits moraux qui protège cette thèse. Ni la thèse ni des extraits substantiels de celle-ci ne doivent être imprimés ou autrement reproduits sans son autorisation.

In compliance with the Canadian Privacy Act some supporting forms may have been removed from this thesis.

While these forms may be included in the document page count, their removal does not represent any loss of content from the thesis.

Conformément à la loi canadienne sur la protection de la vie privée, quelques formulaires secondaires ont été enlevés de cette thèse.

Bien que ces formulaires aient inclus dans la pagination, il n'y aura aucun contenu manquant.

Canada

ABSTRACT

Norbornene monomers bearing carbohydrate groups of relevance for tissue engineering were synthesized via the norbornene acid chlorides, transformed into their ROMP polymers, and reduced to yield saturated neoglycopolymers. These materials bear either O-glycoside groups designed to cross-link collagen via reaction of the ring-open sugar with free NH_2 groups of lysine, or C-glycoside groups. The latter are intended for use as the central block in triblock copolymers terminated with blocks capable of crosslinking: they serve only as potentially biocompatible "spacers" to help span the interlamellar distance in collagen. A third ROMP monomer bearing a succinimide group as an alternative crosslinking agent was also prepared and polymerized. The O-glycoside monomer, bis(1,2;3,4-di-O-isopropylidene-D-galactopyranos-6-O-yl) 5-norbornene-2,3-dicarboxylate **9**, and the succinimide monomer, 5-norbornene-2-carboxylic acid N-hydroxysuccinimide ester **11,** were prepared by the Diels-Alder synthesis of 5-norbornene-2,3-dicarbonyl chloride **7** and 5-norbornene-2-carboxylic acid chloride **8,** and subsequent nucleophilic substitution of the acid chlorides. Synthesis of the C-glycoside monomer, bis(3-(3,4,5-tris-benzyloxy-6-benzyloxymethyl-tetrahydro-pyran-2-yl)-propan-1-O-yl) 5-norbornene-2,3,-dicarboxylate **10**, was accomplished via coupling of an independently-synthesized carbohydrate moiety **5**, in a five-step synthesis with a cumulative yield of 25%. ROMP via $Mo(CHCMe_2Ph)(N\text{-}2,6\text{-}^{i}Pr_2C_6H_3)(O\text{-}t\text{-}Bu)_2$ **18** gave polymers with narrow molecular weight distributions (1.06-1.08), however the procedure was cumbersome, owing to the oxygen- and water-sensitivity of **18**, and the need to effect any subsequent reduction in a separate step. The importance of reducing the polymer was established through an in situ IR study that demonstrated rapid degradation of the

unsaturated polymer. Reduction via use of Pd-C or diimide was inefficient and caused contamination or competitive crosslinking. Homogeneous hydrogenation using $RuCl_2(PCy_3)_2$ **12** and $RuCl_2(PCy_3)$(IMes) **13** as precursors to hydrogenation-active Ru hydrides proved more successful. More efficient, however, was tandem ROMP-hydrogenation, which obviates the need for intermediate workup. Tandem ROMP-hydrogenation via **12** was effected at 1000 psi H_2 and 60°C, in the presence of methanol. Using catalyst **13**, saturated poly(**9**) was obtained in less than 7 hours, compared to 24 hours using the "one-pot" method. Saturated poly(**11**) was prepared in ca. 2.5 hours. Random copolymers of **9** and **11** were also synthesized, as poly(**11**) proved insoluble in water. Deprotection of poly(**9**) or copolymers of **9** and **11** (9:1) could be effected using aqueous trifluoroacetic acid within 20 minutes at RT, affording water-soluble polymers. Preliminary studies of collagen crosslinking and biocompatibility with poly(**9**) show promising utility in the target applications.

TABLE OF CONTENTS

TABLE OF COMPOUND NUMBERS

Number	Compound
1	beta-D-galactose pentaacetate
2	3-(1'-Deoxy-2',3',4',6'-tetra-O-acetyl-alpha-D-galactopyranosyl)prop-1-ene
3	2-Allyl-6-hydroxymethyl-tetrahydro-pyran-3,4,5-triol
4	3-(2',3',4',6'-tetra-O-benzyl-α-D-galactopyranosyl)prop-1-ene
5	3-(3,4,5-Tris-benzyloxy-6-benzyloxymethyl-tetrahydro-pyran-2-yl)-propan-1-ol
6	2,3-Diacetyl-5-norbornene
7	5-Norbornene-2,3-dicarbonyl chloride
8	5-Norbornene-2-carboxylic acid chloride
9	bis(1,2;3,4-di-O-isopropylidene-D-galactopyranos-6-O-yl) 5-norbornene-2,3-dicarboxylate
10	bis(3-(3,4,5-tris-benzyloxy-6-benzyloxymethyl-tetrahydro-pyran-2-yl)-propan-1-O-yl) 5-norbornene-2,3,-dicarboxylate
11	5-Norbornene-2-carboxylic acid N-hydroxysuccinimide ester
12	$RuCl_2(PCy_3)_2$
13	$RuCl_2(PCy_3)(IMes)$
14	$Mo(N\text{-}2,6\text{-}^{i}Pr_2C_6H_3)_2Cl_2(DME)$
15	Magnesium neophyl chloride
16	$Mo(N\text{-}2,6\text{-}^{i}Pr_2C_6H_3)_2(CH_2CMe_2Ph)_2$
17	$Mo(CHCMe_2Ph)(N\text{-}2,6\text{-}^{i}Pr_2C_6H_3)(OSO_2CF_3)_2(DME)$
18	$Mo(CHCMe_2Ph)(N\text{-}2,6\text{-}^{i}Pr_2C_6H_3)(O^{t}Bu)_2$

LIST OF TABLES

LIST OF FIGURES

LIST OF ABBREVIATIONS

Ac	acetyl
atm.	atmosphere (1 atm = 760 mmHg, 101.3 kPa, 14.696 psi)
Ar	aryl
br	broad
°C	degrees Celsius
$^{13}C\{^{1}H\}$	proton-decoupled carbon-13 (NMR)
cm	centimeters
d	doublet
dd	doublet of doublets
DEPT	Distortion Enhancement of Polarization Transfer
DMF	*N,N*-dimethylformamide
DME	1,2-dimethoxyethane
DMSO	dimethylsulfoxide
d.p.	degree of polymerization
EI	electron impact
eq.	equivalents
ESI	electrospray ionization
Et	ethyl
FDA	Food and Drug Administration
GPC	Gel Permeation Chromatography
h	hour
HOMO	Highest Occupied Molecular Orbital
Hz	Hertz
IMes	bis(1,3-(2,4,6-trimethylphenyl)imidazol-2-ylidene)
IR	Infrared
J	coupling constant
LUMO	Lowest Unoccupied Molecular Orbital
[M]	central metal atom in a complex
m	multiplet

M^+	parent molecular ion
min	minutes
Me	methyl
MeOH	methanol
mL	milliliters
mmol	millimoles
M_n(calc.)	calculated molecular weight number
M_n(expt.)	experimental molecular weight number
m.p.	melting point
MS	mass spectrometry or mass spectra
M_W	molecular weight
m/z	mass-to-charge ratio
NBE	norbornene
nm	nanometers
NMR	Nuclar Magnetic Resonance
NHC	N-heterocyclic carbine
p	page
PBS	Phosphate Buffered Saline
PDI	polydispersity index
ppm	parts per million
q	quartet
ROMP	Ring Opening Metathesis Polymerization
RT	Room Temperature
s	singlet
t	triplet
t-Bu	tertiary butyl
TFA	trifluoroacetic acid
THF	tetrahydrofuran
δ	chemical shift (in ppm)
ν	frequency (in cm^{-1})

ACKNOWLEDGMENTS

I thank my supervisor, Professor Deryn Fogg for her vision, support, wisdom and critique. Her research gave me the opportunity to expand my knowledge in the fields of organometallic, polymer, organic, and carbohydrate chemistry.

The encouragement and assistance from Dr. Nemesio Martinez Castro and Dr. Yuwen Liu who worked with me on the Cornea Project are also much appreciated.

I thank my colleague Amir Jabri for his creativity, kindness and companionship during late nights in the lab. Your encouragement to work-out, go enjoy the artistic performances at the National Arts Center, and have a balanced life is greatly valued. I am grateful to all the members of Fogg group, especially Dr. Eduardo N. dos Santos, Dr. Melanie Eelman, Dr. Samantha Drouin, Jay Conrad, Ureshini Dhamensa, Heather Foucault, and Henrietta Parnas for helpful advice and their friendship. Special thanks goes out to Jay for all the favors. To your health - Cheers everyone !

I extend my thanks to Dr. Glen Facey of the NMR Laboratory and Dr. Clement Kazakoff of the Mass Spectroscopy Laboratory at the University of Ottawa for their expertise and assistance.

Finally, I thank my family, my father Antoni, my mother Kazimiera, sister Krystyna, and other family members for all the encouragement and love. Za wszystko dziekuje !

CHAPTER 1

Introduction

1.1. Tissue Engineering and the Cornea

Tissue engineering offers great promise for advances to human health.[1] Prosthetic materials devised from commodity polymers commonly give rise to problems of rejection resulting from immunogenic response.[2,3] An increasingly popular means of enhancing biocompatibility is surface-functionalization of the commodity polymers.[4] Lyses of these groups by enzymatic action can limit the success of this approach. However, specialty polymers in which biocompatible groups are built in at the repeat unit level offer the possibility for significant advances in tissue engineering, via molecular-level design of these materials for the target function and environment.[5] Ring-opening metathesis polymerization (ROMP), described more fully in Chapter 3, is one such method.

As an avascular and immunologically privileged tissue, the cornea is an excellent candidate for tissue engineering.[6] The need for replacement corneal tissues is also a significant and growing issue worldwide, as described below. In the architecture of the eye, the cornea is the main optical element that refracts light for vision (Figure 1.1). Approximately 75% of total refraction of light occurs at the cornea, while the lens then fine-tunes the focus for near or distant objects.[7] As the outermost layer of the transparent window of the eye, the cornea must also serve as a tough protective barrier for delicate internal tissues. It must withstand physical stress while retaining flexibility, transparency and smoothness.[3,8]

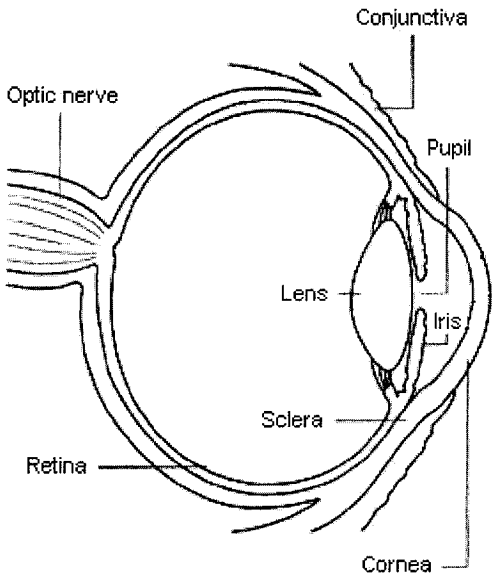

Figure 1.1 Anatomy of the eye. Figure adapted from Ref. 9.[9]

The cornea comprises five major cellular layers (Figure 1.2). These are: (1) an outermost, nonkeratinized epithelium consisting of stratified squamous cells, (2) Bowman's membrane, (3) a middle layer, the stroma, consisting of a hydrated matrix of collagen (20% w/v) networked with proteoglycans, through which fibroblasts are distributed, (4) Descemet's membrane, and (5) an innermost layer of specialized endothelial cells.[3,10] The collagen fibrils in the stroma are ca. 30 nm in diameter, with spacing between the collagen lamellae of ca. 55 nm. This gap is important to allow the free flow of fluids. The size of the gap – significantly less than the wavelength of visible light – is also thought to be important in minimizing light diffraction.[11,12]

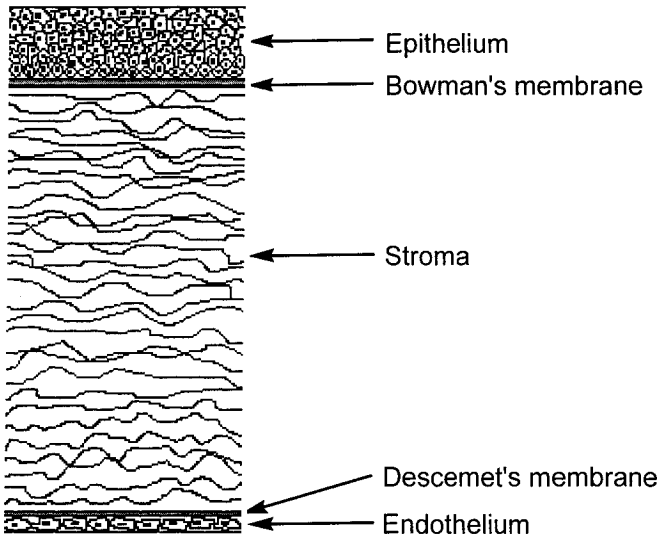

Figure 1.2 Cross-section of the human cornea showing the major tissue layers.

The cornea is one of the most innervated tissues in the body. It is equipped with nociceptive nerve endings (pain-stimuli sensory receptors) that terminate within the epithelium.[13,14] Nerve activity is responsible for maintaining the overall health of the cornea, and loss of innervation can cause "dry eye", a pathological condition that may result in decreased corneal sensitivity and/or corneal epithelial erosion.[15] Loss of sensitivity leaves the eye vulnerable to irreparable corneal injury or ulceration, causing eventual loss of vision and in severe cases, blindness.[16]

In designing corneal replacements, it is desirable to mimic the anatomy and physiology of the human cornea.[17] Important requirements include strength, flexibility, transparency, smoothness, porosity, and biocompatibility. A simple design model comprises the crosslinked collagen matrix sandwiched between two grafted cell layers. The matrix should provide an appropriate microenvironment for cell growth and nutrition.[8,18,19]

1.2. Corneal Diseases

The cornea exposed to the outside environment is vulnerable to mechanical damage.[3,7] While minor scratches are self-regenerated, deeper wounds causing scarring can affect transparency.[9,12,19] Injury or disease that causes the cornea to become permanently opaque results in visual impairment or, in serious cases, corneal blindness. Endothelial cell failure in old age has the same result.

Corneal diseases (Table 1.1) are a major cause of vision loss and blindness, second only to cataracts in overall importance. Corneal scarring as a result of measles is a major cause of blindness in children,[20,21] affecting more then 10 million individuals worldwide. The only treatment for this serious condition is corneal transplantation. Traditional cornea transplantation using human donor corneas has a high success rate (>80%). This relies, however, on the availability of good quality tissue, as well as the patient's condition.[22] For patients with autoimmune disorders or alkali burns (from, for example, cement liquor or KOH bath splashes!), or who have suffered recurrent graft failures, corneal transplantation has a poor prognosis.[23] The increased popularity of corrective laser eye surgery limits the pool of corneas available for transplant, as the weakened mechanical integrity of surgically treated corneas precludes their use in transplantations. Both this factor and the aging population increase the number of individuals requiring transplants, while limiting the donor pool. Worldwide corneal shortages are expected to be compounded by the increasing incidence of infectious diseases such as HIV and hepatitis. For this reason, there is considerable interest in developing an artificial cornea that could be used to replace a damaged cornea.

Table 1.1 Corneal diseases, their progress leading to severe effects, and treatment.[9]

Disease	Cause	Progression	Severe Effect	Treatment
Corneal Infections (Keratitis)	Bacterial/fungal Contact lenses	Reduction in visual clarity Corneal discharges	Erosion of cornea Corneal scarring	Anti-bacterial /fungal treatment **Corneal transplant**
Fuch's Dystrophy	Endothelial cells deteriorate	Corneal swelling Distort vision	Blisters Visual impairment	Ointments **Corneal transplant**
Herpes Zoster (Shingles)	Varicella-zoster virus (also causes chickenpox)	Inflammation	Corneal scaring Permanent decrease in corneal sensitivity	Anti-viral treatment
Iridocorneal Endothelial (ICE) Syndrome	Unknown	Changes in the iris Corneal swelling Development of glaucoma	Movement of endothelial cells from the cornea onto the iris Distortion of the pupil	**Corneal transplant**
Keratoconus	Thinning of the cornea	Corneal bulges Corneal swelling	Corneal scaring	**Corneal transplant**
Lattice Dystrophy	Accumulation of amyloid depositis or abnormal protein fibers	Cloudiness	Epithelial erosion Altered cornea's curvature Severe pain Corneal scarring	Eye drops and ointments **Corneal transplant**
Map-Dot-Fingerprint Dystrophy, (Epithelial Basement Membrane Dystrophy)	Epithelium's basement membrane develops abnormally	Blurred vision Sensitivity to light	Severe pain Excessive tearing Foreign body sensation in the eye	Lubricating eye drops and ointments Anterior corneal punctures Excimer laser
Ocular Herpes	herpes simplex virus	Sore on eyelid Inflammation of the cornea	Blindness Stromal keratitis Corneal scarring	Anti-viral treatment
Pterygium	Unknown (believed to be UV light)	Triangular-shaped tissue growth on the cornea	Swelling	Lubricants Removal by surgery
Stevens-Johnson Syndrome (SJS)	Unknown (believed to be an adverse allergic drug reaction)	Conjunctivitis Iritis	Corneal blisters and erosion Corneal holes Vision loss	Artificial tears Antibiotics Corticosteroids

1.3. Artificial Corneas

Artificial corneas can be divided into two categories: prostheses, and replacement tissues. To date, however, no substitutes are widely accepted. The existing replacements

do not integrate seamlessly into the host tissue, or promote reinnervation, despite the fact that loss of corneal innervation leads to visual loss.[2,17]

Photorefractive surgery is now a very popular technique for correcting corneal refractive errors such as myopia, hyperopia and astigmatism. The method does not require use of external devices and shows long-term stability. Post-surgical problems such as epithelial hypertrophy (an increase in cell size) do occur, however, when this happens secondary procedures must be performed.[24] Implantation of inlays and onlays is also under development for correction of refractive errors. These procedures involve implantation of synthetic lenticules either within the corneal stroma (inlays) or underneath the epithelium (onlays).[3] The methods are not reliable: they tend to fail by causing dry eye, the result of severing the nerve plexus during implantation. The implants also suffer from inadequate flow of nutrients. The latter issue highlights the importance of the porosity of the device. The average pore size in the human corneal basement membrane has a diameter of 92 ± 34 nm, with pores covering 15% of the total surface.[25]

Perfluoropolyether, a transparent, isorefractive polymer that offers high chemical and thermal stability, has been used as a lenticule.[26] Prior to clinical testing the polymer was coated with covalently immobilized type I collagen (the dominant biopolymer that constitutes 70% of the dry weight of the human cornea). Observation of successful growth of the corneal epithelium was attributed to the presence of collagen on the anterior surface of the lenticule. Type I collagen is possibly a necessary component that artificial corneas should contain.

In an interesting alternative approach, bioengineered replacement tissues have been produced that contain human corneal epithelial stem cells in a cross-linked, human

fibrin gel.[27] The artificial tissue degraded within 24 hours unless protease inhibitors such as aprotinin were present in the incubation medium. While this approach is of value in its potential to offer a completely autologous replacement (i.e. using the patient's own cells), it does not produce the normal stratified epithelial architecture, and the issue of adequate optical clarity was not addressed.

The most common solution to corneal replacement is the use of prostheses (keratoprostheses). Current designs comprise a flexible, optically transparent core surrounded by a biointergrable microporous skirt of similar chemical composition and flexibility.[3] The skirt is intended to promote the in-growth of fibroblasts and extracellular matrix collagen: the latter must be sufficient to provide firm anchoring of the device, allowing integration with the host tissues. Such "skirt-and-core" prostheses are typically made from commodity materials such as polyhydroxyethyl methacrylate, polyvinyl alcohol, polybutylmethacrylate, polyhexaethylene glycol methacrylate and polydimethylacrylate, often surface-functionalized to enhance biocompatibility.[2] While many prostheses offer good optical and mechanical properties, biocompatibility is a major problem in vivo. These devices elicit immunogenic responses, fibroblastic membrane development and implant extrusion: especially common is rejection through a condition known as corneal melt, in which enzymes mobilized to digest the synthetic material (which is largely impervious) instead attack native tissue to which the prosthesis is anchored. Corneal melt typically results in extrusion of the device within days to weeks, and is one of the serious problems that leads the FDA to classify such prostheses as "high risk device". Keratoprostheses have been modified with groups that improve cell adhesion, such as RGDS and YIGSR peptides, proteins, or other chemical functionalities.

While cell-polymer interactions can be improved, problems of corneal melt, lack of innervation, loss of touch sensitivity, and degraded hydration feedback still remain.[4,17]

1.4. Biosynthetic Corneal Matrix Replacements

A successfully engineered artificial cornea must provide a visually clear pathway into the retina, be securely integrated with the host tissue and be superior to already available models. An attractive alternative to the keratoprosthetic approach, in which performance is undermined by inherent bioincompatibility, is an implantable artificial cornea possessing properties that more closely resemble the native human cornea.

Griffith *et al.* have developed a prototype replacement cornea fabricated from immortalized human corneal cells and collagen. While use of autologous cells would be envisaged in vivo, the immortalized cells were screened for use to ensure their morphological, biochemical and electrophysiological similarity to their natural counterparts.[8] The tissue used a glutaraldehyde-crosslinked collagen-GAG scaffold.[28] The physical and physiological features of these "corneal equivalents" agree well with those of the natural human cornea: they are very similar in terms of morphology and expression of genes and biochemical markers, as well as transparency and ion and fluid transport. They are already in use in toxicity and drug efficacy testing. Nevertheless, they are too soft to be implantable, and they have limited ability to resist shear or tear stress, and to act as a tough protective covering. These properties are essential for transplantation, suturing and in vivo functioning.

In initial searches for a solution, a hydrogel composed of type I collagen was crosslinked by use of γ-irradiation, urethane/urea, dialdehyde and other aldehyde

generating compounds, N-hydroxysuccinimide, and carbodiimide groups. Some of those methods resulted in materials with enough strength to withstand suture pull during implantation.[10] Collagen crosslinking with an N-hydroxysuccinimide moiety[7] offers improved strength and transparency relative to glutaraldehyde-crosslinked collagen, and is favorable to the ingrowing cells.

The physical properties of the crosslinked collagen matrix are affected by the rate of the crosslinking reaction. Fast crosslinking is found with a number of the agents used above, including the ubiquitous glutaraldehyde, which crosslinks within a few hours.[29,30] This can lead to a problem colloquially known as the "jelly doughnut" structure, with gel formation on the interior but high crosslinking on the outside of the device. Slower crosslinking rates can be beneficial because they give time for the crosslinker to evenly distribute itself throughout the collagen medium.

Other research led to fabrication of collagen-based composites (Figure 1.3) incorporating hydrophilic polymers such as poly(N-isopropylacrylamide-coacrylic acid-coacryloxusuccinimide (TERP), and functionalized with peptide YIGSR, TERP5.[11] The YIGSR peptide is a well known cell adhesion mediator that promotes epithelial growth and enhances neurite extension.[4] In vitro, both hydrogels supported generation of stratified corneal epithelial layer and increase in nerve density. Results were better, however, with the polymer containing YIGSR. In vivo testing, three weeks post-surgery, showed a regenerated epithelium, newly in-grown nerves, and stromal and endothelial cells with cellular morphology mimicking that of the unoperated controls.

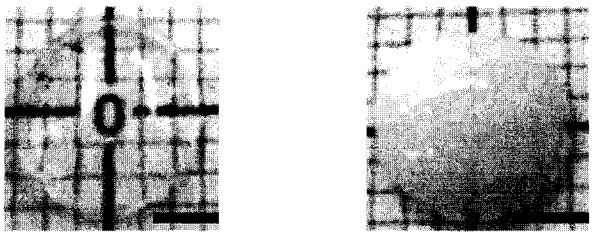

Figure 1.3 Corneal implants comprising collagen-TERP5 (left) and collagen only (right) hydrogels.[11]

Allograft controls of donor cornea did not show subepithelical nerves and stromal cells. Immunohistochemistry indicated that cells within both the implant and allograft were synthesizing pro-collagen I. Touch sensitivity was recovered within 2 weeks while corneal allografts remained anesthetic over 6 week period. The results indicate successful replication of human cornea with retained transparency, flexibility, strength and vital biological properties. However, preliminary results indicated that the polymer of the implanted corneal tissues thins and gradually is replaced by host tissue. The results from artificial cornea implanted in white rabbits showed cells found in stromal pockets that cause slight subepithelial haze near the wound edge.[31] This indicates immunoreactivity and possible polymer degradation.

The ultimate goal of our interdisciplinary research group is to design a biocompatible and biointegrable collagen-based hydrogel that is ideally non-immunogenic, and can maintain the life of the procorneal material. The corneal substitute should posses all the properties of native cornea that to date have been closely mimicked.

1.5. Strategy for Design of Improved Corneal Replacements: Natural-synthetic Biopolymer Composites.

Our design of artificial corneas includes a cell-encapsulated crosslinked collagen matrix. The similarity of ROMP polymers bearing carbohydrate groups to natural carbohydrate polymers inspired our interest in the utility of the former as collagen crosslinkers (Figure 1.4).[32-35] Composites prepared from the natural polymer (collagen) and the synthetic crosslinker should afford a strong and flexible[36] biomatrix that supports cell adhesion, migration and proliferation.[8,11,37]

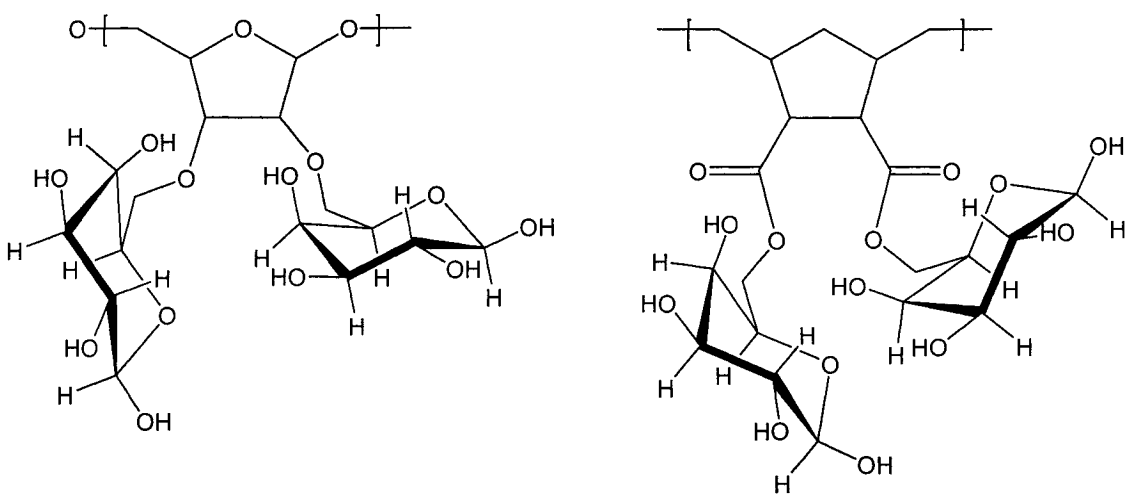

Carbohydrate-based Polymer

Target ROMP Polymer

Figure 1.4 Structure comparison between designed ROMP polymer and a sugar-based analogue.

Our target ROMP polymers and copolymers comprise of the pendant O-glycoside groups that are intended to participate in the crucial crosslinking reaction. Both O-glycoside and C-glycoside carbohydrate groups are also employed to mask the abiological polymer backbone, thus maximizing biocompatibility and reducing cell

toxicity. The non-reducible, unreactive C-glycoside substituents are not intended to participate in crosslinking, but only to span the interlamellar distance, if required. This group will be incorporated in ABA triblock copolymers as the central block. Because of this requirement for rigorous control over block architecture, a living polymerization method such as ROMP is essential. The narrow polydispersities of ROMP polymers may also provide a significant advantage, however, in terms of minimizing the effect of crosslinking on the architecture of the self-assembled collagenous stroma, and thus minimizing light scattering.

Two types of crosslinking moieties, O-glycoside and N-hydroxysuccinimide, were targeted as norbornene substituents. The groups are expected to react with the nucleophilic amine groups of collagen. The O-glycoside, a reducing sugar, is expected to be able to react via its aldehyde form, which exists in equilibrium with the predominant ring-closed isomer (Figure 1.5).[38] Reaction between the free amine of the collagen lysine residues and the aldehyde would give an imine via a reversible equilibrium.[39,40] The reaction rate depends on the pH of the reaction: the fastest rate is at about pH 4-6. (At lower pH, too much amine is protonated, and at higher pH, the proton concentration is too low to allow protonation of the hydroxyl leaving group in the dehydration step. The pH can be adjusted with a phosphate buffered saline, PBS). In water, the imine-aldehyde equilibrium will favour the aldehyde. In order to convert the imine linkage into a permanent form, $NaCNBH_3$ must be added to effect imine reduction (Figure 1.5).[41]

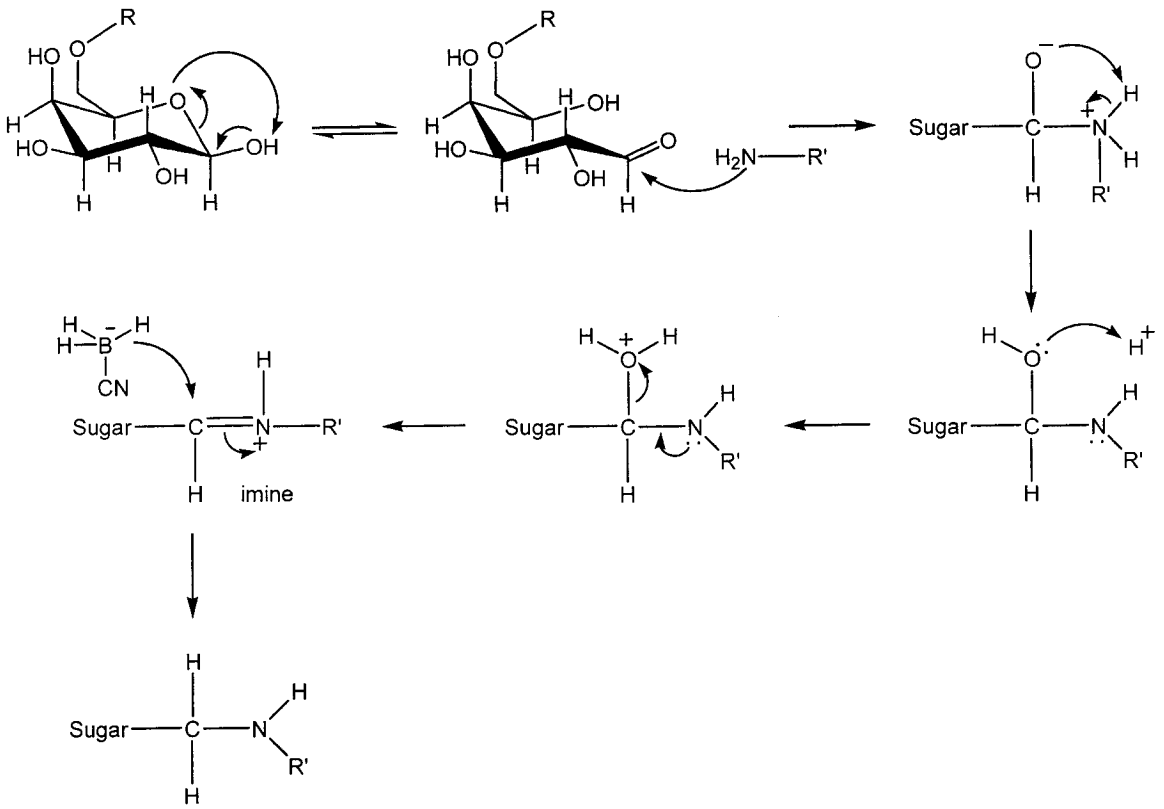

Figure 1.5 Collagen crosslinking via reaction of reduced O-glycoside aldehyde and an amine of the lysine residue of the collagen.

The N-hydroxysuccinimide group undergoes nucleophilic attack on the carbonyl by the lysine amine group, forming a tetrahedral transition state that collapses to release N-hydroxysuccinimide and the new amide bond. N-hydroxysuccinimide is a non-toxic side product (Figure 1.6).[35]

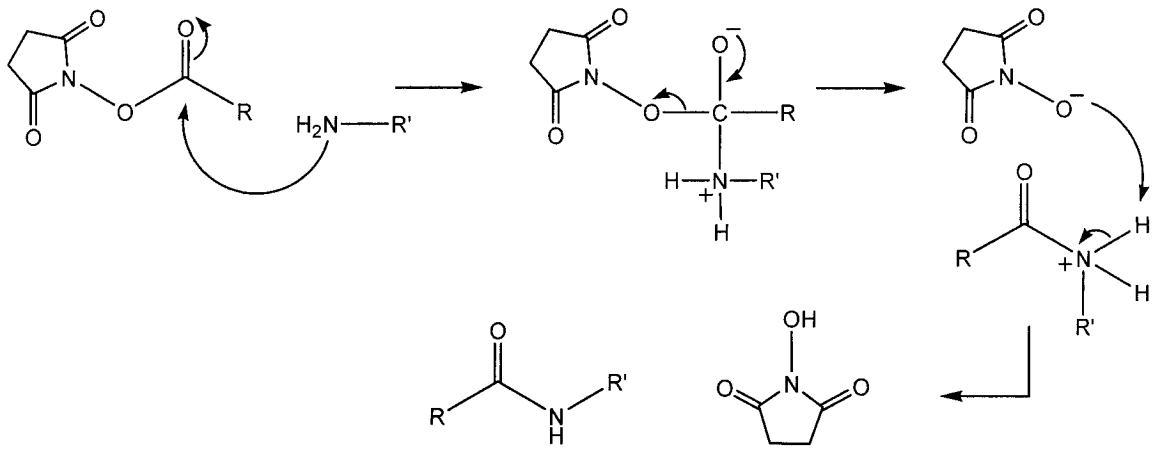

Figure 1.6 Crosslinking collagen using N-hydroxysuccinimide ester moiety.

1.6. Scope of this Thesis

This thesis describes the synthesis of saturated ROMP monomers and polymers that are designed to act as collagen crosslinking agents. Chapter 3 describes synthesis of the O-glycoside, C-glycoside, and N-hydroxysuccinimide functionalized norbornene monomers via Diels-Alder reactions. ROMP polymerization to obtain homo- and co-polymers via molybdenum catalysis is presented.

Chapter 4 describes an investigation of the degradation of the unsaturated polymers, and reduction of the polymers to their saturated forms. Well-known, conventional reduction methods (diimide and Pd-C) are explored, as well as homogeneous hydrogenation and tandem ROMP-hydrogenation methods using Ru catalysis. Hydrolysis of acetal protecting sugar groups to obtain water-soluble saturated polymers is described. The preliminary results of crosslinking via O-glycoside homopolymers are reported in the Appendix. General conclusions and suggestions for future work are outlined in Chapter 5.

1.7. References

1) Laurencin, C. T.; Ambrosio, A. M.; Borden, M. D.; Cooper, A. J. J. *Annual Review of Biomedical Engieering* **1999**, *1*, 19.

2) Hicks, C. R.; Fitton, H. J.; Chirila, T. V.; Crawford, G. J.; Constable, I. J. *Surv. Opthalmol.* **1997**, *42*, 175.

3) Chirila, T. V.; Hicks, C. R.; Dalton, P. D.; Vijayasekaran, S.; Lou, X.; Hong, Y.; Clayton, A. B.; Zieglaar, B. W.; Fitton, J. H.; Platten, S.; Crawford, G. J.; Constable, I. J. *Prog. Polym. Sci.* **1998**, *23*, 447.

4) (a) Kobayashi, H.; Ikada, Y. *Curr. Eye. Res.*, **1991**, *10*, 899. (b) Merrett, K.; Griffith, C. M.; Deslandes, Y.; Pleizier, G.; Sheardown, H. *J. Biomat. Sci. Polymer Ed.*, **2001**, *12*, 647. (c) Kobayashi, H.; Ikada, Y. *Biomaterials*, **1991**, *12*, 747. (d) Xie, R. Z.; Sweeney, D. F.; Beumer, G. J.; Johnson, G.; Griesser, H. J.; Steele, J. G. *Aust. N. Z. J. Ophthalmol.*, **1997**, *25: Suppl. 1*, S46.

5) Sanders, W. J.; Gordon, E. J.; Dwir, O.; Beck, P. J.; Alon, R.; Kiessling, L. L. *The Journal of Biological Chemistry* **1999**, *274*, 5271.

6) Jager, M. J.; Gregerson, D. S.; Streilein, J. W. *Eye* **1995**, *9*, 241.

7) Tortora, G. J.; R., G. S. *Principles of Anatomy and Physiology*; 9th ed.; John Wiley & Sons, Inc.: New York, 2000.

8) Griffith, M.; Osborne, R.; Munger, R.; Xiong, X.; Doillon, C. J.; Laycock, N. L. C.; Hakim, M.; Song, Y.; Watsky, M. A. *Science* **1999**, *286*, 2169.

9) U.S. National Eye Institute, http://www.nei.nih.gov/health/cornealdisease/index.asp#3.

10) Griffith, M.; Trinkaus-Randall, V.; Watsky, M. A.; Liu, C.; Sheardown, H. *Cornea (Chapter 83)*; Academic Press.: New York, 2002, pp 927.

11) Li, F.; Carlsson, D.; Lohmann, C.; Suuronen, E.; Vascotto, S.; Kobuch, K.; Sherdown, H.; Munger, R.; Nakamura, M.; Griffith, M. *PNAS* **2003**, *100*, 15346.

12) Goldman, J. N.; Benedek, G. B.; Dohlman, C. H.; Kravitt, B. *Invest. Ophthalmol.* **1968**, *7*, 501.

13) Rozsa, J.; Beuerman, R. W. *Pain* **1982**, *14*, 105.

14) Gallar, J.; Pozo, M. A.; Tuckett, R. P.; Belmonte, C. *J. Physio. (London)* **1993**, *468*, 609.

15) Stern, M. E.; Beuerman, R. W.; Fox, R. I.; Gao, J.; Mircheff, A. K.; Pflugfelder, S. C. *Adv. Exp. Med. Biol.* **1998**, *438*, 643.

16) Lambiase, A.; Rama, P.; Bonini, S.; Caprioglio, G.; Aloe, L. *N. Engl. J. Med.* **1998**, *338*, 1174.

17) Carlsson, D. J.; Li, F.; Shimmura, S.; Griffith, M. *Current Opinion in Ophthalmology* **2003**, *14*, 192.

18) Chapekar, M. S. *J. Biomed. Mater. Res.* **2000**, *53*, 617.

19) Maurice, D. M. *J. Physiol.* **1957**, *136*, 263.

20) Whitcher, J. P.; Srinivasan, M.; Upqdhyay, M. P. *Bull. W. H. O.* **2001**, *79*, 214.

21) Gilbert, C.; Foster, A. *Bull. W. H. O.* **2001**, *79*, 227.

22) Alldredge, O. C.; Krachmer, J. H. *Arch. Opthalmol.* **1981**, *99*, 599.

23) Chirila, T. V. *Biomaterials* **2001**, *22*, 3311.

24) Belkin, M. W. *Int. Opthalmol. Clin.* **2002**, *42*, 1.

25) Abrams, G. A.; Schaus, S. S.; Goodman, S. L.; Nealey, P. F.; Murphy, C. J. *Cornea* **2000**, *19*, 57.

26) Evans, M. D. M.; Xie, R. Z.; Fabbri, M.; Bojarski, B.; Chaouk, H.; Wilkie, J. S.; McLean, K. M.; Cheng, H. Y.; Vannas, A.; Sweeney, D. F. *Invest. Ophthalmol. Visual Sci.* **2002**, *43*, 3196.

27) Han, B.; Schwab, I. R.; Madsen, T. K.; Trista, K. B. S.; Isseroff, R. R. *Cornea* **2002**, *21*, 505.

28) (a) Minami, Y.; Sugihara, H.; Oono, S. *Invest. Opthalmol. Visual Sci.* **1993**, *34*, 2316 (b) Zieske, J. D.; Mason, V. S.; Wasson, M. E.; Meunier, S. F.; Nolte, C. J.; Fukai, N.; Olsen, B. R. *Exp. Cell Res.* **1994**, *214*, 621 (c) Kahn, C. R.; Young, E.; Lee I. H.; Rhim, J. S. *Invest. Opthalmol. Visual Sci.* **1993**, *34*, 1983 (d) Araki-Sasaki, K.; Ohashi, Y.; Sasabe, T.; Hayashi, K.; Watanabe, H.; Tano, Y.; Handa, H. *Invest. Opthalmol. Visual Sci.* **1995**, *36*, 614 (e) Germain, L.; Auger, F. A.; Grandbois, E.; Guignard, R.; Giasson, M.; Boisjoly, H.; Guerin, S. L. *Pathobiology*, **1999**, *67*, 140.

39) Margolin, A. L.; Navia, M. A. *Angew. Chem. Int. Ed.* **2001**, *40*, 2204.

30) Olde Damink, L. H. H.; Djkastra, P. J.; van Luyn, M. J. A.; van Wachem, P. B.; Nieuwenhuis, P.; Feijen, J. *J. Mater. Sci.: Mater. Med.* **1995**, *6*, 460.

31) Shimmura, S.; Doillon, C. J.; Griffith, M.; Nakamura, N.; Gagnon, E.; Usui, A.; Shinozaki, N.; Tsubota, K. *Cornea* **2003**, *22: Suppl. 1*, S81.

32) Mortell, K. H.; Weatherman, R. V.; Kiessling, L. L. *J. Am. Chem. Soc.* **1996**, *118*, 2297.

33) Manning, D. D.; Hu, X.; Beck, P.; Kiessling, L. L. *J. Am. Chem. Soc.* **1997**, *119*, 3161.

34) Nomura, K.; Schrock, R. R. *Macromolecules* **1996**, *29*.

35) Meier, S.; Resinger, H.; Rainer, H.; Mecking, S.; Mulhaupt, R.; Stelzer, F. *Chem. Commun.* **2001**, 855.

36) Sekiguchi, M.; Otsuki, T.; Ishigaki, T. JP Patent 2001031744, 2001.

37) Lunbard, R. L.; Noyes, C. M. *Chemical reagents for Protein Modification: Chapter 5, The chemical cross-linking of peptide chains*; CRC Press: Florida, U.S., 1984; Vol. II, pp 123.

38) Stick, R. V. *Carbohydrates: The Sweet Molecules of Life*; Academic Press: London, UK, 2001.

39) Wells-Knecht, K. J.; Brinkmann, E.; Baynes, J. W. *J. Org. Chem.* **1995**, *60*, 6246.

40) Lunbard, R. L.; Noyes, C. M. *Chemical reagents for Protein Modification: Chapter 10, Modification of lysine*; CRC Press: Florida, U.S., 1984; Vol. I, pp 127.

41) Clayden, J.; Greeves, N.; Stuart, W.; Wothers, P. *Organic Chemistry*; Oxford University Press: New York, 2001.

CHAPTER 2

Experimental Procedures

Unless otherwise stated, all reactions were carried out at room temperature (RT, ~22°C) and all manipulations involving air-sensitive compounds were performed using standard Schlenk or drybox techniques. Standard purification procedures involved column chromatography with silica gel as the solid phase. High-pressure reactions were conducted in machined steel autoclaves (Parr) equipped with glass liners.

2.1. Instrumentation

Infrared spectra were recorded on a Bomem MB100, Bomem Michelson M129, and Shimazu FTIR-8400S IR spectrometers. The samples were run neat or as KBr pellets (20 mg polymer/200 mg KBr) prepared using a RIIC (Research Industrial Instruments Company) ring press. For temperature-controlled experiments, IR samples were placed in a cylindrical sample holder and heated with a Lambda model LP-521-FM regulated power supply. Nuclear magnetic resonance (NMR) spectra were recorded on a Varian Gemini 200 (200 MHz for ^{1}H) or a Bruker Avance 300 (300 MHz for ^{1}H, 121 MHz for ^{31}P, 75 MHz for ^{13}C, 282 MHz for ^{19}F) FT-NMR spectrometer. For ^{1}H and ^{13}C NMR spectra the residual proton and carbon signals of the deuterated solvent were used as internal standards. Downfield shifts are taken as positive for all nuclei, and chemical shifts are listed in ppm. HMQC, HMBC, and DEPT 135 were carried out on the Bruker Avance 300 instrument. Mass spectrometric analyses were performed by the Ottawa-Carleton Mass Spectrometry Center. Gel Permeation Chromatography (GPC) data were

obtained using CH_2Cl_2 as eluent (flow rate 1.0 mL/min; samples 1-2 mg/mL) on a Wyatt DAWN light-scattering instrument equipped with an Optilab DSP refractometer, an HPLC system with a Waters model 515 pump, Rheodyne model 7725i injector with 200 μL injection loop, and Waters Styragel HR3 and HR4 columns in series.

2.2. Materials

2.2.1. Solvents

Reagent grade tetrahydrofuran, hexanes, toluene and ether were dried and degassed using an Anhydrous Engineering solvent purification system. Anhydrous dimethylformamide (DMF), 1,2-dimethoxyethane (DME) and xylenes were purchased from Aldrich and used without further purification. Other solvents were refluxed over and distilled from an appropriate drying agent under nitrogen atmosphere: benzene over sodium benzophenone ketyl; pentane over sodium; dichloromethane, pyridine, triethyl amine and acetonitrile over calcium hydride; methanol over Mg/I_2; acetone over Drierite (anhydrous $CaSO_4$). All solvents (with the exception of methanol) were stored over Linde 4Å molecular sieves under an atmosphere of N_2.

All deuterated solvents ($CDCl_3$, C_6D_6, and D_2O) were obtained from Cambridge Isotope Laboratories Ltd. $CDCl_3$ was refluxed over and distilled from Drierite under an atmosphere of N_2. C_6D_6 was deoxygenated by consecutive freeze/pump/thaw cycles and stored over Linde 4Å molecular sieves. All deuterated solvents were stored under N_2.

2.2.2. Other Materials

The following materials were purchased from Aldrich Chemical Co. and used without purification: 1,2:3,4-Di-O-isopropylidene-D-galactopyranose, beta-D-galactose pentaacetate, allyltrimethyl silane, boron trifluoride etherate, sodium hydride, benzyl bromide, sodium borohydride, ammonium dimolybdate, neophyl chloride, TMS-Cl, iodine, triflic acid, lithium *t*-butoxide, dimethyl fumarate, fumaryl chloride, acryloyl chloride, 10% Pd-C, *p*-toluenesulphonylhydrazide. 2,6-Diisopropylaniline was distilled over KOH, neophyl chloride over CaH_2. Hydrogen (UHP Grade) was purchased from Praxair and used without purification.

2.3. Synthetic Procedures

2.3.1. Synthesis of C-glycoside

2.3.1.1. 3-(1'-Deoxy-2',3',4',6'-tetra-O-acetyl-alpha-D-galactopyranosyl)prop-1-ene (2) [1,2]

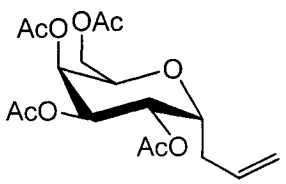

To a stirred solution of β-D-galactose pentaacetate (5.03 g, 12.8 mmol), and allyltrimethyl silane (6 mL, 37.8 mmol) in dry acetonitrile (60.0 mL) at 0 C°, BF_3 etherate (7.01 mL, 55.2 mmol) was added dropwise. The reaction mixture was refrigerated at approximately 4° C for 48 h, then transferred to an ice bath and quenched by dropwise addition of saturated $NaHCO_3$. The product was extracted with EtOAc (3 × 50 mL), dried over Na_2SO_4, and stripped to dryness. Flash chromatography (silica gel, 50

% EtOAc in hexanes) afforded syrupy **2** in 50-68% yield. The NMR data matched values reported in the literature. Literature yield: 80%.

^{1}H NMR ($CDCl_3$), δ: 5.6-5.8 (m, 1 H, C*H*=CH_2, β + α), 5.3 (br, t, 1 H, *J* = 6, *H*-1), 5.1-5.2 (dd, 2 H, *J* = 9 Hz, 5 Hz, CH=C*H*$_2$, β; dd, *J* = 9 Hz, 3 Hz, CH=C*H*$_2$, α), 4.9-5.1 (m, 2 H, C*H*$_2$CH=CH_2), 4.2 (dt, 1 H, *J* = 14 Hz, 7 Hz, *H*-5), 4.1 (dd, 1H, J_d = 15 Hz, 9 Hz, *H*-2), 4.0 (m, 2 H, *H*-3 + *H*-4), 2.2-2.4 (m, 2 H, C*H*$_2$OAc, β + α), 1.8-2.1 (4s, 12 H, C*H*$_3$).

^{13}C{^{1}H} NMR ($CDCl_3$), δ: 170.2 (*C*O, acyl), 169.8 (*C*O, acyl), 169.7 (*C*O, acyl), 169.6 (*C*O, acyl), 133.2 (*C*H=CH_2, β), 133.1 (*C*H=CH_2, α), 117.4 (CH=*C*H$_2$, β), 117.1 (CH=*C*H$_2$, α), 71.9 (*C*-1), 67.9 (*C*-5, *C*-2), 67.6 (*C*-4), 67.4 (*C*-3), 61.3(*C*H$_2$CH=CH_2), 35.8 (*C*H$_2$COAc, β), 30.6 (*C*H$_2$COAc, α), 20.3-20.6 (4 *C*H$_3$).

2.3.1.2. 2-Allyl-6-hydroxymethyl-tetrahydro-pyran-3,4,5-triol (3) [2,3]

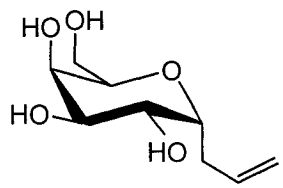

Sodium metal (0.804 g, 34.98 mmol) was added to **2** (3.032 g, 7.77 mmol) in 25 mL methanol. The reaction was stirred for 20 min at 0 C°, and then neutralized with Dowex-50W-hydrogen acid resin. The resin was filtered off and washed with methanol (30 mL). The filtrate was stripped off to give tetrol **3**, which was used without further purification.

2.3.1.3. 3-(2',3',4',6'-tetra-O-benzyl-α-D-galactopyranosyl)prop-1-ene (4) [2,3]

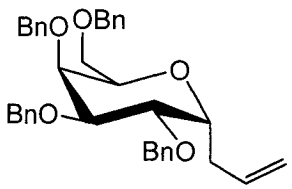

Solidified **3** (1.88 g, 9.21 mmol) was added over 5 min to a stirred suspension of sodium hydride (1.88 g, 60% dispersion in mineral oil, 9.21 mmol) in 20 mL of DMF at 0 °C. The reaction was allowed to warm-up to RT and was stirred for 45 min, then cooled back to 0 C°. Benzyl bromide (4.6 mL, 38.68 mmol) was added dropwise, and the reaction was allowed to warm to RT over 4 h. Excess NaH was then quenched by dropwise addition of brine at RT. DMF was removed under reduced pressure and the solution was extracted with 3 × 50 mL EtOAc. The organic phase was dried (Na_2SO_4), filtered, and stripped to a yellowish syrup. Flash chromatography (silica gel, 10% EtOAc in hexanes) afforded **4** as a clear syrup in 75% yield. The NMR data matched values reported in the literature. Reported yield: 90%.

^{1}H NMR ($CDCl_3$), δ: 7.5 (m, 20 H, Ar*H*), 6.0 (m, 1 H, C*H*=CH_2, β + α), 5.0-5.3 (m, 2 H, CH=CH_2, β + α), 4.5-5.0 (m, 6 H, CH_2Ph), 3.6-4.4 (m, 7 H, *H*-1 *H*-2 *H*-3 *H*-4 *H*-5, CH_2CH=CH_2), 2.5 (m, CH_2OCH_2Ph). **^{13}C{^{1}H} NMR** ($CDCl_3$), δ: 139.1 (*ipso*-Ar*C*H), 139.0 (2 *ipso*-Ar*C*H), 138.8 (*ipso*-Ar*C*H), 135.7 (*C*H=CH_2), 127.9-128.9 (20 C, Ar*C*H), 117.3 (CH=*C*H_2), 78.1 (*C*-1), 77.7 (*C*-5), 77.3 *(C*-2), 76.9 (*C*-4), 74.7 (*C*-3), 73.5-73.6 (4 C, *C*H_2Ph), 67.7 (*C*H_2CH=CH_2), 67.3 (*C*H_2OBn).

2.3.1.4. 3-(3,4,5-Tris-benzyloxy-6-benzyloxymethyl-tetrahydro-pyran-2-yl)-propan-1-ol (5) [2,4]

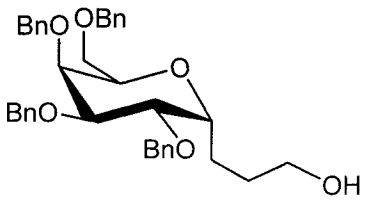

Solid $NaBH_4$ (0.067 g, 2 equiv) was added to a solution of C-glycoside **4** (0.5 g, 0.8 mmol) in 10 mL THF. The reaction was stirred for 30 min until a homogeneous dispersion formed, then cooled to 0 C° in an ice bath. Boron trifluoride etherate was added dropwise over 10 min at RT, after which the reaction was heated to 40 C° for 1 h. The excess BF_3 was quenched by dropwise addition of water at ice temperatures, after which freshly prepared 3N NaOH and 5% H_2O_2 (5 mL each) were added together, and the reaction was heated at 50 C°. After 1 h, the reaction was allowed to cool, and the product was extracted with EtOAc (3 × 20 mL). The organic phase was dried over Na_2SO_4, and stripped to dryness. Flash chromatography (silica gel, 50% EtOAc in hexanes) afforded **5** as a colourless syrup in 75% yield. The NMR data matched values reported in the literature. The reported yield of the reaction was 73%.

ESI-MS (NH_4^+, *m/z*): M^++1 583 (calcd 582). **IR** (neat, cm^{-1}): 3458 υ(OH). **^{1}H NMR** ($CDCl_3$), δ: 7.3-7.5 (m, 20 H, Ar*H*), 4.5-5.0 (m, 8 H, C*H*$_2$Ph), 3.5-4.0 (m, 6 H, *H*-6, *H*-5, *H*-4, *H*-3, *H*-2, *H*-1), 2.5 (br, s, 1 H, O*H*, D_2O exchange), 1.5-2.0 (br, m, 2H, C*H*$_2$C*H*$_2$CH$_2$OH). **^{13}C{^{1}H} NMR** ($CDCl_3$), δ: 139.0 (*ipso*-Ar*C*H), 138.9 (*ipso*-Ar*C*H), 138.8 (*ipso*-Ar*C*H), 138.6 (*ipso*-Ar*C*H), 127.9-128.8 (Ar*C*H), 78.1 (*C*-1), 77.7 (*C*-5), 77.3 (*C*-2), 77.2 (*C*-4), 74.8 (*C*-3), 73.6-73.7 (4 C, *C*H$_2$Ph), 62.7 (overlapping, 2*C*, *C*H$_2$OBn, *C*H$_2$OH), 30.0 (overlapping, 2 *C*, *C*H$_2$*C*H$_2$CH$_2$OH).

2.3.2. Monomer Synthesis

The following preparations are based on literature methods. These compounds were either used directly as substrates in ROMP experiments, or as starting materials for the synthesis of other monomers. The norbornene ring numbering shown in Figure 2.1 is provided to aid in the NMR analysis.

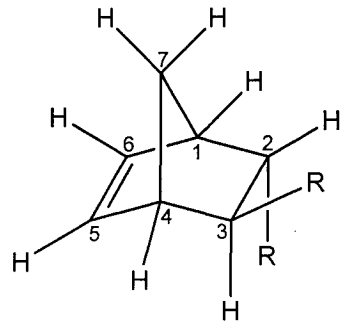

Figure 2.1 Representative numbering of the norbornene carbons.

2.3.2.1. 2,3-Diacetyl-5-norbornene (6) [5]

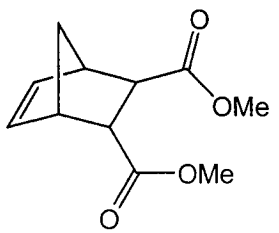

An ice-cold solution of dimethyl fumarate (30.00 g, 208 mmol) in 50 mL of CH_2Cl_2 was added to 11 mL of freshly cracked cyclopentadiene (13.7 g, 208 mmol). The solution was stirred for 30 minutes, then allowed to warm up to RT over 24 hours. The solvent was then evaporated and the product was purified by vacuum distillation (bp 78-80°C at 25 mm Hg) to yield 35.86 g (82%) of clear oil which formed a white solid at RT.

The NMR data matched values reported in literature and the reported yield of the reaction was 94%.

IR (Nujol, cm^{-1}): 1731 υ(C=O). **^{1}H NMR** ($CDCl_3$), δ: 6.2 (m, 1 H, CH=C*H*), 6.0 (m, 1 H, C*H*=CH), 3.6 (s, 3 H, CH_3), 3.4 (s, 3 H, CH_3), 3.25 (s, 1 H, C*H*COOMe), 3.18 (m, 1 H, C*H*COOMe), 3.0 (m, 1 H, C-1), 2.6 (m, 1 H, C-4), 1.6 (m, 1 H, C-7), 1.4 (m, 1 H, bridge). **^{13}C{^{1}H} NMR** ($CDCl_3$), δ: 174.8 (*C*=O), 173.6 (*C*=O), 137.5 (*C*H=CH), 135.1 (CH=*C*H), 52.0 ($CHCO_2CH_3$), 51.8 ($CHCO_2CH_3$), 47.8 (C-1), 47.5 (C-4), 47.2 (C-7), 47.0 ($CHCO_2CH_3$), 45.5 ($CHCO_2CH_3$).

2.3.2.2. 5-Norbornene-2,3-dicarbonyl chloride (7) [6]

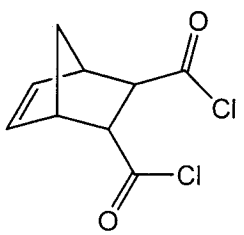

An ice-cold solution of 17.8 mL of fumaryl chloride (25.00 g, 163 mmol) in 50 mL of dry diethyl ether was added to 13.5 mL of freshly cracked cyclopentadiene (11 g, 163 mmol). The solution was stirred for 30 minutes, then allowed to warm up to RT over 24 hours. The solvent was then evaporated and the product was purified by vacuum distillation (bp 69-72°C at 25 mm Hg) to yield 23.22 g (65%) of clear oil. The NMR data matched values reported in literature. The reported yield of the reaction was 57%.

^{1}H NMR ($CDCl_3$), δ: 6.35 (m, 1 H, CH=C*H*), 6.20 (m, 1 H, C*H*=CH), 3.82 (t, 1 H, C*H*COOCl), 3.52 (s, br, 1 H, C*H*COOCl), 3.42 (s, br, 1 H, C-1), 3.17 (m, 1 H, C-4), 1.60

(m, 2 H, C-7). **$^{13}C\{^{1}H\}$ NMR** ($CDCl_3$), δ: 174.9 (*C*=O), 173.4 (*C*=O), 138.1 (*C*H=CH), 135.6 (CH=*C*H), 60.2 (*C*HCO_2Me), 59.6 (*C*HCO_2Me), 48.6 (C-1), 47.7 (C-4), 47.1 (C-7).

2.3.2.3. 5-Norbornene-2-carboxylic acid chloride (8) [7,8]

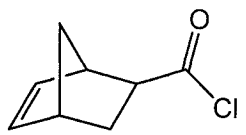

An ice-cold solution of acryloyl chloride (27.17 g, 300 mmol) in 50 mL of dry diethyl ether was added to freshly cracked cyclopentadiene (19.85 g, 300 mmol). The solution was stirred for 30 minutes, then allowed to warm up to RT over 24 hours. The solvent was then evaporated and the product was purified by vacuum distillation (bp 58-63°C at 25 mm Hg) to yield 33.23 g (71%) of clear oil. The NMR data matched values reported in the literature.

^{1}H NMR ($CDCl_3$), δ: 6.22 (dd, 1 H, CH=C*H*), 5.99 (dd, 1 H, C*H*=CH), 3.39 (s, 2 H, C*H*COOCl and C-1), 2.95 (s, 1 H, C-4), 1.91 (m, 1 H) 1.47 (m, 2 H, C-3, C-7), 1.29 (m, 1 H, C-7).**$^{13}C\{^{1}H\}$ NMR** ($CDCl_3$), δ: 175.4 (*C*=O), 139.1 (*C*H=CH), 131.9 (CH=*C*H), 56.8 (*C*HCOCl, C-2), 49.6 (CH_2, C-7), 47.5 (*C*H, C-1), 43.3 (*C*H, C-4), 30.4 (C-3).

2.3.2.4. Bis(1,2;3,4-di-O-isopropylidene-D-galactopyranos-6-O-yl) 5-norbornene-2,3-dicarboxylate (9) [9]

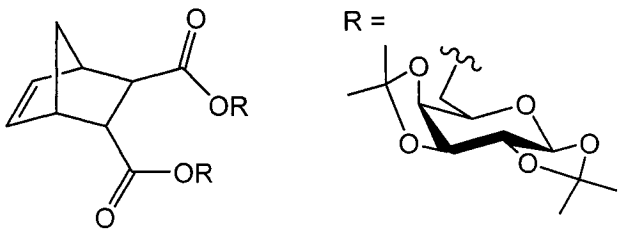

A solution of 5-norbornene-2,3-carboxylic dicarbonyl chloride **7** (3.42 g, 15.55 mmol) in ether (10 mL) was added dropwise to a solution of 1,2;3,4-di-O-isopropylidene-D-galactopyranose (8.0 g, 30.73 mmol) and triethylamine (3.12 g, 30.72 mmol) in ether (80 mL) at -78°C. The reaction mixture was stirred overnight; a white precipitate deposited as it slowly warmed to room temperature. The reaction mixture was washed twice each with saturated Na_2CO_3 and brine, and dried over $MgSO_4$. The organic extracts were combined, the solvent was evaporated, and the product was purified by column chromatography using 35% ethyl acetate in hexanes. After drying under vacuum (25 mm Hg) the reaction afforded 8.0 g (77% yield) of white powder. The NMR data matched values reported in literature. The reported yield of the reaction was 80%.

^{1}H NMR ($CDCl_3$), δ: 6.25 (m), 6.10 (m) (2 H, C-6, C-7), 5.5 (t, 2 H, anomeric protons), 4.6 (d, 2 H), 4.4-3.9 (m, 8 H) (sugar group protons), 3.4 (br s, 1 H), 3.25 (m, 1 H), 3.1 (br s, 1 H), 2.7 (br s, 1 H), 1.7 (br s, 1 H), 1.5 (m, 1 H) (C-1, C-2, C-3, C-4, C-7), 1.45 (d, 6 H), 1.4 (s, 6 H), 1.25 (s, 12 H) (cyclic acetal protons). **^{13}C{^{1}H} NMR** ($CDCl_3$), δ: 174.67, 174.52, 173.41, 173.37 (carbonyl), 137.76, 135.98, 135.78 (olefinic carbon), 110.01, 109.91, 109.05 (isopropylidene), 96.67, 96.59, 71.35, 71.08, 71.03, 70.81, 70.78, 66.54, 66.35, 66.26, 66.21, 63.94 (sugar group), 48.15, 48.11, 47.99, 47.50, 47.42, 46.15, 46.09 (C-1, C-2, C-3, C-4, C-7), 26.35, 25.28, 24.75 (isopropylidene methyl).

2.3.2.5. Bis(3-(3,4,5-tris-benzyloxy-6-benzyloxymethyl-tetrahydro-pyran-2-yl)-propan-1-O-yl) 5-norbornene-2,3,-dicarboxylate (10)

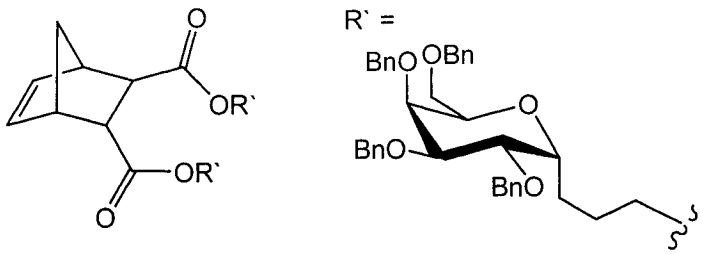

A solution of 5-norbornene-2,3-carboxylic dicarbonyl chloride **7** (1.13 g, 5.16 mmol) in ether (10 mL) was added dropwise to a solution of C-glycoside **10** (6.0 g, 10.30 mmol) and triethylamine (1.14 g, 11.30 mmol) in 80 mL ether at -78°C. The reaction mixture was allowed to warm to room temperature overnight, over which time a white precipitate deposited. The reaction mixture was washed twice with saturated Na_2CO_3, twice with brine, and dried over $MgSO_4$. The organic extracts were combined, the solvent evaporated, and the product purified by column chromatography using 30% ethyl acetate in hexanes. After drying under vacuum (25 mm Hg) the reaction afforded 4.9 g (73% yield) of a thick, clear and sticky oil.

^{1}H NMR ($CDCl_3$), δ: 7.35 (m, 40 H, benzyl group protons), 6.3 (m), 6.1 (m) (C-6, C-7), 4.5-5.0 (m, 8 H, CH_2Ph), 3.6-4.0 (m, 6 H, *H*-6, *H*-5, *H*-4, *H*-3, *H*-2, *H*-1, sugar protons), 3.45 (br s, 1 H), 3.3 (m, 1 H), 3.2 (br s, 1 H), 2.8 (br s, 1 H), 1.7 (br s, 1 H), 1.5 (m, 1 H) (C-1, C-2, C-3, C-4, C-7), 2.0 (s), 1.5-2.0 (br, m) ($CH_2CH_2CH_2O$). **^{13}C{^{1}H} NMR** ($CDCl_3$), δ: 174.8 (*C*=O), 173.6 (*C*=O), 139.0 (*ipso*-Ar*C*H), 138.9 (*ipso*-Ar*C*H), 138.8 (*ipso*-Ar*C*H), 138.6 (*ipso*-Ar*C*H), 137.5 (*C*H=CH), 135.1 (CH=*C*H), 128.8-127.9 (*Ar*CH), 73.7, 73.5, 73.4, 72.6, 68.1 (sugar carbons and OCH_2Ph), 65.2, 64.9 (CH_2CO_2), 48.3, 47.8, 47.7, 46.2 (C-1, C-2, C-3, C-4, C-7), 25.7, 24.1 ($CH_2CH_2CH_2O$).

2.3.2.6. 5-Norbornene-2-carboxylic acid N-hydroxysuccinimide ester (11) [10]

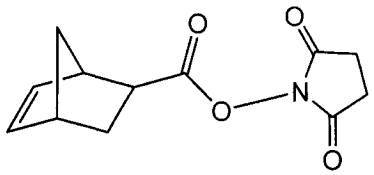

A solution of 5-norbornene-2-carboxylic acid chloride **8** (1.36 g, 8.69 mmol) in 10 mL ether was added dropwise to a solution of N-hydroxysuccinimide (1.0 g, 8.69 mmol) and triethylamine (0.88 g, 8.69 mmol) in ether (60 mL) at -78°C. The reaction mixture was stirred overnight and worked up as in Section **2.3.2.5**. After drying under vacuum (25 mm Hg) the reaction afforded 1.8 g (87% yield) of white crystalline powder. The NMR data matched values reported in literature. The literature yield was 80%.

IR (neat, cm^{-1}): 1804, 1778 ν(CO) of the succinimide, 1729 overlap of ν(CO) and ν(CH=CH). **^{1}H NMR** ($CDCl_3$), δ: 6.25-6.10 (m, 2 H, C*H*=CH, C-5, C-6), 3.4 (s, 1 H, C-1), 3.25 (m, 1 H, C*H*COON, C-2), 2.9 (s, 1 H, C-3), 2.75 (m, 4 H, CH_2 of the succinimide), 1.9 (m, 1 H), 1.45 (m, 1 H) (C-3), 1.45 (m, 1H), 1.25 (d, 1 H) (C-7). **^{13}C{^{1}H} NMR** ($CDCl_3$), δ: 170.35, 169.71 (*C*O), 138.52, 132.52 (*C*H=*C*H), 50.03 (C-7), 46.82 (C-1), 42.89 (C-4), 40.97 (*C*HCO$_2$, C-2), 29.93 (C-3), 25.96 (*C*H$_2$*C*H$_2$).

2.3.3. Synthesis of Catalysts

$RuCl_2(PCy_3)_2$ **12** and $RuCl_2(PCy_3)$(IMes) **13** catalysts were prepared according to literature procedures[11-13] by Jay Conrad of the Fogg group. The Schrock Mo catalyst was also prepared according to the literature procedure. [14]

2.3.3.1. Mo(N-2,6-$^{i}Pr_2C_6H_3)_2Cl_2$(DME) (14)

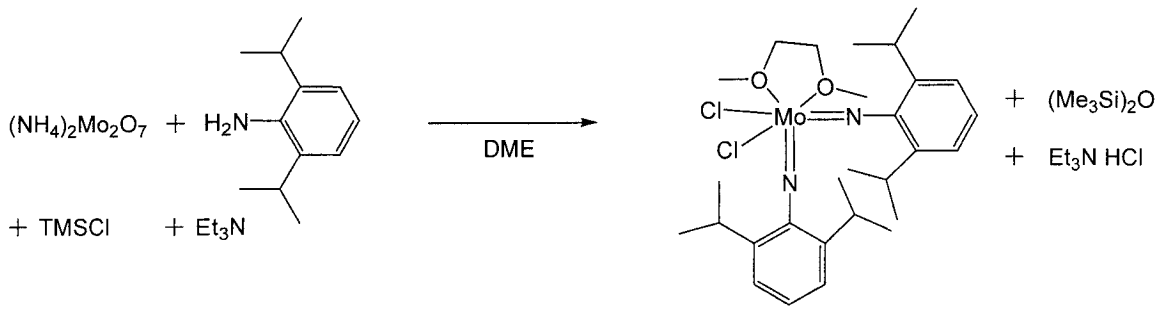

In a 500 mL Schlenk flask, ammonium dimolybdate (10 g, 29.41 mmol) was suspended in DME (150 mL) and stirred vigorously while a solution of NEt_3 (23.81 g, 235.29 mmol) in DME (10 mL) was added over 10 min. A solution of TMS-Cl (54.32 g, 500 mmol) in DME (10 mL) was then added over 30 min. The white mixture turned gray and 2,6-diisopropylaniline (20.86 g, 117.65 mmol) in DME (10 mL) was added. The mixture turned yellow and was left to stir overnight in the drybox. After 12 hours the color of the reaction was brick-red. The reaction was then removed from the drybox and stirred at 65 °C for 6 hours under N_2. It was then returned to the glovebox, filtered through Celite, and washed with DME until the washings were colorless. The filtrate was stripped to dryness leaving a brick-red solid. Yield: 34 g, 95%. The product is stable at room temperature under N_2.

^{1}H NMR ($CDCl_3$), δ: 7.02-6.86 (6H, aromatic protons), 4.34-4.25 (4H, 4C*H*Me_2), 3.44 (6H, O-C*H*$_3$), 3.17 (4H, O-CH_2CH_2-O), 1.26-1.08 (24H, 4CH*Me*$_2$).

2.3.3.2. Magnesium neophyl chloride (15)

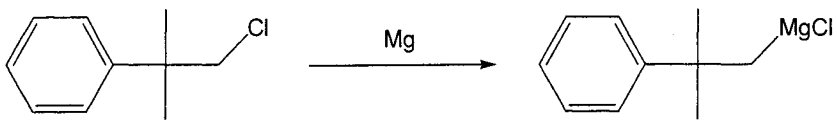

Mg (6.1 g, 250 mmol) was added to a 500 mL 3-neck round-bottom flask containing 100 mL Et_2O. The flask was fitted with two stoppers and a dropping funnel containing the neophyl chloride (31.47 g, 186 mmol) layered with Et_2O (10 mL) to wash it down. Two or three crystals of iodine were added to initiate the reaction, the dropping funnel was fitted with a gas release adaptor, and the assembly was removed from the drybox and connected to a Schlenk manifold. The middle stoppers was removed and fitted with a condenser under nitrogen. About 10 mL neophyl chloride was added and the flask was gently warmed up until the reaction started. The neophyl chloride was added slowly to keep the reaction refluxing smoothly. When addition was completed, the reaction was refluxed overnight. The solution was then cooled, cannulated into a Schlenk tube equipped with a Kontes valve, and taken into the drybox. The proportion of active Grignard reagent was measured by titration. A known volume of magnesium neophyl chloride (100 μL) was added to a solution of 1,10-phenanthroline in THF, and the mixture was titrated by adding MeOH via a 10 μL syringe until the endpoint was reached. The endpoint was indicated by a change in color from deep purple to light yellow.

2.3.3.3. Mo(N-2,6-$^{i}Pr_2C_6H_3)_2(CH_2CMe_2Ph)_2$ (16)

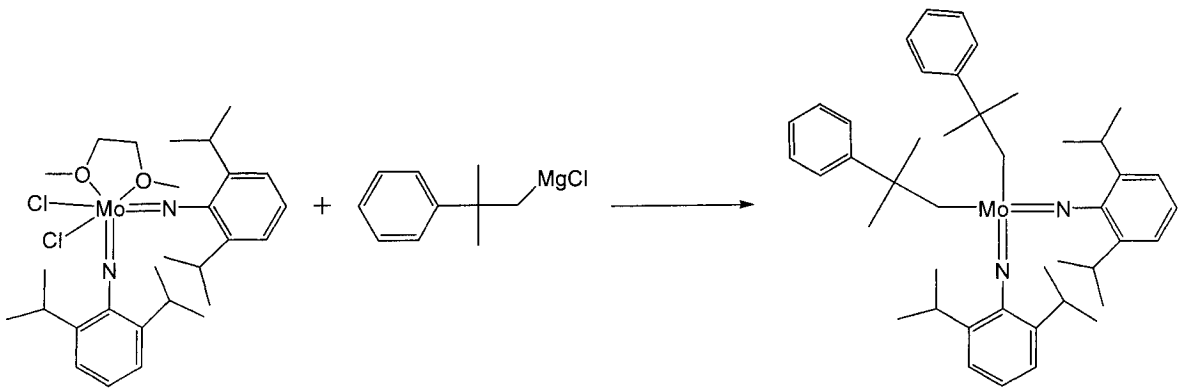

A solution of magnesium neophyl chloride (1.46 M, 16.46 mmol) in Et_2O was added slowly to a cooled solution (freezer; -35°C; 1 h) of Mo(N-2,6-$^{i}Pr_2C_6H_3)_2Cl_2$(DME) **14** (5.00 g, 8.23 mmol) in 100 mL Et_2O, to avoid refluxing. The mixture was stirred overnight. The solution was then filtered through Celite and washed with Et_2O until the washings were colorless. The filtrate was concentrated until a bright orange precipitate was evident. The latter was filtered off and quickly washed with cold hexanes. Precipitation was repeated until no more product was collected. Total yield of 5 crops: 4.2 g, 72%.

^{1}H NMR ($CDCl_3$), δ: 7.46-6.94 (16H, aromatic protons), 3.69-3.60 (2H, 4C*H*Me), 1.71 (4H, 2 CH_2 in C*H*$_2$CMe$_2$Ph), 1.48 (12H, 4CH_3 in CH2C*Me*$_2$Ph), 1.47-1.07 (24H, CH_3 in CH*Me*$_2$).

2.3.3.4. Mo(CHCMe$_2$Ph)(N-2,6-^{i}Pr$_2$C$_6$H$_3$)(OSO$_2$CF$_3$)$_2$(DME) (17)

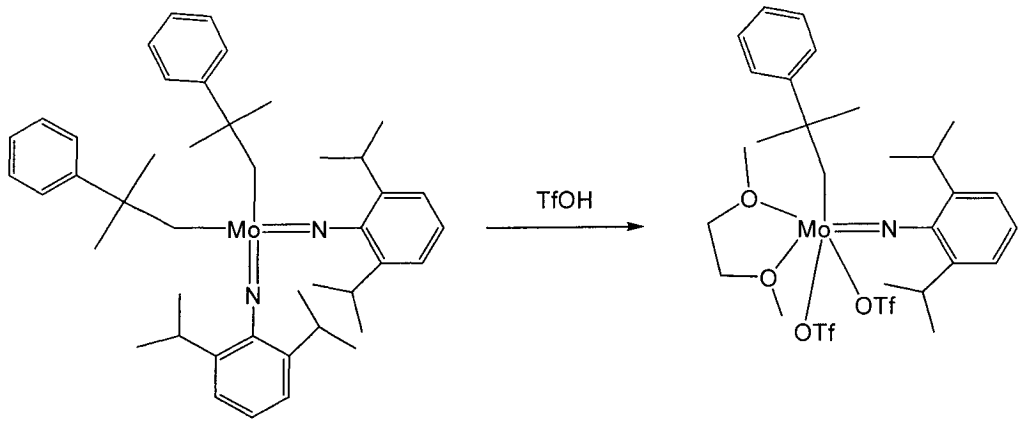

To test if the quality of the DME is adequate for the reaction, a small amount of triflic acid, chilled in the freezer for ca. 30 min, was added to 1 mL of chilled DME. A colour change of the solution to black indicates DME decomposition. If the DME remained colorless or slightly yellow, the synthesis was carried out. To a solution of Mo(N-2,6-^{i}Pr$_2$C$_6$H$_3$)$_2$(CH$_2$CMe$_2$Ph)$_2$ **16** in DME (150 mL, chilled in the freezer for ca. 1 hour) was added a solution of cold triflic acid (5 g, 33.32 mmol) in 10 mL DME. The resulting red-orange reaction mixture was allowed to stir overnight at room temperature. A dark yellow reaction solution resulted, which was stripped of solvent. The residue was extracted with chilled toluene and filtered through Celite until the washings were colourless. The filtrate was concentrated and refrigerated to precipitate the product as a yellow solid, which was filtered off and washed with cold Et$_2$O. The precipitation process was repeated until no more product was obtained. Yield: 6.5 g, 74%. The product was stored in the freezer.

^{1}H NMR ($CDCl_3$), δ: 14.45 (1H, C*H*CMe$_2$), 7.59-6.90 (8H, aromatic), 3.84 (2H, C*H*Me$_2$), 3.74 (3H, OC*H*$_3$), 3.18 (2H, OC*H*$_2$), 2.78 (5H, OC*H*$_3$, OC*H*$_2$), 1.91 (6H, CHC*Me*$_2$Ph), 1.39-1.37 (6H, CH*Me*$_2$), 1.23-1.20 (6H, CH*Me*$_2$).

2.3.3.5. Mo(CHCMe$_2$Ph)(N-2,6-^{i}Pr$_2$C$_6$H$_3$)(O^{t}Bu)$_2$ (18)

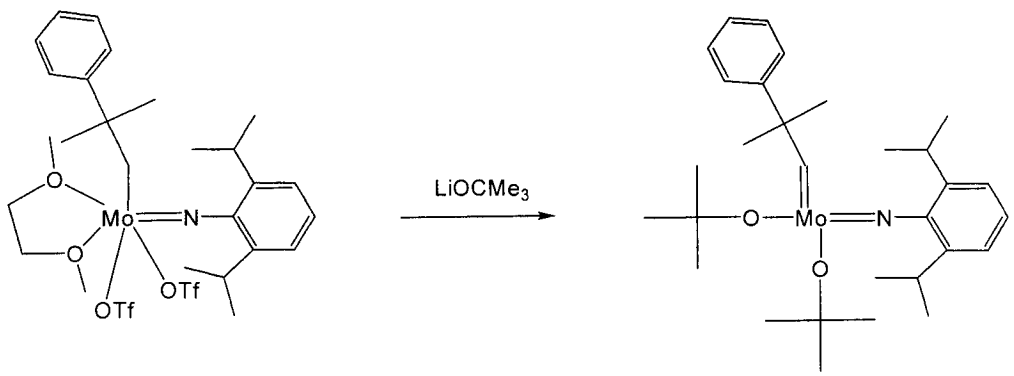

Mo(CHCMe$_2$Ph)(N-2,6-^{i}Pr$_2$C$_6$H$_3$)(OSO$_2$CF$_3$)$_2$(DME) **17** was dissolved in 50 mL Et_2O to give a yellow solution, which was chilled for 30 min in the drybox freezer. Solid $LiOCMe_3$ (208 mg, 2.60 mmol) was added in one portion and the reaction was allowed to warm to room temperature (orange color). After 45 min, the solvent was removed in vacuo and the resulting solid was extracted with 20 mL pentane and washed with pentane until the washings were colorless. Pentane was evaporated under reduced pressure until 3-5 mL of solvent remained, and the viscous solution was then placed in the freezer. After ca. 1 hour crystals were collected by filtration. The product was quickly washed with a minimal amount of cold pentane, and dried in vacuo. Yield: 377 mg, 53% (first crop, bright yellow-orange color). The product was stored in the freezer.

^{1}H NMR ($CDCl_3$), δ: 11.32 (1H, C*H*CMePh), 7.45-7.02 (8H, aromatic), 4.04-3.95 (2H, C*H*Me$_2$), 1.70-1.05 (36H, CHC*Me$_2$*, CH*Me$_2$*, OC*Me$_3$*).

2.3.4. ROMP via Molybdenum Catalysis [9]

*Synthesis of Poly(**9**)*

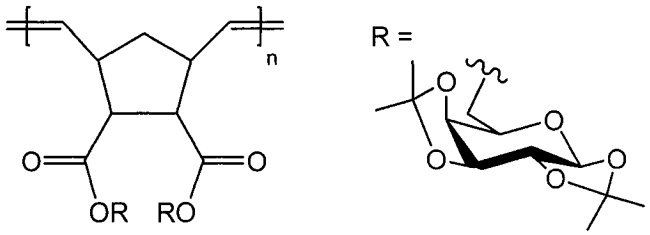

In a representative procedure, a benzene (2 mL) solution of **9** (182 mg, 0.273 mmol) was added in one portion to a rapidly stirred solution of $Mo(CHCMe_2Ph)(N\text{-}2,6\text{-}{}^{i}Pr_2C_6H_3)(O^{t}Bu)_2$ **18** (3 mg, 0.005 mmol) in 5 mL benzene. The reaction was followed by ^1H NMR. After complete conversion the polymerization was quenched by adding benzaldehyde, and stirred for 20 minutes. The solvent was removed under reduced pressure, the resulting solid dissolved in a minimum amount of CH_2Cl_2, and this solution added dropwise to vigorously stirred cold methanol (~ 100 mL) to afford a white to pale yellow precipitate. The polymer was collected by centrifugation, purified by column chromatography (30% ethyl acetate in hexanes) and dried in vacuo.

^1H NMR ($CDCl_3$), δ: 5.5-5.2 (br) (anomeric carbon proton *H-1*, and olefinic C-5, C-6), 4.6 (br s), 4.4-4.0 (br), 3.9 (br s) (*H-6, H-5, H-4, H-3, H-2,* sugar group protons), 3.2 (br s), 2.9 (br s), 2.7 (br s), 1.8 (br s), 1.6 (s) (C-1, C-2, C-3, C-4, C-7), 1.5 (s, 3 H, Me), 1.4 (s, 3 H, Me) 1.3 (s, 6 H, Me) (4(CH_3) acetal). **$^{13}C\{^1H\}$ NMR** ($CDCl_3$), δ: 174.1, 173.8, 173.0-173.3 (CO), 134.6, 130.7, 129.9, 129.2, 128.4, 125.5 (olefinic carbon, C-5, C-6), 109.6, 108.9 (isopropylidene), 96.4, 71.1, 70.9, 70.7, 65.8, 63.6 (sugar group), 53.2-52.8, 52.3-51.7, 47.2-46.5, 45.6-45.3, 39.0-38.7 (C-1, C-2, C-3, C-4, C-7), 26.2, 25.2, 24.7 (isopropylidene). **GPC**: n = 10: M_n(calc.) = 6670; M_n(expt.)= 12320; PDI = 1.06, n = 50:

M_n(calc.) = 33350; M_n(expt.) = 35090; PDI = 1.08, n = 100: M_n(calc.) = 66700; M_n(expt.) = 97360; PDI = 1.08.

*Poly(**6**)*

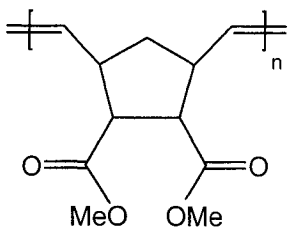

ROMP of 2,3-diacetyl-5-norbornene **6** was used to check the glovebox atmosphere for the presence of O_2 or H_2O (Sections 3.3. and 3.3.1.) This "test" reaction was carried out prior to ROMP of any sugar monomer.

^{1}H NMR ($CDCl_3$), δ: 5.5-5.2 (br) (olefinic protons, C-5, C-6), 3.6 (s, 3 H, Me), 3.55 (s, 3 H, Me), 3.2 (br, s), 2.9 (br, m), 2.6 (br, s), 1.6-1.45 (br, m) (C-1, C-2, C-3, C-4, C-7). **GPC**: Range 1.04 – 1.40 depending on the drybox atmosphere.

*Poly(**11**)*

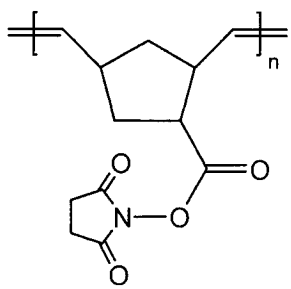

IR (neat, cm^{-1}): 1808, 1777 ν(CO) of the succinimide, 1731-1675 overlap of ν(CO) and ν(CH=CH). **^{1}H NMR** ($CDCl_3$), δ: 5.7-5.3 (br, olefinic protons C-5, C-6) , 2.8 (br, s) (succinimide methylene protons), 3.2 (br), 2.6-2.5 (br), 2.2 (br), 2.0-1.7 (br), 1.5-1.2 (br)

(C-1, C-2, C-3, C-4, C-7). **GPC**: n = 60: M_n(calc.) = 14082; M_n(expt.) = 15240; PDI = 1.12.

*Random copolymer of **9** and **11***

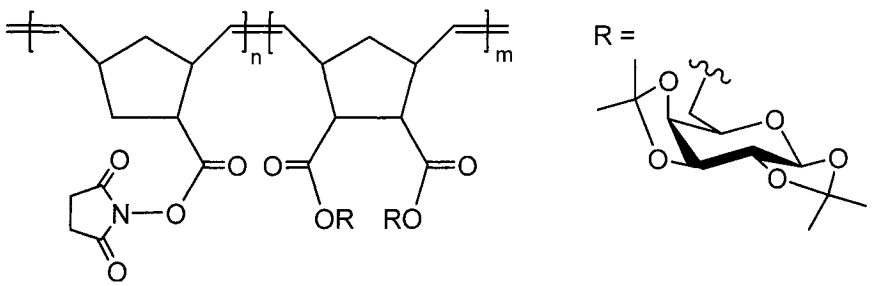

Norbornene O-glycoside **9** (0.200 g, 0.150 mmol) and norbornene N-hydroxysuccinimide ester **11** (0.014 g, 0.030 mmol) were dissolved in 2 mL of benezene and added to a rapidly stirring solution of Mo(CHCMe$_2$Ph)(N-2,6-^{i}Pr$_2$C$_6$H$_3$)(O^{t}Bu)$_2$ **18** (3.0 mg, 0.003 mmol) in 5 mL benzene. ROMP was followed by ^{1}H NMR analysis; after complete conversion the reaction was quenched with benzaldehyde. The solvent was removed under reduced pressure and the resulting solid was dissolved in a minimum amount of CH_2Cl_2. This solution was added dropwise to vigorously stirring methanol (100 mL) at ice temperatures to afford a pale yellow precipitate. The polymer was collected by centrifugation, purified by column chromatography (30% ethyl acetate in hexanes) and dried in vacuo. The obtained NMR spectrum revealed overlapping peaks of norbornene N-succinimide and O-glycoside polymers.

^{1}H NMR ($CDCl_3$), δ: 5.5-5.2 (br) (anomeric carbon proton *H-1*, and olefinic C-5, C-6), 4.6 (br s), 4.4-4.0 (br), 3.9 (br s) (*H-6, H-5, H-4, H-3, H-2,* sugar group protons), 3.2 (br s), 2.8 (br s), 2.2-1.8 (br), 1.6 (br s) (C-1, C-2, C-3, C-4, C-7, methylenes of the

succinimide), 1.5 (s, 3 H, Me), 1.4 (s, 3 H, Me) 1.3 (s, 6 H, Me) (4(CH_3) acetal). **GPC**: n = 10, m = 50: M_n(calc.) = 35 697; M_n(expt.) = 48770; PDI = 1.13.

Triblock copolymer ***(9)$_5$(10)$_{10}$(9)$_5$***

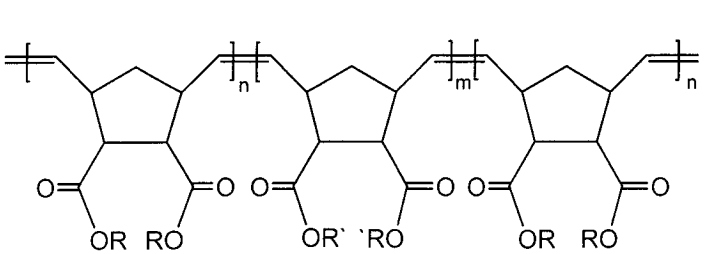

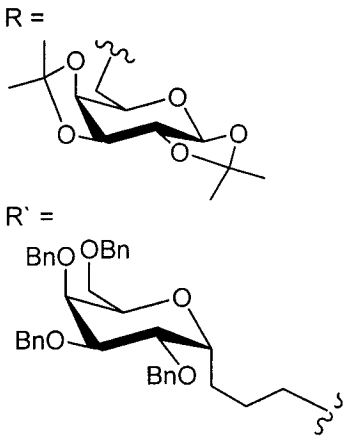

To a benzene (8.0 mL) solution of O-glycoside monomer **9** (0.1 g, 0.15 mmol) was added the catalyst **18** (0.016 g, 0.03 mmol) in benzene (1.0 mL) and stirred for 30 min (polymerization monitored by ^{1}H NMR). The C-glycoside monomer **10** (0.393 g. 0.3 mmol) in 1.0 mL of benzene was added and stirred for 1 hour (polymerization monitored by ^{1}H NMR). Again, O-glycoside monomer **9** (0.100 g, 0.15 mmol) in 1.0 mL of benzene was added and stirred for another 30 min. After the complete conversion, the polymerization was quenched by adding benzaldehyde and stirred for 20 min. The polymer A_5-B_{10}-A_5 was precipitated from cold MeOH. The polymer was collected by centrifugation, purified by column chromatography (30% ethyl acetate in hexanes) and dried in vacuo. The obtained NMR corresponds to poly(9) and poly(10) and is indistinguishable.

IR (neat, cm^{-1}): 1731 ν(CO). **^{1}H NMR** ($CDCl_3$), δ: 7.25 (benzyl protons), 5.52 (C-5, C-6, olefinic protons), 4.86-3.52 (sugar protons), 3.26-1.82 (five-member ring, and C-

glycoside linkage), 1.53-1.35 (isopropylidene). **^{13}C NMR** ($CDCl_3$), δ: 173.9, 173.3 (carbonyl), 139.1-138.8 (benzyl quaternary carbon), 128.1-134.0 (C-5, C-6, olefinic carbon), 128.7, 127.8 (Ar*C*H), 109.8, 109.1 (isopropylidene), 96.6, 74.9-63.8 (sugar group). 52.5-31.0 (five-member ring), 26.4-23.4 (isopropylidene). **GPC**: n = 5, m = 10: M_n(calc.) = 19780; M_n(expt.) = 20050; PDI = 1.12.

2.3.5. Saturated ROMP Polymers

2.3.5.1. Hydrogenation of Isolated Polymers

*Pd-C hydrogenation of norbornene Poly(**9**) made with catalyst **18***

In a representative procedure, poly(**9**) (300 mg), 10% Pd-C (150 mg) and EtOAc (10 mL) were added to a glass-lined autoclave. The reactor was closed, taken out of the glovebox, purged with H_2, pressurized to 500 psi and stirred at room temperature for 24 hours. The solvent was then evaporated and the resulting solid was dissolved in a minimum amount of CH_2Cl_2. The solution was added dropwise to a vigorously stirring cold methanol (~100 mL) and the polymer was obtained as a pale yellow to white precipitate. The polymer was isolated by centrifugation and drying under vacuum.

*Hydrazide hydrogenation of Poly(**9**) made with catalyst **18*** [15-17]

In a representative procedure, poly(**9**) (n=50) (0.9 g, 0.026 mmol) was dissolved in xylenes (30 mL) and *p*-toluenesulphonylhydrazide (0.5 g, 2.6 mmol) was added. The reaction mixture was stirred at 130°C for 3 hours, then allowed to cool to RT. The solution was then added dropwise to ice-cold methanol (~150 mL) to afford the saturated

polymer as a pale yellow to white precipitate. The polymer was isolated by centrifugation, and dried in vacuo.

GPC: n = 10: M_n(calc.) = 6670; M_n(expt.) = 16390; PDI = 1.15, n = 50: M_n(calc.) = 33350; M_n(expt.) = 35310, PDI = 1.14, n = 100: M_n(calc.) = 66700; M_n(expt.) = 86850; PDI = 1.11.

2.3.5.2. "One-pot" ROMP and Hydrogenation

*Use of Catalyst **12** to hydrogenate Poly(**9**) made with catalyst **18***

Representative procedure: To a solution of poly(**9**) (100 mg, 0.9881 mmol) in CH_2Cl_2 (8 mL) in in a glass-lined autoclave was added the Grubbs catalyst **12** (1.2 mg, 0.0015 mmol), NEt_3 (1.1 mg, 0.0110 mmol) and 2 mL of methanol. The reaction mixture was sealed, taken out of the drybox, purged with H_2, pressurized to 500 psi, and stirred at 60°C. The hydrogenation was followed by ^{1}H NMR. After 96 hours the solvent was evaporated and the resulting solid was dissolved in minimum amount of CH_2Cl_2. This solution was added dropwise into vigorously stirred cold methanol (~ 100 mL) to afford a pale yellow precipitate; conversion >95%. Hydrogenation was confirmed by the absence of olefinic peaks at 5.3 ppm.

*Saturated poly(**9**)*

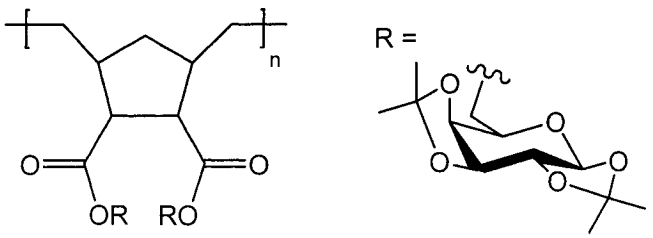

^{1}H NMR ($CDCl_3$), δ: 5.5-5.4 (br) (anomeric carbon proton, *H-1*), 4.6 (br s), 4.4-4.0 (br), 3.9 (br s) (*H-6, H-5, H-4, H-3, H-2,* sugar group protons), 3.2 (br s), 2.8 (br s), 2.2-1.8 (br), 1.6 (br s) (C-1, C-2, C-3, C-4, C-7), 1.5-1.2 (br) (C-5, C-6, methylenes of the polymer backbone), 1.5 (s, 3 H, Me), 1.4 (s, 3 H, Me) 1.3 (s, 6 H, Me) (4(CH_3) acetal). **GPC**: n = 47: M_n(calc.) = 31349; M_n(expt.) = 31660; PDI = 1.13.

2.3.5.3. Tandem ROMP-hydrogenations[18-20]

To a vigorously stirring solution of catalyst **12** (0.003 g, 0.004 mmol) in CH_2Cl_2 (2 mL) a CH_2Cl_2 solution (2 mL) of O-glycoside **9** (0.15 g, 0.23 mmol) was added. After complete ROMP was verified by ^{1}H NMR analysis, the reaction mixture was transferred to a glass-lined autoclave and 12 mL of THF was added as cosolvent. The reactor was taken out of the glovebox, purged with H_2, pressurized to 1000 psi and the reaction mixture was stirred at 60°C. The hydrogenation was monitored by ^{1}H NMR analysis of 1 mL samples taken at 1 hour time intervals. After the reaction was completed the solvent was evaporated and the resulting solid was dissolved in a minimal amount of CH_2Cl_2. This solution was added dropwise to vigorously stirred cold methanol to afford a white to yellow precipitate.

A similar procedure was employed using catalyst **13** and norbornene O-glycoside **9**, norbornene N-hydroxysuccinimide ester **11**, or mixture of those monomers, except that up to 20% of methanol was used as co-solvent. In synthesis of poly(**11**), only 16% of methanol could be used for reasons of solubility. Random copolymers were prepared using 10%, 20% and 40% of **11**. No polymer precipitation was observed when adding 20% methanol. Reaction time for ROMP and hydrogenation using catalyst **13** was much

shorter compared to catalyst **12**, though results vary depending on the catalyst concentration.

(The following polymers were prepared using catalyst **13** in tandem ROMP-hydrogenation).

*Saturated homopolymer of **9***

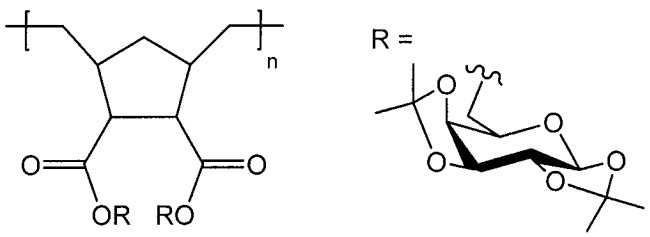

IR (neat, cm^{-1}): 1730 ν(CO). **^{1}H NMR** ($CDCl_3$), δ: 5.5-5.4 (br) (anomeric carbon proton, *H-1*), 4.6 (br s), 4.4-4.0 (br), 3.9 (br s) (*H-6, H-5, H-4, H-3, H-2,* sugar group protons), 3.2 (br s), 2.8 (br s), 2.2-1.8 (br), 1.6 (br s) (C-1, C-2, C-3, C-4, C-7), 1.5-1.2 (br) (C-5, C-6, methylenes of the polymer backbone), 1.5 (s, 3 H, Me), 1.4 (s, 3 H, Me) 1.3 (s, 6 H, Me) (4(CH_3) acetal).

*Saturated homopolymer of **11***

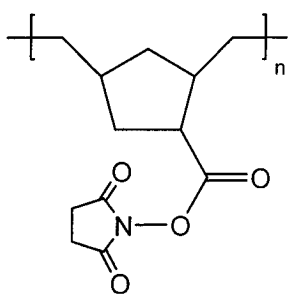

IR (neat, cm^{-1}): 1804, 1778 ν(CO) of the succinimide, 1734 ν(CO). **^{1}H NMR** ($CDCl_3$), δ: 2.8 (br, s) (succinimide protons), 3.2 (br), 2.6-2.5 (br), 2.2 (br), 2.0-1.7 (br), 1.5-1.2 (br) (C-1, C-2, C-3, C-4, C-7, and C-5, C-6, methylenes of the polymer backbone).

*Saturated random copolymer of **9** and **11***

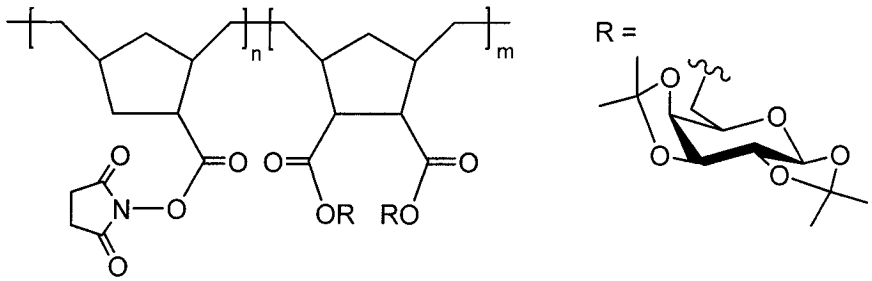

IR (neat, cm^{-1}): 1805, 1778 ν(CO) of the succinimide, 1737 ν(CO). **^{1}H NMR** ($CDCl_3$), δ: 5.5-5.4 (br) (anomeric carbon proton, *H-1*), 4.6 (br s), 4.4-4.0 (br), 3.9 (br s) (*H-6, H-5, H-4, H-3, H-2,* sugar group protons), 3.2 (br s), 2.8 (br s), 2.2-1.8 (br), 1.6 (br s) (C-1, C-2, C-3, C-4, C-7, methylenes of the succinimide), 1.5 (s, 3 H, Me), 1.4 (s, 3 H, Me) 1.3 (s, 6 H, Me) (4(CH_3) acetal), 1.5-1.2 (br) (C-5, C-6, methylenes of the polymer backbone).

2.3.6. Hydrolysis Procedure[9]

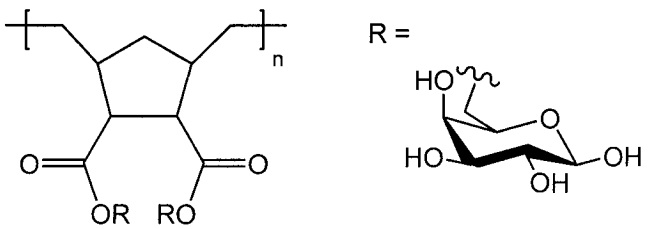

To the acetal-protected poly(**9**) (100 mg), trifluoroacetic acid in H_2O (9/1, v/v, 1 mL) was added and the reaction was stirred for 20 minutes. If the polymer did not completely dissolve, the reaction was stirred for several extra minutes and if necessary more TFA/H_2O was added. The reaction mixture was then added dropwise to vigorously

stirred THF (50 mL) at 0°C resulting in a white precipitate. The polymer was washed with THF (40 mL), Et2O (2 x 40 mL) and hexanes (2 x 40 mL). The white powder was centrifuged and dried under vacuum (25 mm Hg); 78 mg, 89% yield.

IR (neat, cm^{-1}): 3343 ν(OH), 1721 (CO). **^{1}H NMR** ($CDCl_3$), δ: 5.2 (br) (anomeric carbon proton, *H-1*), 4.9-4.6 (OH groups, D_2O exchange), 4.6 (br s), 4.1 (br), 3.7 (br), 3.6 (br) (*H-6, H-5, H-4, H-3, H-2,* sugar group protons), 3.4 (br), 3.2 (br), 2.8 (br), 2.0 (br) (C-1, C-2, C-3, C-4, C-7), 1.3-1.0 (br) (C-5, C-6, methylenes of the polymer backbone).

This hydrolysis procedure was employed for any polymer containing acetal-protected **9**.

2.4. References

1) Giannis, A.; Sandhoff, K. *Tetrahedron Letters* **1985**, *26*, 1479.

2) Arya, P.; Berkley, A.; Randell, K. D. *Journal of Combinatorial Chemistry* **2002**, *4*, 193.

3) Arya, P.; Ben, R.; Qin, H. *Tetrahedron Letters* **1998**, *39*, 6131.

4) Martin, A.; Salazar, J. A.; Suarez, E. *J. Org. Chem.* **1996**, *61*, 3999.

5) Lee, P. S.; Sakai, S.; Honsternmann, P.; Roth, W. R.; Kaller, E. A.; Houk, K. N. *J. Am. Chem. Soc.* **2003**, *125*, 5839.

6) Nelson, W. L.; Freeman, D. S.; Sankar, R. *J. Org. Chem.* **1975**, *20*, 3658.

7) Jacobine, A. F.; Glaser, D. M.; Nakos, S. T. *ACS Polym. Mater. Sci. Eng.* **1989**, *60*, 211.

8) Ripoll, J.; Lasne, M. *Tetrahedron Letters* **1978**, *19*, 5201.

9) Nomura, K.; Schrock, R. R. *Macromolecules* **1996**, *29*, 540.

10) Strong, L. E.; Kiessling, L. L. *J. Am. Chem. Soc.* **1999**, *121*, 6193.

11) Schwab, P.; Grubbs, R. H.; Ziller, J. W. *J. Am. Chem. Soc.* **1996**, *118*, 100.

12) Arduengo, III, A. J.; Krafczyk, R.; Schmutzler, R.; Craig, H. A.; Goerlich, J. *Tetrahedron*, **1999**, *55*, 14523.

13) Scholl, M.; Ding, S.; Lee, C. W.; Grubbs, R. H. *Org. Lett.* **1999**, *1*, 953.

14) Schrock, R. R.; Murdzek, J. S.; Bazan, G. C.; Robbins, J.; DiMare, M.; O'Regan, M. *J. Am. Chem. Soc.* **1990**, *112*, 3875.

15) Edwards, H. G. M.; Farrell, D. W.; Johnson, A. F.; Lewis, I. R.; Ward, N. J.; Webb, N. *Macromolecules* **1992**, *25*, 525.

16) Amir-Ebrahimi, V.; Corry, D. A. K.; Hamilton, J. G.; Rooney, J. J. *Journal of Molecular Catalysis A: Chemical* **1998**, *133*, 115.

17) Kanai, M.; Mortell, K. H.; Kiessling, L. L. *J. Am. Chem. Soc.* **1997**, *119*, 9931.

18) Drouin, S. D.; Yap, G. P. A.; Fogg, D. E. *Inorg. Chem.* **2000**, *39*, 5412.

19) Drouin, S. D.; Zamanian, F.; Fogg, D. E. *Organometallics* **2001**, *20*, 5495.

20) Fogg, D. E.; dos Santos, E. N. *Coordination Chemistry Reviews* **2004**, (Invited contribution: special issue on transition metals in catalysis), accepted.

CHAPTER 3

Synthesis of Monomers and Polymers as Potential Collagen Cross-linking Agents

3.1. Introduction

Well developed methods such as radical, anionic and cationic polymerizations allow large-scale production of materials ranging from highly crystalline to amorphous polymers. Much current interest lies, however, in obtaining materials possessing low polydispersity index (PDI) which these methods do not provide. Powerful and efficient homogeneous catalytic reactions such as ring opening metathesis polymerization (ROMP) give access to narrow-PDI polymer materials.[1,2,3] ROMP via well-defined transition metal catalysts affords polymers with excellent control over both PDI values and polymer block architecture.[1,3] The generally accepted reaction mechanism involves 2+2 cyclo-addition to form a metallacyclobutane intermediate, which then undergoes retro-addition to yield a new propagating unit (Figure 3.1).[4,5] The reaction sequentially repeated results in a growing polymer chain. The initial addition reaction is an equilibrium: it can be shifted in favor of the product by using highly strained cyclic monomers. The reaction is then driven by relief of ring strain, and is essentially irreversible. An example of such a strained monomer is bicyclo[2.2.1]hept-2-ene (norbornene) which upon ring opening releases energy of ~15 kcal/mol.[6] As the electron density and ring strain of the cyclic monomer changes depending on its substituents, different monomers have different rates of initiation, propagation, and termination.[7,8]

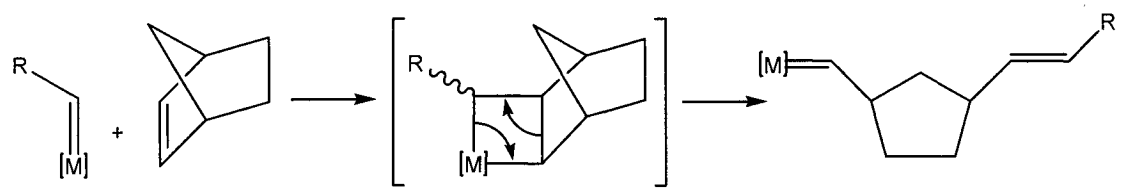

Figure 3.1 Mechanism of ROMP of norbornene.

A wide range of functionalized norbornene monomers is easily accessible via the Diels-Alder reaction. This reaction was discovered by Otto Diels and Kurt Alder in 1928, and won them a Nobel Prize in 1950. This pericyclic reaction involves no intermediates: the mechanism involves movement of electrons around the circle (Figure 3.2).

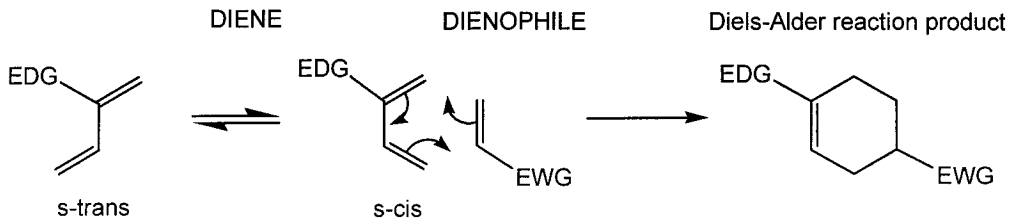

Figure 3.2 The Diels-Alder reaction.

The reaction takes place between a conjugate diene and an alkene, or dienophile. The diene component of the Diels-Alder reaction must have the s-cis conformation in order to position itself close to the alkene and undergo an electron shift, thus forming new bonds. Exceptionally good are cyclic dienes permanently locked in an s-cis conformation, with no equilibrium formation of the energetically favored s-trans conformation. The dienophile must have an electron-withdrawing group conjugated to the alkene. This lowers the LUMO energy of the alkene, resulting in a better orbital overlap with the high-energy HOMO of the electron-rich diene in the transition state. The Diels-Alder reaction

works so well because of the appropriate HOMO and LUMO symmetry overlap of the diene and the dienophile. As the stereochemistry of the reaction is retained, cis and trans dienophiles give different diastereoisomeric products. Enantiomers are obtained in reaction with trans dienophiles (Figure 3.3).[9]

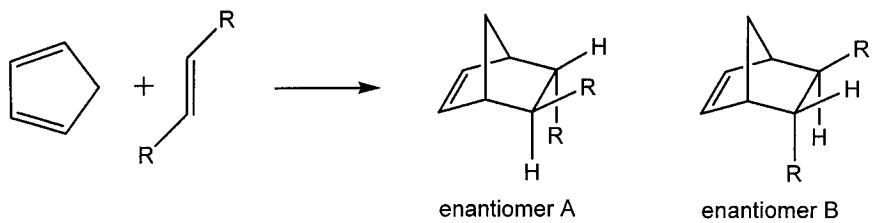

Figure 3.3 The Diels-Alder reaction resulting in mixture of two enantiomers.

In the reaction between cyclic dienes and dienophiles, both exo and endo adducts can be formed, with endo being the kinetic, less energetically stable product, and the exo being the thermodynamic product. The two conformations are easily observed in reaction between cyclopentadiene and maleic anhydride (Figure 3.4). The exo adduct is more stable due to the smaller hindrance between one bridging carbon of the bicyclic ring and the anhydride. The endo adduct and is more readily formed because of the secondary orbital interaction of the C=O groups of the dienophile and the developing π bond at the back of the diene (Figure 3.4).[10]

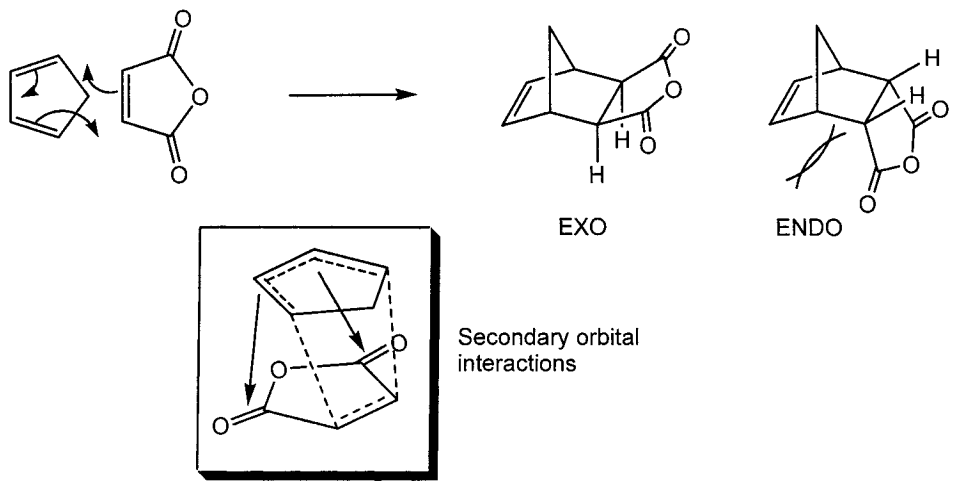

Figure 3.4 Endo/exo conformers of the Diels-Alder reaction.

Norbornene is easily derivatized at positions 2 and 3, and its ROMP polymers thus provide a versatile platform for presentation of functional groups. Of particular interest for tissue engineering purposes, Kiessling *et al.* reported use of glucose-functionalized polynorbornenes and polyoxanorbornenes as cell agglutination inhibitors, while Grubbs used oligopeptide-substituted polynorbornenes to enhance cell adhesion to fibronectin inhibitors.[11,12,13] Norbornene-based ROMP polymers also serve in industrial applications as semiconductors, photoconductors and non-linear optical materials.[14-18] Our interest rests in the possible utility of functionalized ROMP polymers as collagen crosslinking agents. With this in mind, we targeted synthesis of norbornene functionalized with several crosslinking groups.

This chapter describes the synthesis of ROMP monomers and polymers for tissue engineering. The targets are norbornenes functionalized with C-glycoside, O-glycoside, and N-hydroxysuccinimide groups (Figure 3.5). The norbornene O-glycoside and N-hydroxysuccinimide monomers **9** and **11** are known compounds, which were prepared by the literature routes (Figure 3.6). Monomers related to C-glycoside **10** have been previously reported, but in all cases these contain a two-carbon linkage between the norbornene ester or amide groups, and the sugar substituent. In monomer **10**, the linkage is extended to three carbons (Figure 3.5)[19,20] for ease of synthesis.

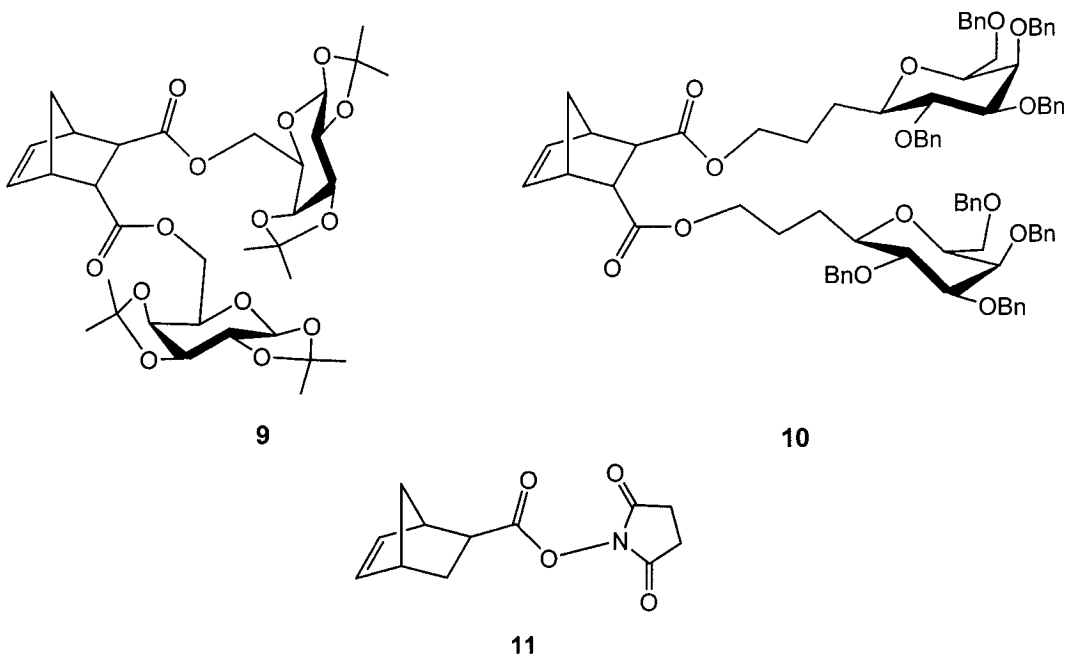

9 **10** **11**

Figure 3.5 Target ROMP-active monomers.

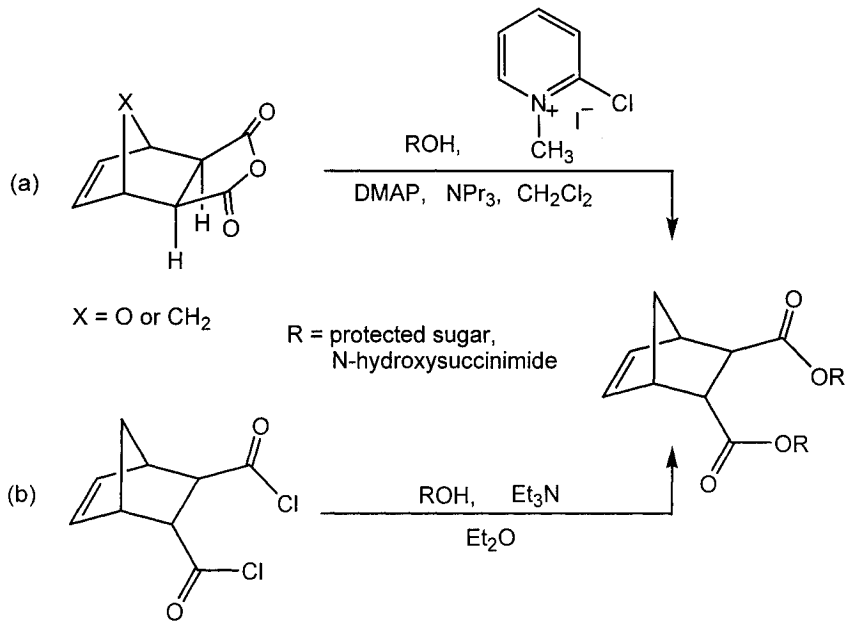

Figure 3.6 Literature routes to sugar functionalized norbornene, (a) utilized by Kiessling *et al.*, (b) utilized by Schrock *et al.* and Grubbs *et al.* [21-23]

The O-glycoside and the N-hydroxysuccinimide groups in **9** and **11** are intended to effect crosslinking of collagen via nucleophilic reaction with the free amine groups of lysine. The C-glycoside monomer is unable to participate in such reactions: instead, it is designed to function as a "linker" group separating two terminal crosslinking blocks: this triblock copolymer may therefore span the gap between collagen lamellae without interfering with lamellar stacking. ROMP of these monomers to give homopolymers and random copolymers is described in the following Sections. Their application in collagen crosslinking by other members of this interdisciplinary research group is reported in the Appendix.

3.2. Monomer Synthesis

Routes to target ROMP monomers utilize the known[24-26] acid chloride norbornene derivatives **7** and **8**. Monomers **6**, **7** and **8** were prepared by the literature procedures in 65-82% yield.[24-27] Dicyclopentadiene was freshly cracked at 170°C to generate cyclopentadiene, which was collected in an ice-cooled round-bottom flask. To a CH_2Cl_2 solution of cyclopentadiene, a solution of dimethyl fumarate in CH_2Cl_2 was added dropwise at 0°C. The reaction began to heat up as more cyclopentadiene was added, as expected for the exothermic Diels-Alder reaction. Once addition was complete, the mixture was allowed to warm to room temperature overnight. The same procedure was used to synthesize acid chlorides **7** and **8** (Figure 3.7) from fumaryl chloride and acryolyl chloride, respectively.

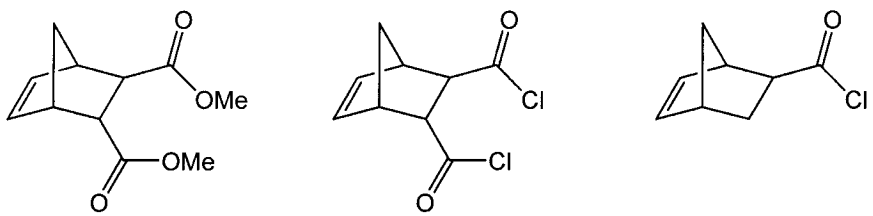

6 **7** **8**

Figure 3.7 ROMP "Test" monomer (**6**) and monomer precursors (**7** and **8**).

Norbornene dimethyl ester **6**, norbornene diacid chloride **7** and norbornene acid chloride **8** were all purified by vacuum distillation. A potential problem during purification of **6** is its spontaneous solidification in the condenser during distillation. In order to avoid problems associated with buildup of pressure in the still apparatus, the condenser was replaced by a short adapter attached to an ice-cooled round-bottom flask.

Carefully distilled **6** was collected as a white solid. This monomer was used only as a test monomer to optimize polymerization conditions, as described in Section 3.3.1.

Characteristic ^{1}H and ^{13}C NMR features common to products **6, 7, 8, 9, 10** and **11** are shown in Figure 3.8. Unique to **6** are methyl signals at 3.6 and 3.4 ppm, which integrate to the expected three protons each. For diacid chloride **7**, the C-7 proton signals appear as a multiplet at 1.6 ppm, while the (mono)acid chloride **8** gives rise to overlapping methylene (C-3 and C-7) signals at 1.91 (1 H), 1.47 (2 H) and 1.29 (1 H) ppm. Assignments for **8** were verified by HMQC and DEPT 135 analysis, and were confirmed by comparison to literature values. [25]

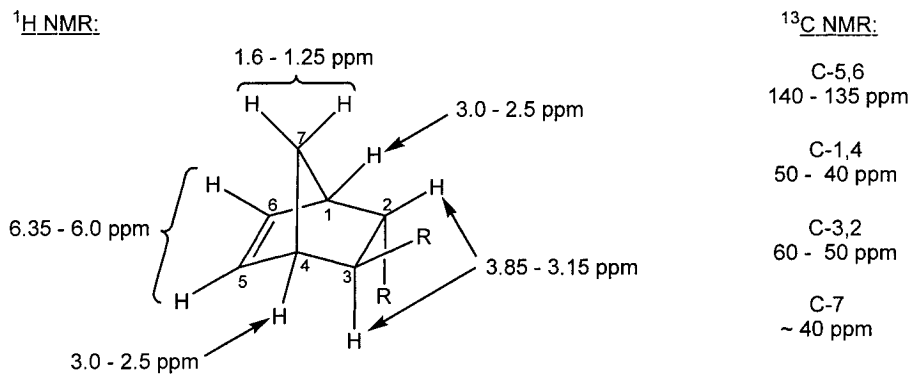

Figure 3.8 Characteristic ^{1}H and ^{13}C NMR values for norbornenes **6 - 11**. While *J* values vary for each compound, most signals appear as multiplets.

3.2.1. Synthesis of O-glycoside Monomer 9

Synthesis of norbornene O-glycoside **9** was accomplished by the literature procedure[22], via dropwise addition of acid chloride **7** to the 1,2;3,4-di-O-isopropylidene-D-galactopyranose in the presence of triethylamine as a proton acceptor.[22] A slight excess (2.1 equiv) of glycoside is used to drive the reaction. The addition was carried out at low

temperature (-78° C), after which the reaction was allowed to warm to room temperature overnight. A white salt of Et_3N•HCl precipitated, but redissolved on aqueous workup. The solution was extracted with ethyl acetate and purified by column chromatography to remove the unreacted 1,2;3,4-di-O-isopropylidene-D-galactopyranose. Flash chromatography was incompletely successful in effecting a clean separation. The product was obtained as a sweet-smelling, colourless, and sticky oil, which could be converted to a free-flowing white powder by prolonged (72 h) drying under vacuum, in ca. 80% yield. The monomer was stored under nitrogen in the drybox at –35 °C, in order to prevent unwanted polymerization.

Characteristic peaks in the ^{1}H NMR spectrum of **9** include overlapping resonances for the anomeric and olefinic protons, at 6.25-6.10 ppm. The methylene signals for the O-CH_2-sugar group overlap with those for the galactose ring, in the range 3.9-4.4 ppm. These data agree with those reported.[22]

3.2.2. Synthesis of C-glycoside Monomer 10

3.2.2.1. Synthesis of the C-glycoside Unit

Synthesis of the C-glycoside monomer **10** requires preparation of the C-glycoside unit shown in Figure 3.9. A route to this monomer was developed by Ranga Reddy of this research group. The synthesis is accomplished over four steps in ca. 25% yield from β-D-galactose pentaacetate. In order to generate the hydroxyl group in the last step of the C-glycoside synthesis, the literature methods utilize an ozonolysis reaction, which requires a special apparatus. We therefore turned to an alternative strategy involving hydroboration, as shown in Figure 3.9.

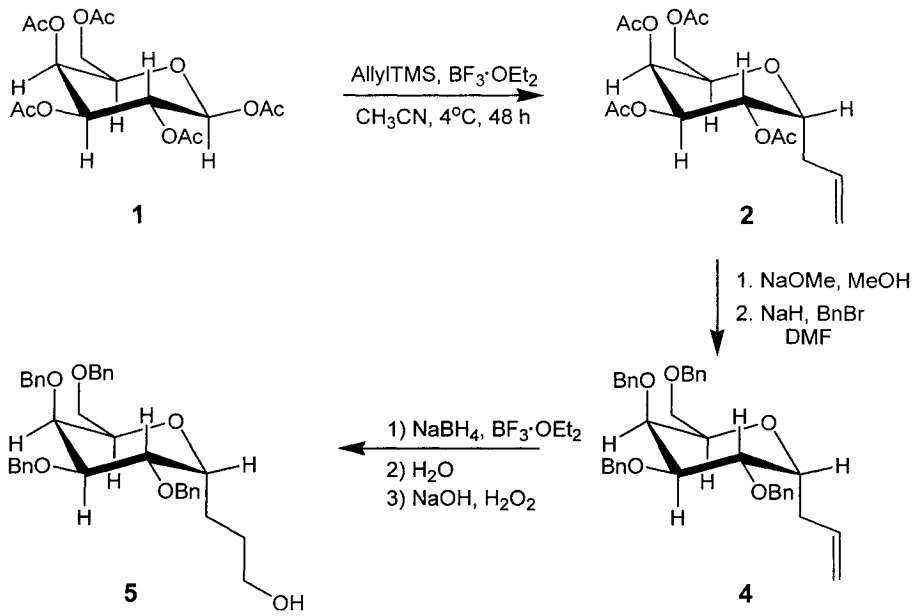

Figure 3.9 Synthesis of C-glycoside.

The allyl functionality was introduced at the C-1 position by treating β-D-galactose pentaacetate **1** with allyl TMS and BF_3 etherate in acetonitrile at 0°C for 48 hours. A yellow-brown product was obtained on quenching the reaction with $NaHCO_3$, extracting with ethyl acetate and purifying by column chromatography. Pure **2** was obtained as a colorless and viscous oil in 50-68% yield. The reaction is selective for substitution at C-1, owing to the anomeric effect.[28-30] The α isomer was obtained in >90% yield, as the combined result of the anomeric effect, the nitrilium effect[31] of the acetonitrile, and the use of low temperatures, which retards the kinetic formation of the β isomer.

From a mechanistic perspective the reaction may proceed via two pathways (Figure 3.10). The first involves (1) BF_3 coordination to acetate at C-1, (2) elimination of the acetate-BF_3 at C-1, with anchimeric assistance through α-coordination of the C-2 acetate, (3) oxonium ion formation (anomeric effect) and (4) reaction of the allyl TMS at

C-1 to form the α anomer. For the second pathway, steps (1) and (2) are unchanged, but are followed by (3) blockage of the β anomeric position by reaction with acetonitrile and (4) SN_2 reaction of the allyl TMS at C-1, again forming the α anomer.

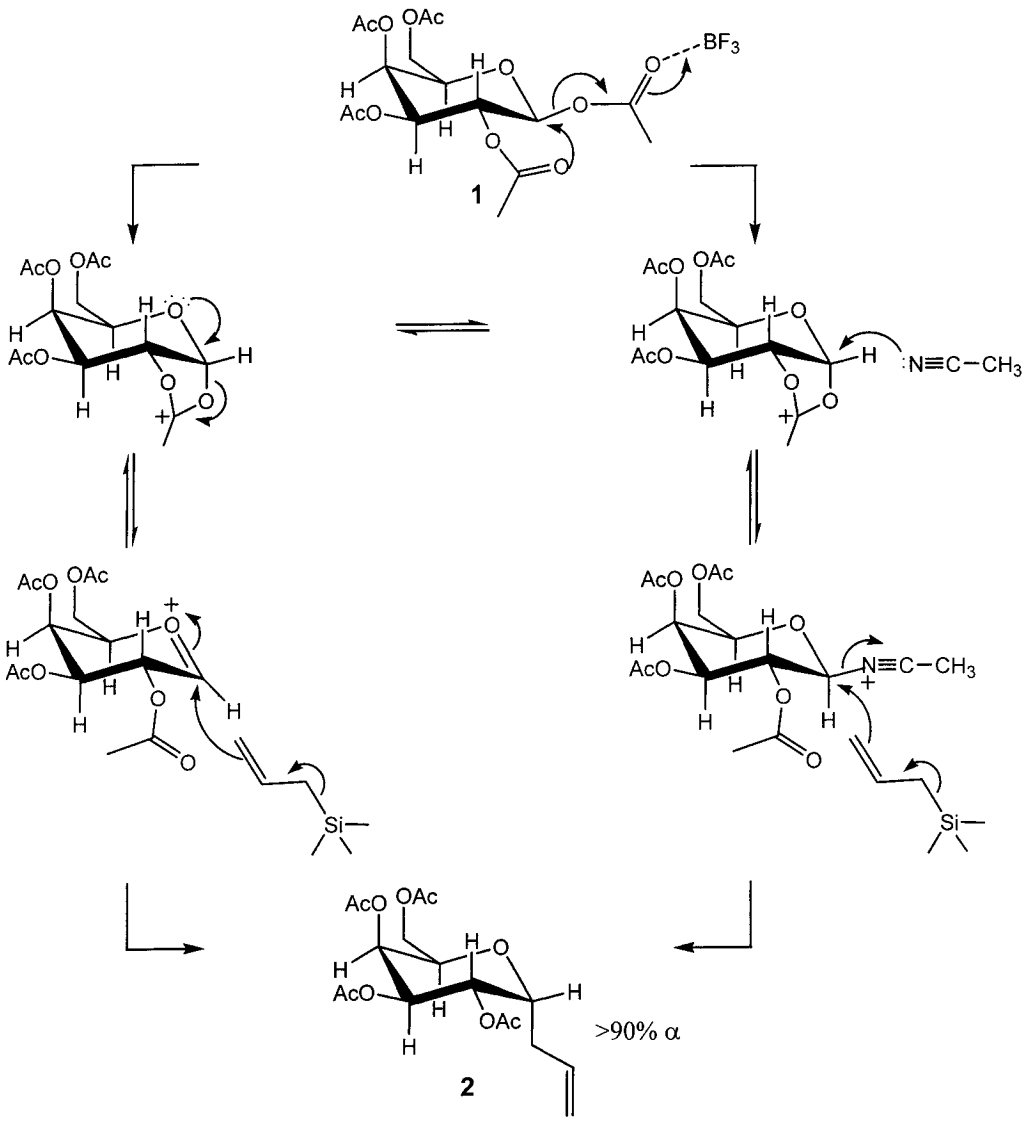

Figure 3.10 Proposed mechanism of anchimeric group participation, anomeric effect and nitrilium effect giving rise to >90% of the α anomer.

The ^{1}H NMR spectrum of **2** revealed multiplets for the vinyl group at 5.8-5.6 (CH=CH_2) and 5.2-5.1 (CH=CH_2) ppm, and resonances for the twelve methyl protons at 2.1-1.8 ppm. The ^{13}C NMR spectrum reveals characteristic olefinic signals at 133.2 (CH=CH_2, β), 133.1 (CH=CH_2, α) and 117.4 (CH=CH_2), 117.1 (CH=CH_2). These NMR values agree with those reported.[32]

In order to carry out subsequent steps of the synthesis, exchange of the acetyl protecting groups for benzyl was necessary. The acetyl groups are prone to enolate and aldol chemistry in the presence of strong bases, which could interfere with the chemistry of interest.[33] Replacement of the protecting groups was performed in two steps. First, the acetyl-protected sugar **2** was deprotected with sodium methoxide (Zemplén reaction) generated in situ by addition of sodium metal to methanol. The deprotected tetrol was isolated by neutralizing the reaction medium with Dowex-50-hydrogen resin, filtering off the resin and stripping off the solvent. ^{1}H NMR analysis confirmed disappearance of the acetyl groups. The benzyl protection was carried out by adding sodium hydride to the (unpurified) product **3** at 0°C in DMF, followed by treatment with benzyl bromide. Large quantities of H_2 were released on addition of the sodium hydride, requiring the addition of further DMF in order to convert the foamy reaction mixture back to solution. After 4 hours of stirring at RT, DMF was removed under vacuum and the reaction was extracted with H_2O and EtOAc. The organic extracts were combined, dried over Na_2SO_4 and the solvent was evaporated. After column chromatography, **4** was obtained as a clear sticky oil in 75 % yield. The identity of the product is supported by ^{1}H NMR analysis. Multiplet for the benzylic phenyl groups appears at 7.5 ppm, which integrates to the expected twenty protons. The ^{13}C NMR spectrum also shows the aromatic singlets for the benzyl

protecting group (127.9-128.9 ppm) and the ipso-carbons of the phenyl ring (139.1 (1 C), 139.0 (2 C) and 138.8 (1 C) ppm). The NMR analysis agrees with the literature values.[34]

The benzyl-protected sugar **4** was converted into a primary alcohol by hydroboration with $NaBH_4$, followed by dropwise addition of BF_3 in dry THF at room temperature. The reaction involves addition of the borane across the double bond to give a trialkyl borane (Figure 3.11). The addition is selective as the boron always adds to the less substituted end of the alkene in anti-Markovnikov fashion, forming the more stable cationic intermediate.[9]

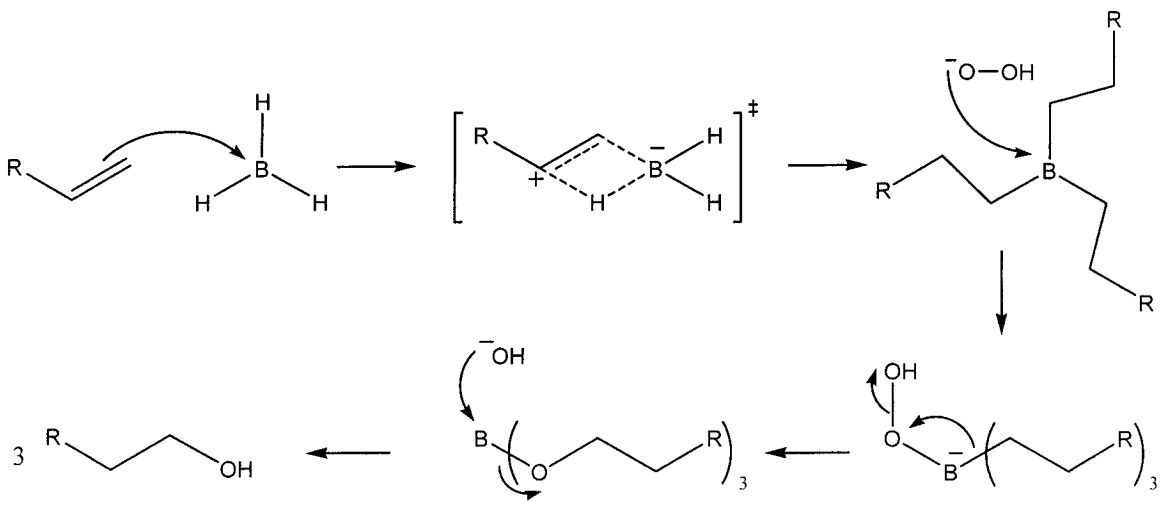

Figure 3.11 Hydroboration following oxidation reaction.

The reaction was heated to 40°C for 1 hour to complete hydroboration. Since organoboranes can be easily converted to alcohols by peroxide oxidation, the intermediate alkylborane was then oxidized by addition of 3N sodium hydroxide and 5 % hydrogen peroxide at 0°C, followed by warming to 50°C. After 1 hour the reaction was cooled, extracted and purified by column chromatography to yield a clear, colorless, semicrystalline sticky oil in 75% yield. ^{1}H and ^{13}C NMR analysis confirmed

disappearance of the vinylic resonances, and the IR spectrum revealed the expected O-H stretching band at 3500 cm^{-1}. ESI-MS analysis confirmed a molecular weight of 582 g/mol (M+1 = 583) consistent with the expected value. NMR values agreed with the literature values.[35]

3.2.2.2. C-glycoside Monomer 10

The C-glycoside monomer **10** was prepared in the same manner as the O-glycoside monomer **9**, except that the C-glycoside building block described above was used instead of 1,2;3,4-di-O-isopropylidene-D-galactopyranose. The reaction yielded 73% of a thick, clear and sticky oil. The product was characterized by ^{1}H NMR analysis, which revealed 40 benzyl-group proton peaks at 7.35 ppm and two olefinic protons at 6.3 and 6.1 ppm. The olefinic and benzyl protecting group carbons give rise to ^{13}C NMR signals at 137.5 and 135.1, and 128.8-127.9 ppm, respectively.[22]

3.2.3. Synthesis of N-hydroxysuccinimide Monomer 11

The N-hydroxysuccinimide monomer **11** was synthesized by dropwise addition of an ethereal solution of **8** to N-hydroxysuccinimide and triethylamine in diethyl ether at -78°C. The mixture was allowed to warm to room temperature overnight, then extracted and purified by column chromatography to yield the product as a white solid in 87% yield. The identity of the product was confirmed by NMR analysis: N-hydroxysuccinimide methylene signals appear at 2.75 ppm (^{1}H NMR) and 25.96 ppm (^{13}C NMR). These assignments are consistent with literature values.[7]

3.3. Synthesis of Polymers

Examples of the two most prominent classes of ROMP catalysts are Schrock's well-known catalyst Mo(N-2,6-i-Pr_2-C_6H_3)(O-*t*-Bu)$_2$($CHCMe_2Ph$) **18**, and the ruthenium complexes shown in Figure 3.12.[36-42] The first of these, $RuCl_2(PCy_3)(L)(CHPh)$ (L = PCy_3), is often referred to as the "Grubbs catalyst". The second (L = N-heterocyclic carbene) was simultaneously reported by the groups of Nolan, Grubbs, and Herrmann, and is often termed a "second generation" catalyst.

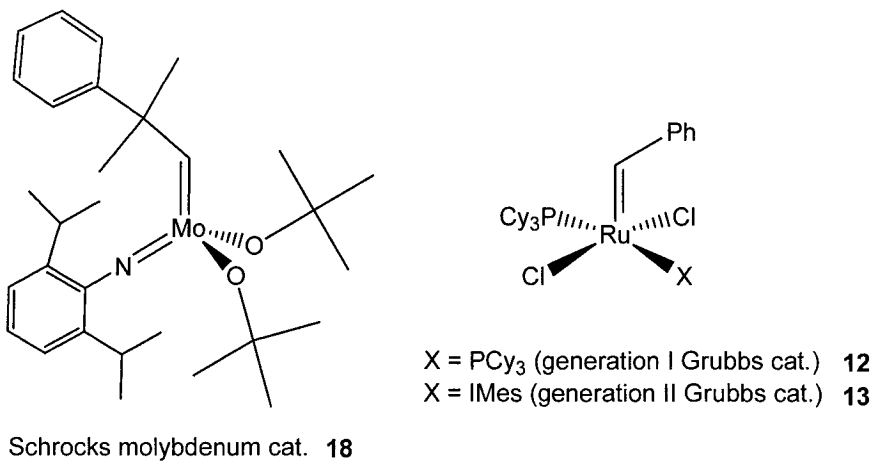

Figure 3.12 Molybdenum and ruthenium metathesis catalysts.

The Mo catalyst can produce polymers with polydispersities as low as 1.04.[22,43] The living nature of Mo polymerizations also allows preparation of block copolymers with specified endgroups, and excellent control over chain lengths and block architecture. A disadvantage to using this catalyst, however, is its sensitivity to even trace amounts (ppm) of water or oxygen, which can cause complete deactivation. Rigorously anhydrous and anaerobic conditions are necessary for successful use of the Mo catalyst. Ruthenium ROMP catalysts, while less active, are much less sensitive to aerial oxidation and

hydrolysis. Kiessling's group has used the ruthenium "Grubbs" catalyst to effect ROMP of norbornenes functionalized with sugars containing free hydroxyl groups,[8,44] though it may be noted that the polydispersity of the product suffers, almost certainly due to decomposition during reaction.

ROMP of monomers **9** and **11** was carried out using Mo complex **18** as an initiator.[32] The sensitivity of this catalyst to water and oxygen often resulted in broadening of PDI values and formation of some high molecular weight polymer, as detected by GPC (Figure 3.13). Water is thought to effect hydrolysis of the Mo-imido functionality, resulting in a short-lived but very active species that produces high molecular weight polymer. Contamination by oxygen gives rise to GPC peak at double the expected molecular weight, owing to polymer dimerization (Figure 3.14).

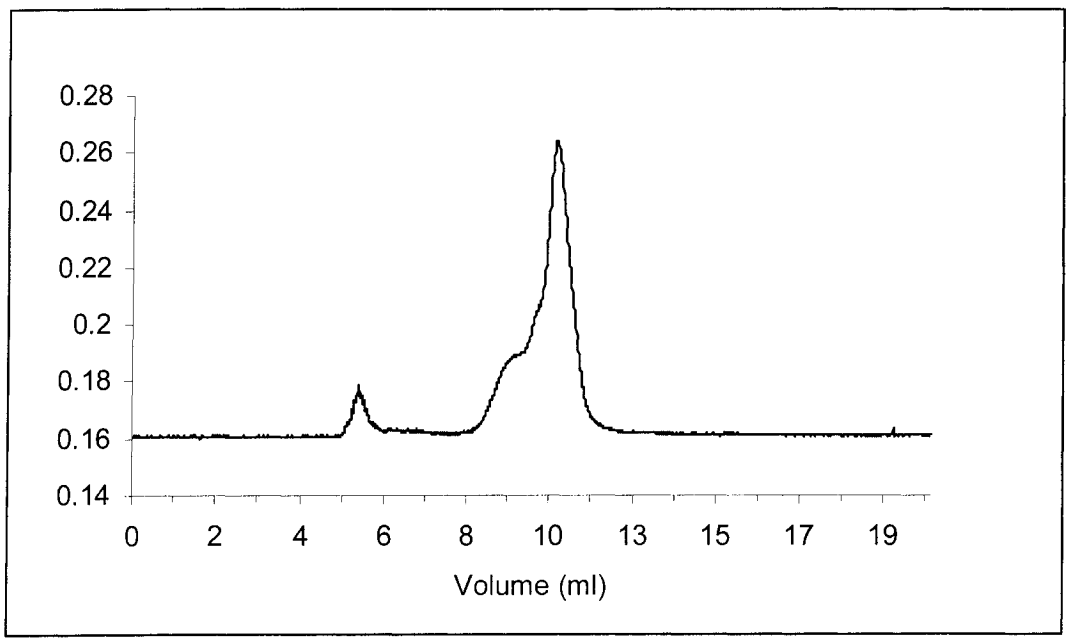

Figure 3.13 GPC spectrum showing "extra" peaks resulting from the presence of water (elution volume 5.5 mL), and oxygen (shoulder at elution volume 9 mL).

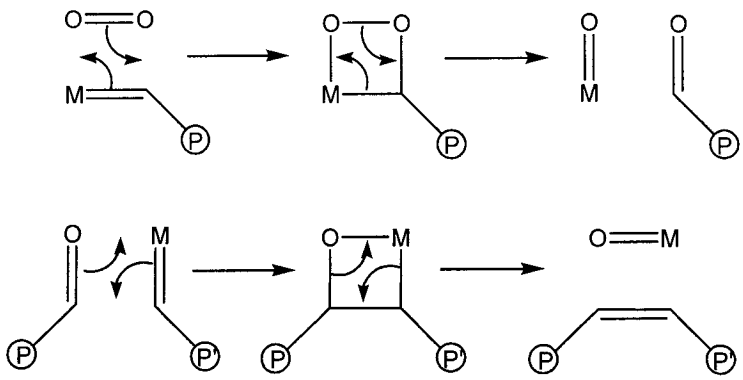

Figure 3.14 Generation of double molecular weight polymer by reaction with oxygen.

3.3.1. Use of "Test" Monomer to Optimize ROMP Conditions

In order to limit waste of the monomers of interest, all ROMP syntheses were preceded by a "test" polymerization using the inexpensive and easily synthesized dimethyl ester of norbornene. Prior to polymerization, glovebox detectors were checked to ensure that concentrations of O_2 and H_2O were below 0.5 ppm. Elevated levels were lowered by 20 minutes of N_2 purging, followed by switching the glovebox to circulation mode for approximately 1 hour. The polymerization solvent was checked by addition of one drop of a THF solution of sodium benzophenone ketyl to 5 mL of solvent. A change of color from purple to yellow indicated the presence of oxygen. Where these tests were satisfactory, the test polymerization was performed. Where the GPC spectrum was satisfactory, ROMP of the sugar or N-hydroxysuccinimide monomers was carried out. If polymerization was unsuccessful, the catalyst was purified by recrystallization, or, if necessary, the benzaldehyde used to terminate ROMP (see next section) was distilled and degassed.

3.3.2. Synthesis of Polynorbornenes Bearing Crosslinking Groups

Homopolymers of O-glycoside monomer **9** were prepared in benzene by adding *n* equivalents of the monomer to a rapidly-stirring solution of the initiator (Table 3.1).[23] The reaction was quenched by addition of benzaldehyde to cleave the polymers from the metal in a Wittig-like reaction.[4,5] The reaction mixture was then concentrated and the polymer precipitated by dropwise addition to ice-cold methanol. The pale yellow polymer was collected by centrifugation. Yields are limited to ca. 90% by the partial solubility of the sugar-functionalized polymers in methanol. The polymer products showed a satisfactory degree of polymerization (d.p.). Values of 18, 52 and 145 were determined by GPC: calculated d.p. values were 10, 50, and 100. The discrepancy is probably due to errors in catalyst weighing, as the reactions were carried out on a small scale (1-5 mg catalyst). Catalyst deactivation during the reaction may also be a contributor; however, this would result in higher molecular weight products and slightly broader polydispersities. The identity of the products was supported by ^{1}H NMR analysis, which shows the diagnostic upfield shift in the olefinic signals (from 6.25-6.10 ppm in the monomers, to 5.5-5.2 ppm in the ring-opened products).

Table 3.1 ROMP of norbornene O-glycoside using Mo catalyst **18**.[a]

Entry	Equiv.	M_n(calc.)	M_n(expt.)	PDI
1	10	6 670	12 320	1.06
2	50	33 350	35 090	1.08
3	100	66 700	97 360	1.08

[a] ROMP was carried out in 8 mL CH_2Cl_2; reaction was complete in 1 hour.

A triblock polymer, poly(**9**)$_5$(**10**)$_{10}$(**9**)$_5$ was synthesized via **18**, by sequential addition of each monomer. The consumption of the monomer was followed by ^{1}H NMR analysis, following which another monomer was added. Time to complete polymerization of poly(**9**)$_5$ was determined to be 30 min, and that of poly(**10**)$_{10}$ 1 hour. The polymer was isolated by precipitation. The obtained molecular weight (M_n(expt.) = 20050) closely corresponded to the calculated value (M_n(calc.) = 19780). PDI value of the triblock was determined to be 1.11, which is very narrow for such procedure.

A homopolymer of the N-hydroxysuccinimide monomer **11** was synthesized by rapid addition of **11** in benzene to a benzene solution of catalyst **18**. ROMP was complete in 45 min, as judged by ^{1}H NMR analysis. The polymer was isolated as a pale yellow powder by precipitation from methanol and centrifuging, as before. However, the polymer was insoluble in water. This precludes its use as a crosslinking agent, given that the collagen crosslinking reaction is carried out in an aqueous medium.

In the hope of obtaining water-soluble polymers, we turned to copolymerization of the non-polar monomer **11** with polar O-glycoside monomer **9**. A random copolymer was synthesized in quantitative yield by ROMP of these monomers in 1:5 ratio. The presence of both repeat units was verified by IR analysis, which revealed the succinimide ν(C=O) stretching bands at 1804 and 1778 cm^{-1}, accompanied by an ester stretching band at 1737 cm^{-1}. The ^{1}H NMR spectrum was less informative, owing to overlap of both the olefinic and the aliphatic peaks. The unique, sharp singlet due to the succinimide methylene group is apparent, however, at 2.8 ppm. Satisfactory ^{13}C NMR spectra could not be obtained because of low solubility.

3.4. Conclusions

The forgoing described the successful syntheses of ROMP monomers **9**, **10**, and **11**. Their preparation is accomplished via functionalization of norbornene acid chlorides. Synthesis of **10** required preparation of the C-glycoside which was accomplished in four steps through allylation, protecting group exchange, and hydroboration reactions.

Highly active but very sensitive catalyst **18** was used to polymerize monomers **9**, **10** and **11**, giving homopolymers with narrow polydispersities (1.06-1.08). Synthesis of triblock copolymer incorporating **9** and **10** was successful. Narrow molecular weight distribution (PDI = 1.11) was obtain which corresponded to the calculated value (M_n(expt.) = 20050, M_n(calc.) = 19780). As the poor solubility of poly(**11**) in water limits its utility for collagen crosslinking, synthesis of random copolymers of **9** and **11** was also undertaken. Deprotection of the O-glycoside groups, as well as reduction of these unsaturated polymers, is described in Chapter 4.

3.5. References

1) Recent reviews: (a) Trnka, T. M.; Grubbs, R. H. *Acc. Chem. Res.* 2001, *34*, 18. (b) Fürstner, A. *Angew. Chem. Int. Ed.* 2000, *39*, 3012. (c) Schrock, R. R. *Tetrahedron,* 1999, *55*, 8141. (d) Buchmeiser, M. R. *Chem. Rev.* 2000, *100*, 1565.

2) Conrad, J. C.; Amoroso, D.; Czechura, P.; Yap, G. P. A.; Fogg, D. E. *Organometallics* 2003, *22*, 3634.

3) For recent reviews on olefin metathesis, see: (a) Barrett, A. G. M.; Hopkins, B. T.; Köbberling, J. *Chem. Rev.* 2002, *102*, 3301. (b) Frenzel, U.; Nuyken, O. *J. Polym. Sci. Part A: Polym. Chem.* 2002, *40*, 2895. (c) Trnka, T. M.; Grubbs, R. H. *Acc. Chem. Res.* 2001, *34*, 18. (d) Dragutan, V.; Dragutan, I. *Platinum Metals Rev.* 2001, *45*, 155. (e) Buchmeiser, M. R. *Chem. Rev.* 2000, *100*, 1565.(f) Fürstner, A. *Angew. Chem. Int. Ed.* 2000, *39*, 3012. (g) Schuster, M.; Blechert, S. *Angew. Chem. Int. Ed. Engl.* 1997, *36*, 2036. (h) Armstrong, S. K. *J. Chem. Soc., Perkin Trans. 1* 1998, 371.

4) Herisson, J.-L.; Chauvin, Y. *Makromol. Chem.* 1971, *141*, 161.

5) Sanford, M. S.; Ulman, M.; Grubbs, R. H. *J. Am. Chem. Soc.* 2001, *123*, 749.

6) Adlhart, C.; Chen, P. *J. Am. Chem. Soc.* 2004, *126*, 3496.

7) Strong, L. E.; Kiessling, L. L. *J. Am. Chem. Soc.* 1999, *121*, 6193.

8) Kanai, M.; Mortell, K. H.; Kiessling, L. L. *J. Am. Chem. Soc.* 1997, *119*, 9931.

9) Clayden, J.; Greeves, N.; Stuart, W.; Wothers, P. *Organic Chemistry*; Oxford University Press: New York, 2001.

10) Vollhardt, K. P. C.; Schore, N. E. *Organic Chemistry: Structure and Function*; 4th ed.; W. H. Freeman and Company: New York, 2002.

11) Mann, D. A.; Kanai, M.; Maly, D. J.; Kiessling, L. L. *J. Am. Chem. Soc.* 1998, *120*, 10575.

12) Schuster, M. C.; Mortell, K. H.; Hegeman, A. D.; Kiessling, L. L. *Journal of Molecular Catalysis A: Chemical* 1997, *116*, 209.

13) Maynard, H. D.; Okada, S. O.; Grubbs, R. H. *J. Am. Chem. Soc.* 2001, *123*, 1275.

14) Fogg, D. E.; Radzilowski, L. H.; Balinski, R.; Schrock, R. R.; Thomas, E. L. *Macromolecules* 1997, *30*, 417.

15) Weck, M.; Mohr, B.; Bob, M. R.; Grubbs, R. H. *Macromolecules* 1997, *30*, 6430.

16) Kim, S.; Lee, H.; Jin, S.; Cho, H.; Choi, S. *Macromolecules* 1993, *26*, 846.

17) (a)Yamamoto, Y. S., Tadahiro; Takao, T.; Ikeda, K.; Fukuda, T. Japan. Patent 2001027803, 2001. (b) Sunaga, T.; Okita, M.; Asanuma, T. U.S. Patent 6,197,894, 2001. (c) Kamijima, T.; Otsuki, T. Japan. Patent 2001064367, 2001. (d) Bansleben, D. A.; Huynh-Tran, T.-C.; Blanski, R. L.; Hughes, P. A.; Roberts, W. P.; Grubbs, R. H.; Hatfield, G. R. PCT Int. Appl. WO 2000018579, 2000. (e) Suzuki, T.; Obuchi, K.; Tokoro, M. Japan. Patent 11130846, 1999. (f) Sekiguchi, M.; Otsuki, T.; Ishigaki, T. Japan. Patent 2001031744, 2001. (g) Murakami, T.; Tada, M.; Tsunogae, Y. U.S. Patent 5,905,129, 1999. (h) Chen, Y.; Dujardin, R.; Bruder, F.-K.; Rechner, J. U.S. Patent 5,990,246, 1999.

18) Kohara, T. *Macromol. Symp.* 1996, *101*, 571.

19) Mortell, K. H.; Gingras, M.; Kiessling, L. L. *J. Am. Chem. Soc.* 1994, *116*, 12053.

20) Weatherman, R. V.; Mortell, K. H.; Chervenak, M.; Kiessling, L. L.; Toone, E. J. *Biochemistry* 1996, *35*, 3619.

21) Mortell, K. H.; Weatherman, R. V.; Kiessling, L. L. *J. Am. Chem. Soc.* 1996, *118*, 2297.

22) Nomura, K.; Schrock, R. R. *Macromolecules* 1996, *29*, 540.

23) Fraser, C.; Grubbs, R. H. *Macromolecules* 1995, *28*, 7248.

24) Nelson, W. L.; Freeman, D. S.; Sankar, R. *J. Org. Chem.* 1975, *20*, 3658.

25) Jacobine, A. F.; Glaser, D. M.; Nakos, S. T. *ACS Polym. Mater. Sci. Eng.* 1989, *60*, 211.

26) Ripoll, J.; Lasne, M. *Tetrahedron Letters* 1978, *19*, 5201.

27) Arjona, O.; Fernandez de la Pradilla, R.; Plumet, J.; Viso, A. *J. Org. Chem.* 1991, *56*, 6227.

28) Ellervik, U.; Magnusson, G. *Tetrahedron Letters* 1997, *38*, 1627.

29) Herzig, J.; Hudelman, A.; Gottlieb, H. E.; Fischer, B. *J. Org. Chem.* 1986, *51*, 727.

30) Lemieux, R. U.; Hendriks, K. B.; Stick, R. V.; James, K. *J. Am. Chem. Soc.* 1975, *97*, 4056.

31) Braccini, I.; Derouet, C.; Esnault, J.; de Penhoat, C. H.; Mallet, J. M.; Michon, V.; Sinay, P. *Carbohydrate Research* 1993, *246*, 23.

32) Giannis, A.; Sandhoff, K. *Tetrahedron Letters* 1985, *26*, 1479.

33) Carey, F. A.; Sundberg, R. J. *Advanced Organic Chemistry, Part A: Structure and Mechanisms*; Plenum Press: New York, 1990; Vol. 3rd.

34) Arya, P.; Berkley, A.; Randell, K. D. *Journal of Combinatorial Chemistry* 2002, *4*, 193.

35) Wellner, E.; Gustafsson, T.; Backlund, J.; Holmadahl, R.; Kihlberg, J. *ChemBioChem* 2000, *1*, 272.

36) Schrock, R. R.; Murdzek, J. S.; Bazan, G. C.; Robbins, J.; DiMare, M.; O'Regan, M. *J. Am. Chem. Soc.* 1990, *112*, 3875.

37) Lynn, D. M.; Kanaoka, S.; Grubbs, R. H. *J. Am. Chem. Soc.* 1996, *118*, 784.

38) Arduengo, A. J.; Dias, H. V. R.; Harlow, R. L.; Kline, M. *J. Am. Chem. Soc.* 1992, *114*, 5530.

39) Arduengo III, A. J.; Davidson, F.; Dias, H. V. R.; Goerlich, J. R.; Khasnis, D.; Marshall, W. J.; Prakasha, T. K. *J. Am. Chem. Soc.* 1997, *119*, 12742.

40) Schwab, P.; Grubbs, R. H.; Ziller, J. W. *J. Am. Chem. Soc.* 1996, *118*, 100.

41) Scholl, M.; Ding, S.; Lee, C. W.; Grubbs, R. H. *Org. Lett.* 1999, *1*, 953.

42) Scholl, M.; Trnka, T. M.; Morgan, J. P.; Grubbs, R. H. *Tetrahedron Lett.* 1999, *40*, 2247.

43) Schrock, R. R. *Acc. Chem. Res.* 1990, *23*, 158.

CHAPTER 4

Synthesis of Saturated Neoglycopolymers via "One-pot" or Tandem ROMP-hydrogenation

4.1. Introduction

4.1.1. Polymer Degradation

In order to obtain water-soluble polymers suitable for crosslinking, it was necessary to deprotect the glycopolymers of Chapter 3. As this Chapter will demonstrate, polymer hydrogenation was also essential in order to obtain polymers that were less prone to degradation by intermolecular crosslinking or oxidative degradation. The latter processes can cause significant alterations in the physical properties of unsaturated polymers.[1,2] Intermolecular crosslinking, with formation of new bonds between individual macromolecules, leads to uncontrolled increases in polymer chain length and microstructure: in the extreme, it can lead to new superstructures.[3] Such alterations would seriously hamper development of structure-property correlations for the ROMP polymers used to crosslink collagen, and could also result in deterioration of the composites in vivo. It should be recognized that the ROMP polymers are particularly susceptible to intermolecular crosslinking owing to the unsaturated present in the polymer backbone. Oxidation of the double bonds, leading to hydroperoxides, can likewise initiate a radical chain reaction which can be terminated by radical coupling reactions. In order to prevent such reactions, we found that it was essential to store the ROMP polymers under inert atmosphere at low temperatures.[4]

In order to quantify the degradation problems, we undertook an in situ IR spectroscopic analysis. In this experiment, a KBr pellet containing finely-dispersed polymer (200 mg KBr/20 mg polymer) was heated at 60°C, and IR spectra were recorded every 15 minutes for 4 hours (Figure 4.1). The integrated intensity of the C=O and C=C stretching bands was then plotted as a function of time (Figure 4.2). Degradation of the functional group is inferred from a loss of integrated intensity.

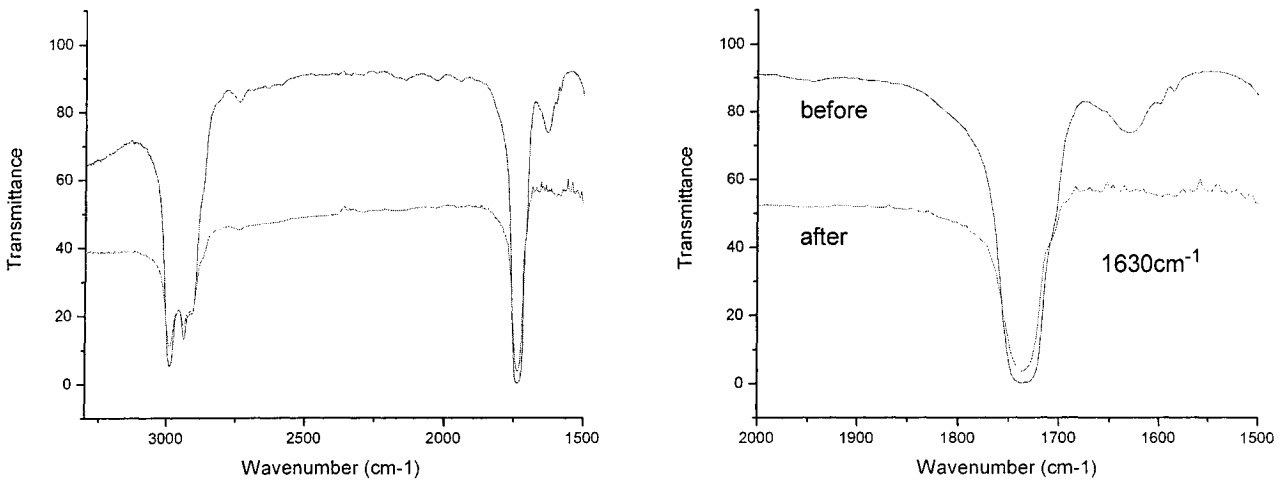

Figure 4.1 Change in intensity of infrared ν(C=C) band (1630-1650 cm^{-1}) in poly(**9**) (O-glycoside homopolymer). KBr pellet monitored over 4 hours at 60°C.

This analysis revealed essentially no change in the intensity of the ν(C=O) band, while the ν(C=C) band dramatically decreased in intensity over the first hour, and continued to decrease throughout the experiment. Similar effects are found at room temperature over longer periods of time.

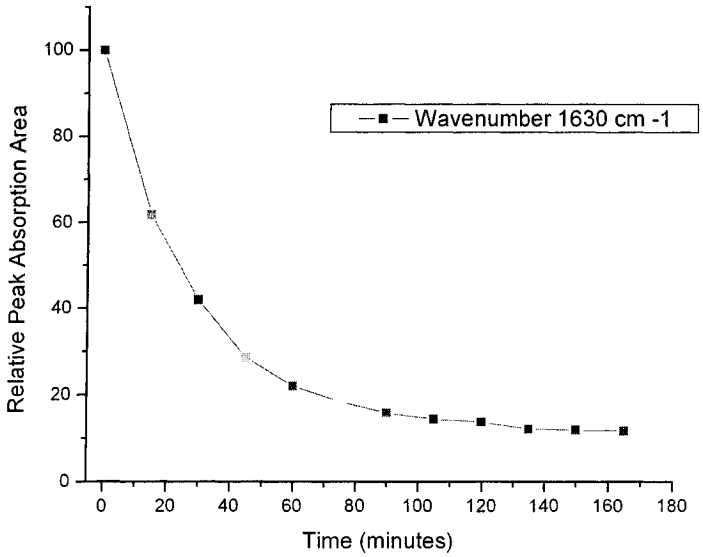

Figure 4.2 Thermal degradation of C=C double bonds at 60°C. Decrease of IR ν(C=C) stretching band with time.

Degradation of the polymers may also result from reaction of the pendant glycoside groups. While the protected sugars are not anticipated to cause problems, unwanted side-reactions may occur under the acidic conditions required to deprotect the acetal groups.[5] The reaction time must be limited in order to minimize such reactions. For example, sugars are known to dimerize under acidic conditions, and prolonged hydrolysis time could thus lead to crosslinking.[6]

4.1.2. Solutions to Polymer Degradation

In order to overcome degradation issues two solutions can be considered: addition of antioxidants, or hydrogenation.[4] Antioxidants function as radical scavengers, interfering with free radical reactions that lead to incorporation of oxygen into

macromolecules by inhibiting or retarding formation of hydroperoxides which initiate radical chain reactions. Various types of stabilizers have been reported, which function in different ways. An example is a stabilizer XH such as butylated hydroxytoluene (BHT) or diphenylamine,[3] which competes with the polymer to donate hydrogen atoms to the free radical (Eqn.1). This generates an unreactive free radical X• which is incapable of propagating the chain reaction. We rejected this approach, however, out of concern that these molecular antioxidizing agents could trigger unwanted reactions (in vivo) in the corneal implants. Instead, we turned to hydrogenation of the ROMP polymers.

$$ROO\bullet + HX \longrightarrow ROOH + X\bullet \qquad (1)$$

Hydrogenation of internal olefins is a challenging problem. Polymeric olefins are particularly problematic, since polymers are by their nature exceptionally bulky, and issues of diffusion control also make it difficult for the catalyst to reach the unsaturated sites. Especially resistant to reduction are polymers such as those formed in Chapter 3, with a predominance of trans olefinic groups in the polymer backbone.[7,8]

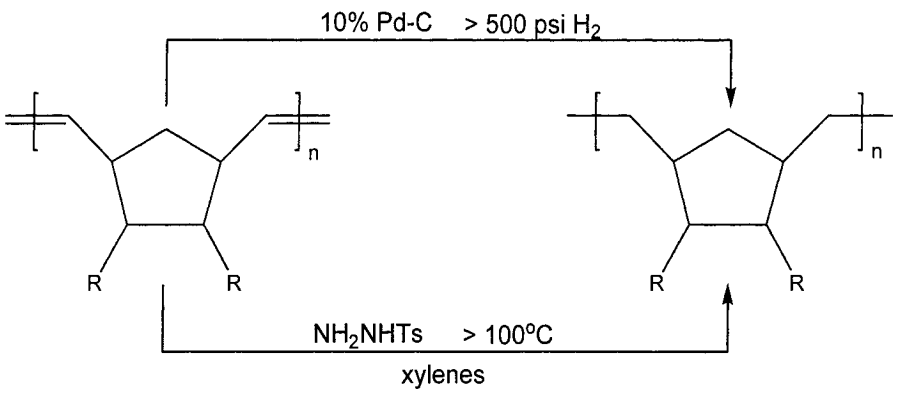

Figure 4.3 Conventional hydrogenation methods of unsaturated polymers.

Two widely used polymer hydrogenation methods make use of Pd-C and hydrazide as reducing agents.[9-12] These methods work well in reduction of the olefins present in small organic molecules, but may be less successful in polymer hydrogenation. Unwanted reactions may result if forcing reaction conditions are required. Hydrogenation via diimide, for example, can be accompanied by side reactions in which the tosyl hydrazide fragment functionalizes the polymer chains (Figure 4.4).[13] Pd-C hydrogenation of polymers can show low activity and long reaction times[17] if the surface of the heterogeneous palladium particles has difficulty in approaching the unsaturated sites.[9] If these reaction require elevated temperatures (100-130°C), [14-16] polymer crosslinking may also be competitive with reduction.

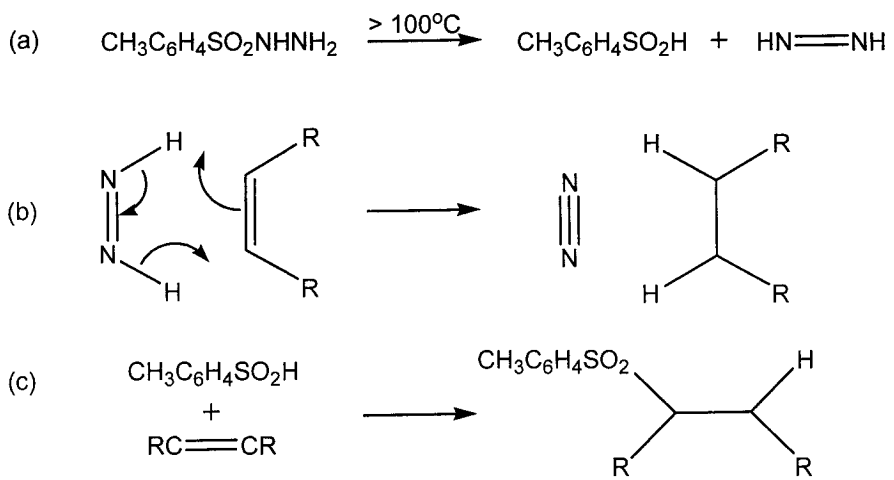

Figure 4.4 Hydrogenation via p-toluenesulfonyl hydrazide: (a) chemical decomposition to hydrogenation-active diimide, (b) reaction mechanism, (c) unwanted tosylation.

Homogeneous hydrogenation may be preferred for polymer reduction, as soluble catalysts can access the unsaturated sites much more easily than heterogeneous catalysts.[18] An alternative route to saturated ROMP polymers involves hydrogenation via

the Grubbs catalyst **12** (Figure 4.5), using a protocol developed and patented by the Fogg group.[19-23] While homogeneous nickel and rhodium catalyst also promote reduction of ROMP polymers, forcing conditions are required (100-135°C and 300 psi).[24] Milder conditions are possible using **12**. Optimized conditions involve use of mixed CH_2Cl_2 - MeOH solvent systems,[22] in which methanol functions as a source of CO, aiding transformation of **12** into a highly active hydridocarbonyl catalyst **21** (Figure 4.5). High activity requires use of amine base in excess, probably owing to chlorination of the metal hydride by CH_2Cl_2. [22]

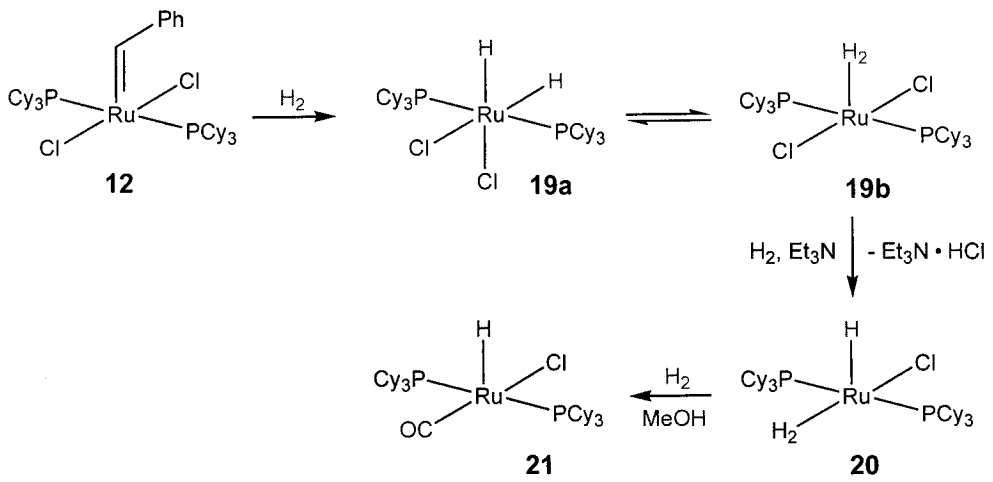

Figure 4.5 Formation of hydrogenation-active species by hydrogenolysis of $RuCl_2(PCy_3)_2(CHPh)$ in presence of CH_2Cl_2:MeOH (80/20%) and Et_3N under 1000 psi H_2. [21]

The Ru catalyst **12** is, of course, much more commonly used as a ROMP initiator.[25-27] Indeed, earlier work from our group demonstrated the utility of **12** in effecting sequential processes of ROMP and hydrogenation of simple monomers such as cyclooctene and norbornene (Figure 4.6). The utility of this approach for synthesis of

more challenging targets, such as the saturated sugar polymers, is thus of interest. Such "tandem catalysis" processes involve a single catalytic precursor that first effects ROMP, and then hydrogenation.[21-23,28] Attractive features of the tandem catalysis approach are the fact that no intermediates need to be isolated: hence there is no need to quench the reaction, or to precipitate or purify the unsaturated polymers.[29] PDI values obtained by Ru ROMP are generally rather broader then those obtained using Mo catalysis (via **18**), but the lower air- and water-sensitivity of the ruthenium catalyst means that formation of very high-molecular weight and double-molecular weight materials is minimized.

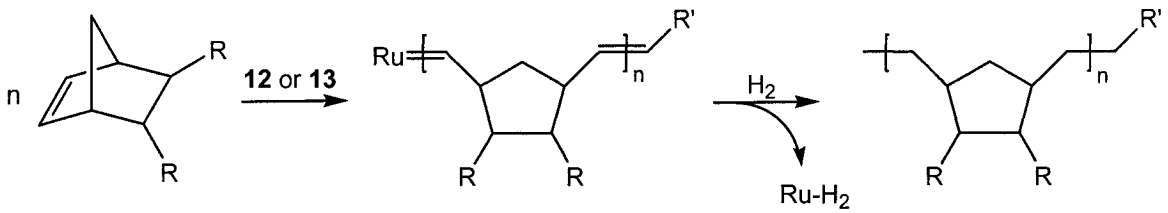

12 = $RuCl_2(PCy_3)_2(CHPh)$
13 = $RuCl_2(PCy_3)(IMES)(CHPh)$

Figure 4.6 Tandem catalytic ROMP-hydrogenation of norbornene monomers.

This chapter describes an investigation of the Pd-C and hydrazide hydrogenation, as well as "one-pot" or tandem homogeneous hydrogenation via **12** and **13**. The latter methods allow efficient synthesis of saturated polymers via tandem ROMP-hydrogenation.

4.2. Hydrogenation of O-glycoside Homopolymer, Poly(9)

4.2.1. Pd-C Hydrogenation

Hydrogenation of the O-glycoside homopolymer using 10% Pd-C was completed within 24 hours at 500 psi and RT, but very high catalyst loadings (50% by weight or larger) were necessary. Use of lower loadings resulted in incomplete hydrogenation even after 72 hours. After hydrogenation was complete (as deduced by disappearance of the olefinic signal at 5.3 ppm in the ^{1}H NMR spectrum), the reaction solution was concentrated and filtered though packed Celite, then silica, to remove Pd. The solution appeared gray even after three filtrations, presumably owing to contamination by Pd residues leached off the carbon support into solution. Reprecipitation of the filtered and concentrated reaction mixture by addition to cold methanol resulted in a grayish material even after three purification cycles. This is a concern, as the presence of Pd could raise toxicity levels in the crosslinked collagen composite. Alternative hydrogenation routes were therefore explored.

4.2.2. Diimide Hydrogenation

Stochiometric reduction of poly(**9**) with tosyl hydrazide gave the reduced product in quantitative yields[13,15] within 3 h at 130°C. Again, hydrogenation was confirmed by loss of the olefinic peak at 5.3 ppm in the NMR spectrum. While the reaction has minimal effect on the average molecular weight, the PDI values change significantly (Table 4.1), presumably because some crosslinking occurs under the forcing conditions.

Table 4.1 Comparison of PDI and M_n of poly(**9**) before and after diimide hydrogenation.

Expected d.p.	Before hydrogenation		After hydrogenation	
	M_n (d.p.)	PDI	M_n (d.p.)	PDI
10	12320 (18)	1.06	16390 (25)	1.15
50	35090 (53)	1.08	35310 (53)	1.14
100	97360 (146)	1.08	86850 (130)	1.11

4.2.3. "One-pot" Homogeneous Hydrogenation

4.2.3.1. "One-pot" ROMP-Hydrogenation Using Catalyst 12

"One-pot" homogeneous hydrogenation was applied to reduction of ROMP polymers prepared via Mo initiator **18**. Despite some possibility of polymer cross-metathesis, catalyst **12** was used as the precursor for the hydrogenation-active species, as indicated in Figure 4.5. Hydrogenation was carried out with a substrate:catalyst ratio of 100:1 equivalents, in the presence of excess base (15 equiv. NEt_3), as well as 20% methanol by volume. Hydrogen pressures of 500 psi were used, and the reaction was carried out at 60°C. The reaction was complete after 96 hours (^{1}H NMR analysis), though it must be noted that this is a maximum figure, as samples were not taken at shorter reaction times. The satisfactory results, however, led us to explore more efficient procedures.

4.2.3.2. "One-pot" Hydrogenation Using Catalyst 13

Parallel work in the Fogg group indicates that incorporation of an N-heterocyclic carbene (NHC) ligand into Ru hydride catalysts results in a significant increase in hydrogenation activity.[30] Again, preliminary "one-pot" reactions were carried out using

O-glycoside ROMP-polymer prepared via catalyst **18**, and treating these with Ru-NHC catalyst **13** as hydride precursor. The same conditions as for hydrogenation with **12** were used, except that the ratio of olefinic sites to Ru was decreased to 27:1, in the interest of obtaining saturated polymers for cross-linking experiments (Appendix). Because of this, however, the "one-pot" hydrogenation processes using **12** and **13** are not comparable. It should also be noted that no base was added in these experiments, regardless of the base requirement noted above. Despite this, completely saturated polymer was obtained in 24 hours, as verified by ^{1}H NMR analysis. We speculate that the PCy_3 ligand released during hydrogenation (which occurs via a dissociative mechanism) serves as the required base. Indeed, protonation of the released phosphine can help to drive the reaction by preventing recoordination of PCy_3.

4.3. Tandem ROMP-Hydrogenation

4.3.1. Tandem ROMP-Hydrogenation of Norbornene O-glycoside 9 Using Catalyst 12

The success of the "one-pot" ROMP-hydrogenation experiments led us to investigate tandem ROMP-hydrogenation. The tandem catalyses were carried out by polymerizing the O-glycoside monomer in 2 mL CH_2Cl_2, transferring the reaction to a glass-lined high pressure autoclave, diluting with 12 mL of THF and 2 mL of CH_2Cl_2, pressurizing the reactor with H_2 and heating at 60°C. THF was added in order to minimize chlorination of the active catalyst by CH_2Cl_2, despite the potential for it to coordinate to the metal center (as also proposed for ROMP).[31,32] Polymerization and hydrogenation were monitored by withdrawing 1 mL samples for NMR analysis. ROMP-

hydrogenation experiments with Grubbs catalyst **12** show complete polymerization in 72 hours, and hydrogenation in 87 hours (Figure 4.7).

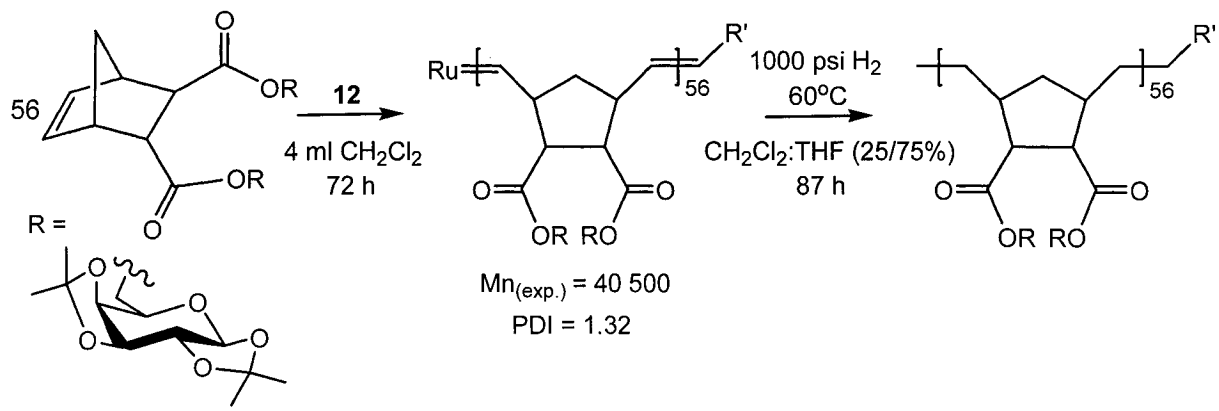

Figure 4.7 Tandem ROMP-hydrogenation of norbornene O-glycoside using catalyst **12**.

4.3.2. Tandem ROMP-Hydrogenation of Norbornene O-glycoside 9 Using Catalyst 13

Complete polymerization and hydrogenation via **12** required one week. Tandem ROMP-hydrogenation experiments were thus investigated using more active **13**. Best results, generated at [S]:[C] ratios of 70:1, show complete reaction in 7 hours (Table 4.2, entry 2). At a ratio of 200:1, the reaction time increases to 12 hours (Table 4.2, entry 4). ROMP polymerization and hydrogenation can therefore be completed in ca. 12 hours, as compared to one week when catalyzed by **12**. Entries 5 and 6 (Table 4.2), where large-scale hydrogenations were performed, suggest possible industrial use of the tandem process.[33] Polydispersities are 1.19-1.37 versus 1.06-1.08 for ROMP via molybdenum catalyst **11**. However, the efficiency of the tandem polymerization and reduction is very advantageous.

Table 4.2 Tandem ROMP-hydrogenation of norbornene O-glycoside **9** using catalyst **13**.

Entry	Ring Opening Metathesis Polymerization							Hydrogenation
	Catalyst (mmol)	Monomer (mmol)	Equiv.	CH_2Cl_2 (mL)	Time (hours)	$M_n \times 10^4$ (g/mol)	PDI	Time (hours)
1	0.0047	0.39	84	5	5	1.49	1.30	<12
2	0.0047	0.33	70	3	3	2.72	1.22	4
3	0.0023	0.47	200	2	6	20.4	1.36	3
4	0.0023	0.47	200	2	5	27.4	1.37	12
5	0.053	1.79	34	16	5	14.2	1.19	< 12

Conditions: Polymerization performed at room temperature while hydrogenation at 60°C. Hydrogenation was performed with 20% methanol as co-solvent and under 1000 psi H_2.

4.3.3. Tandem ROMP-Hydrogenation of N-hydroxysuccinimide Monomer 10 Using Catalyst 13

Tandem ROMP-hydrogenation via **13** was also used to synthesize the saturated N-hydroxysuccinimide homopolymer (Figure 4.8). Polymerization of 50:1 equivalents of monomer to catalyst in 3 mL of CH_2Cl_2 gave a viscous solution within 20 minutes at RT, which showed complete ROMP by NMR analysis. This reaction is clearly much faster then ROMP of O-glycoside monomer **9**, reflecting the steric influence of the two monomers: O-glycoside monomer **9** has two substituents, while N-hydroxysuccinimide monomer **11** has only one. The reaction was transferred to a high pressure autoclave for hydrogenation, and 10.5 mL of CH_2Cl_2 and 2.5 mL of methanol were added. Use of larger amounts of methanol caused the polymer to precipitate. Compared to poly(**9**), poly(**11**) is less polar, limiting the proportion of methanol that can be used to 16 % by volume. The autoclave was pressurized with H_2 to 1000 psi and heated at 60°C. After hydrogenation was complete, the solution was concentrated and the polymer was

precipitated by addition to methanol. Following centrifuging and decanting the product appeared as gray-white polymer clumps, which could not be dissolved in most organic solvents (CH_2Cl_2, EtOAc, acetone, MeOH) or water. At 0.010 g/mL it was soluble in DMF. IR analysis showed the presence of the two distinct υ(C=O) ester stretching bands; two for the succinimide amide groups (1804 and 1778 cm^{-1}), and one for the ester (1734 cm^{-1}).

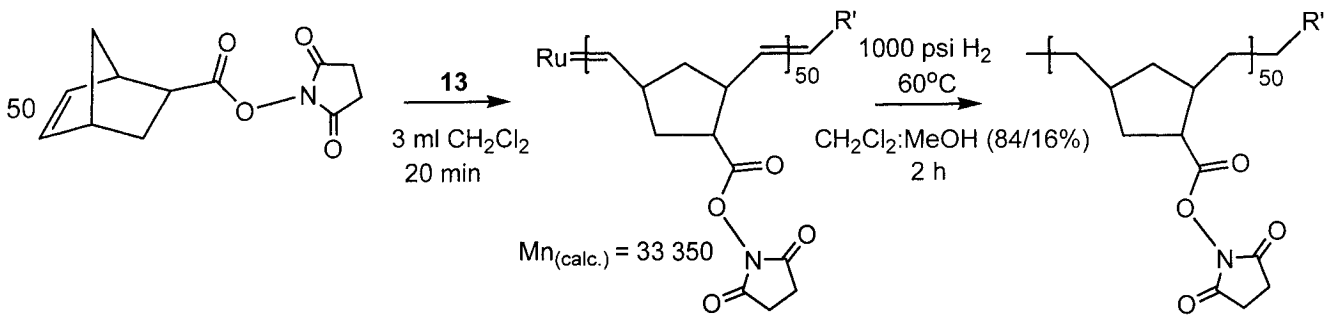

Figure 4.8 Tandem ROMP-hydrogenation of norbornene N-hydroxysuccinimide using ruthenium catalyst **13**.

4.3.4. Preparation of Random Copolymers via Tandem ROMP-Hydrogenation Using Catalyst 13

In order to obtain water-soluble polymers containing the N-hydroxysuccinimide group, we investigated preparation of random co-polymers of **9** and **11**. N-hydroxysuccinimide monomer **11** and O-glycoside monomer **9** were was copolymerized and reduced via tandem ROMP-hydrogenation (Figure 4.9). The norbornene N-hydroxysuccinimide content in the polymers was 10%, 20%, and 40%, and a total of 50 equivalents of monomer to 1 equivalent of catalyst was used. The enhanced solubility

conferred by the O-glycoside monomer allowed addition of 20% of methanol to the reaction mixture prior to hydrogenation. The solubility of the polymers after hydrogenation in CH_2Cl_2 did not significantly decrease: a higher proportion of the N-hydroxysuccinimide is apparently needed in order to confer solubility in hydrocarbon solvents. The presence of both types of repeat unit was verified by IR and ^1H NMR analysis, as for the random copolymers prepared with molybdenum catalyst **18** (Section 3.3.2.) We note, however, that the rate of polymerization is faster for N-hydroxysuccinimide monomer **11** than the corresponding O-glycoside monomer **9**. Since the monomers were polymerized simultaneously, we speculate that instead of obtaining a true random copolymer, blocky polymer structure may have been formed. The blocky polymer would likely exhibit lower solubility, possibly resulting from formation of micelles.

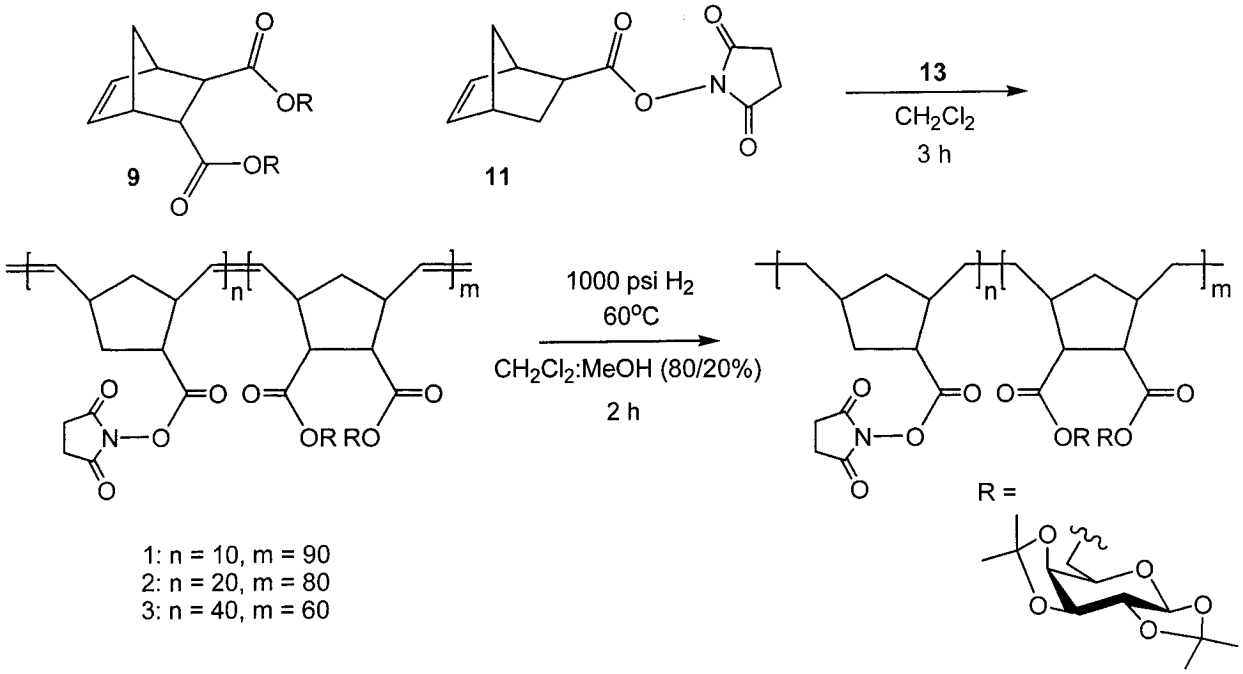

Figure 4.9 Copolymer synthesis via tandem ROMP-hydrogenation of monomers **9** and **11** using catalyst **13**.

4.4. Hydrolysis of Protected Sugar Polymers

To obtain water-soluble saturated polymers, the O-glycoside acetal protecting groups were removed by reaction with 9:1 trifluoroacetic acid in water for 20 minutes at room temperature.[26] The time constraint is imposed by the possibility of sugar dimerization. The polymer was precipitated in THF and further washed with THF, ether and hexanes. Following centrifuging and decanting, the product was dried under vacuum to afford a white powder in quantitative yield. Complete deprotection is indicated by the disappearance of the ^{1}H NMR singlets for the methyl protons of the acetal protecting groups (1.45, 1.4 and 1.25 ppm). The broad signals for the methylene protons of the polymer backbone are observed at 1.3-1.0 ppm.

Sugar homopolymers prepared by tandem ROMP-hydrogenation showed excellent solubility in water. This implies that the tandem ROMP-hydrogenation process is the most effective, as well as the most efficient, of the methods explored. The sequence of the reactions affords polymers that are synthesized quickly, are easily isolated, and that possess the expected physical properties.

Random copolymers were hydrolyzed as well, but their solubility in water varied depending on the ratio of N-hydroxysuccinimide to O-glycoside. The copolymers contain both hydrophilic sugar groups, and hydrophobic N-hydroxysuccinimide groups. Solubility in water increases, not surprisingly, as the proportion of the carbohydrate repeat unit is increased to 100% (Table 4.3). If the copolymers deviate towards block structures, formation of micelles is likely. As amphiphilic polymers have a variety of applications, however, including drug delivery, these polymers may find other possible uses in addition to collagen crosslinking.

Table 4.3 Deprotection reactions carried out in 9:1 TFA/H_2O.

Entry	[N-hydroxysuccin.]$_n$ [O-glyc.]$_m$		Solubility in H_2O (w/v)
	N	M	
1	10	90	0.005 g/mL
2	20	80	< 0.001 g/mL
3	40	60	Insoluble

Preliminary collagen crosslinking experiments using O-glycoside homopolymer (d.p. = 34, M_n(expt.) = 14 200, PDI = 1.19) are described in the Appendix. The results show very promising utility of these saturated neoglycopolymers as biocompatible collagen crosslinking agents towards construction of a cell-based artificial cornea.

4.5. Conclusions

The forgoing describes infrared investigations of the thermal degradation of ROMP polymers, and alleviation of these problems by polymer hydrogenation. Standard reduction methods using Pd-C and diimide hydrogenation are unsatisfactory, owing to purification problems and cost issues associated with high catalyst loadings, or polymer crosslinking under the harsh reaction conditions required. "One-pot" hydrogenation using catalyst **12** as precursor to hydrogenation-active Ru hydrides effect hydrogenation with better efficiency, but better yet is the NHC catalyst **13**, particularly when used in a tandem ROMP-hydrogenation procedure. This enables synthesis of saturated ROMP polymers in <12 hours from the free monomer. Deprotection of the acetal-protected O-glycoside polymers gave water-soluble materials.

These polymers were used to effect collagen crosslinking, as described in the Appendix. Preliminary results show excellent refractive index, swelling, and mechanical

properties of the composites. Ingrowth of cells though the crosslinked collagen matrices also suggest that the materials are biocompatible under the conditions explored to date.

4.6. References

1) (a) McManus, N. T.; Rempel, G. L. *J. Macromol. Sci., Rev. Macromol. Chem. Phys.* **1995**, *C35*, 239. (b) Maréchal, E. In *Comprehensive Polymer Science*; Eastmond, G. C., Ledwith, A., Russo, S., Sigwalt, P., Eds.; Pergamon: Toronto, 1989; Vol. 6.

2) (a) Sohn, B. H.; Gratt, J. A.; Lee, J. K.; Cohen, R. E. *J. Appl. Polym. Sci.* **1995**, *58*, 1041. (b) Yoshida, Y.; Yoshinari, M.; Iko, A.; Komiya, Z. *Polymer J.* **1998**, *30*, 819. (c) Kohara, T. *Macromol. Symp.* **1996**, *101*, 571.

3) Schnabel, W. *Polymer Degradation: Principles and Practical Applications*; Hanser International: New York, 1981.

4) Grassie, N.; Scott, G. *Polymer Degradation and Stabilization*; Cambridge University Press: Cambridge, 1985.

5) Nomura, K.; Schrock, R. R. *Macromolecules* **1996**, *29*.

6) Stick, R. V. *Carbohydrates: The Sweet Molecules of Life*; Academic Press: London, UK, 2001.

7) Ivin, K. J.; Mol, J. C. *Olefin Metathesis and Metathesis Polymerization*; Academic Press: New York, 1997.

8) Schwab, P.; Grubbs, R. H.; Ziller, J. W. *J. Am. Chem. Soc.* **1996**, *118*, 100.

9) For examples, see: (a) Creighton, C. J.; Reitz, A. B. *Org. Lett.* **2001**, *3*, 893. (b) Wallace, D. J.; Goodman, J. M.; Kennedy, D. J.; Davies, A. J.; Cowden, C. J.; Ashwood, M. S.; Cottrell, I. F.; Dolling, U.-H.; Reider, P. J. *Org. Lett.* **2001**, *3*, 671. (c) Fürstner, A.; Thiel, O. R.; Kindler, N.; Bartkowska, B. *J. Org. Chem.* **2000**, *65*, 7990.

10) Sohn, B. H.; Gratt, J. A.; Lee, J. K.; Cohen, R. E. *J. Appl. Polym. Sci.* **1995**, *58*, 1041.

11) Al-Samak, B.; Amir-Ebrahimi, V.; Carvill, A. G.; Hamilton, J. G.; Rooney, J. J. *Polymer Intl.* **1996**, *41*, 85.

12) Hahn, S. F. *J. Pol. Sci. A* **1992**, *30*, 397.

13) Edwards, H. G. M.; Farrell, D. W.; Johnson, A. F.; Lewis, I. R.; Ward, N. J.; Webb, N. *Macromolecules* **1992**, *25*, 525.

14) Novak, B. M.; Grubbs, R. H. *J. Am. Chem. Soc.* **1988**, *110*, 960.

15) Amir-Ebrahimi, V.; Corry, D. A. K.; Hamilton, J. G.; Rooney, J. J. *Journal of Molecular Catalysis A: Chemical* **1998**, *133*, 115.

16) Manning, D. D.; Hu, X.; Beck, P.; Kiessling, L. L. *J. Am. Chem. Soc.* **1997**, *119*, 3161.

17) Parshall, G. W.; Ittel, S. D. *Homogeneous Catalysis*; 2nd ed.; Wiley-Interscience: Toronto, 1992.

18) Widegren, J. A.; Finke, R. G. *Journal of Molecular Catalysis A: Chemical* **2003**, *298*, 317.

19) Chaloner, P. A.; Esteruelas, M. A.; Joo, F.; Oro, L. A. *Homogeneous Hydrogenation*; Kluwer: Boston, 1994.

20) James, B. R. *Homogeneous Hydrogenation*; John Wiley & Sons: Toronto, 1973.

21) Drouin, S. D.; Yap, G. P. A.; Fogg, D. E. *Inorg. Chem.* **2000**, *39*, 5412.

22) Drouin, S. D.; Zamanian, F.; Fogg, D. E. *Organometallics* **2001**, *20*, 5495.

23) Fogg, D. E.; Drouin, S. D.; Zamanian, F. ; U. S. Patent 6,486,263, 2001.

24) (a) Kodemura, J.; Natsuume, T. *Polym. J.* **1995**, *27*, 1167. (b) Yi, K. S.; Tenney, L. P.; Lane, P. C.; Wessel, J. V.; Marchant, N. S. US Patent 5,705,572, 1998.

25) Chen, Y.; Dujardin, R.; Pielarzik, H.; Franz, U. W. ; U. S. Patent 5,932,664: US, 1997.

26) McLain, S. J.; McCord, E. F.; Arthur, S. D.; Hauptman, E.; Feldman, J.; Nugent, W. A.; Johnson, L. K.; Mecking, S.; Brookhart, M. *Polym. Mater. Sci. Eng.* **1997**, *76*, 246.

27) Wagener, K. B.; Watson, M. D. ; U.S. Patent 6,107,237, 2000.

28) Fogg, D. E.; dos Santos, E. N. *Coordination Chemistry Reviews* **2004**, (Invited contribution: special issue on transition metals in catalysis), accepted.

29) For recent examples of multifunctional tandem catalysis see: (a) Sutton, A. E.; Seigal, B. A.; Finnegan, D. F.; Snapper, M. L. *J. Am. Chem. Soc.* **2002**, *124*, 13390. (b) Motherwell, W. B. *Pure Appl. Chem.* **2002**, *74*, 135. (c) Bielawski, C. W.; Louie, J.; Grubbs, R. H. *J. Am. Chem. Soc.* **2000**, *122*, 12872. (d) Louie, J.; Bielawski, C. W.; Grubbs, R. H. *J. Am. Chem. Soc.* **2001**, *123*, 11312. (e) Watson, M. D.; Wagener, K. B. *Macromolecules* **2000**, *33*, 3196. (f) Wagener, K. B.; Watson, M. D. U.S. Patent 6,107,237, 2000. (g) Chen, Y.; Dujardin, R.; Pielarzik, H.; Franz, U. U. S. Patent 5,932,664, 1997. (h) McLain, S. J.; McCord, E. F.; Arthur, S. D.; Hauptman, E.; Feldman, J.; Nugent, W. A.; Johnson, L. K.; Mecking, S.; Brookhart, M. *Polym. Mater. Sci. Eng.* **1997**, *76*, 246.(i) Borstin, P.; Nielsen, P. *Chem. Commun.* **2002**, 2140.(j) Thadani, A. N.; Rawal, V. H. *Org. Lett.* **2002**, *4*, 4317. (k) Thadani, A. N.; Rawal, V. H. *Org. Lett.* **2002**, *4*, 4321. (l) Choudary, B. M.; Chowdari, N. S.; Jyothi, K.; Kumar, N. S.; Kantam, M. L.

Chem. Commun. **2002**, 586. (m) Teoh, E.; Campi, E. M.; Jackson, W. R., Robinson, A. J. *Chem. Commun.* **2002**, 978. (n) Evans, P. A.; Robinson, J. E. *J. Am. Chem. Soc.* **2001**, *123*, 4609. (o) Ikeda, S.-I. *Acc. Chem. Res.* **2000**, *33*, 511. (p) Eilbracht, P.; Bärfacker, L.; Buss, C.; Hollmann, C.; Kitsos-Rzychon, B. E.; Kranemann, C. L.; Rische, T.; Roggenbuck, R.; Schmidt, A. *Chem. Rev.* **1999**, *99*, 3329. (q) Molander, G. A.; Harris, C. R. *Chem. Rev.* **1996**, *96*, 307.

30) Fogg, D. E.; Dharmasena, U.; Martinez Castro, N.; Czechura, P.; dos Santos, E. N. *N-Heterocyclic Carbenes as Activating Ligands in Olefin Hydrogenation*: Philadelphia, PA, United States, August 22-26, 2004, pp Abstract of Papers.

31) Nguyen, S. T.; Johnson, L. K.; Grubbs, R. H.; Ziller, J. W. *J. Am. Chem. Soc.* **1993**, *115*, 9858.

32) Sanford, M. S.; Ulman, M.; Grubbs, R. H. *J. Am. Chem. Soc.* **2001**, *123*, 749.

33) Yi, K. S.; Tenney, L. P.; Lane, P. C.; Wessel, J. V.; Marchant, N. S. ; U.S. Patent 5,705,572, 1998.

CHAPTER 5

Conclusions and Recommendations for Future Work

The work summarized in this thesis establishes efficient routes to saturated neoglycopolymers and succinimide-functionalized polymers via tandem ROMP-hydrogenation process. ROMP of the monomers via Mo catalysis afforded polymers with narrow polydispersity, nevertheless with less overall efficiency than the tandem catalysis route described in Chapter 4. The importance of hydrogenation of these materials in order to prevent crosslinking and oxidative degradation was confirmed by IR studies. Conventional reduction methods (Pd-C, diimide) were much less efficient than tandem ROMP-hydrogenation, which afforded the saturated poly(**9**)$_{70}$ in seven hours. The efficiency of the tandem catalysis varied with catalyst to monomer ratio, as well as the volume of solvent used for ROMP. The reaction conditions may be optimized further through addition of base, which will promote formation of the catalytically-active hydridochloro species.

Water-soluble polymers were obtained after cyclic acetal hydrolysis using TFA/H_2O. Random copolymers of poly(**9**)$_n$(**11**)$_m$ increased in solubility as the proportion of **9** increased. Homopolymers of the O-glycoside monomer proved very promising in collagen crosslinking, however future work will need to examine, in comparative studies, the efficacy of poly(**9**)$_n$ with different chain lengths (where n is 10, 50, and 100). This will aid in establishing the optimum chain length for fabrication of a strong crosslinked collagen matrix. Also to be investigated is the mechanical strength and biocompatibility of collagen crosslinked with triblock copolymers containing O-glycoside and C-glycoside groups. Incorporation of succinimide crosslinkers may also be useful, but it is likely that

these will need to be used within a random copolymer, owing to the poor solubility in water of the succinimide homopolymers. It may be noted that the N-hydroxysuccinimide group can also be valuable as a "handle" to attach cell-recognition peptides such as YIGSR (known to promote epithelial growth and enhance neurite extension). Reaction of YIGSR with norbornene N-hydroxysuccinimide ester in DMF couples the peptide to norbornene within 48 h at room temperature.

The extent of crosslinking via the O-glycoside homopolymer, the triblock copolymer, and the random carbohydrate-succinimide polymer must be assessed through comparative assays of mechanical strength and biocompatibility. Depending on the outcome of the biocompatibility assays, it may be valuable to increase the similarity of our polymers to carbohydrate analogues by using furan instead of cyclopentadiene in the Diels-Alder synthesis of the base monomer. Also, changing sugar-norbornene ester linkage to an amide or a short carbon chain maybe beneficial to the polymer stabilization.

Further, the transparency of the hydrogels may be improved using collagen from a different source. The collagen composition varies depending on its source, and can give different transparencies with different crosslinkers. Upon optimizing mechanical strength, biocompatibility and transparency, in vivo testing will be undertaken in order to assess polymer decomposition.

Current and future work in the laboratory is directed at optimizing catalyst architecture for tandem ROMP-hydrogenation. Should this enable living polymerization, synthesis of triblock copolymer will be possible via Ru catalysis, circumventing the problems of catalyst degradation associated with Mo catalysis.

APPENDIX

Polymer applications

Preliminary studies of the collagen crosslinking capabilities and biocompatibility of the saturated O-glycoside homopolymer, poly(**9**), were carried out by other members of this interdisciplinary research group, Dr. Yuwen Liu (National Research Council) and Dr. Donna Grant (University of Ottawa Eye Institute).

A.1. Collagen Crosslinking

Collagen crosslinking was investigated with a sample of poly(**9**) characterized in Table 4.2 (Entry 5, d.p. = 213). Porcine collagen (Nippon Ham, Japan, 10% w/w, containing 3 x 38 NH_2 groups per mole of collagen from amino acid analysis) was mixed in 1:1, 2:1 and 4:1 weight ratios relative to homopolymer. Sodium cyanoborohydride (2 eq. per 1 eq. of lysine NH_2) was then added, and the gel was incubated for one week at room temperature, then for 24 hours at 37°C. A control sample had no added $NaBH_3CN$. The collagen gel used as the control appeared opaque and was very weak (Figure 1.3). The crosslinked collagen composites (or hydrogels) were slightly cloudy, but were strong and elastic, as determined by the testing protocols described below.

A.2. Refractive Index Measurements

The index of refraction n, a measure of the transparency of any medium, is defined as the ratio of the speed of light in a vacuum, c, to the speed of light in the medium of interest, m. It is beneficial for the crosslinked collagen composites to have a refractive index as low as possible, or close to that of air (approximately 1.0003).[1]

Refractive index data (Table A.1) show that all composite samples have a refractive index much close to H_2O than to that of human cornea. These results indicate that the crosslinked collagen matrix (hydrogels) have better transparency than the human cornea.

Table A.1 Refractive indexes of the collagen-homopolymer hydrogels.

Sample	1:1	1:1 (without $NaBH_3CN$)	2:1	4:1	PBS	H_2O	Human cornea
Refractive Index	1.3485	N/A	1.3452	1.3432	1.3348	1.3332	1.3850

A.3. Hydrogel Swelling Properties

Swelling properties were investigated by submerging the hydrogels in phosphate buffered solution (PBS) overnight at 4°C. The excess PBS was then taken up using Kimwipes, and the hydrogels were immediately weighed. The swelling ratio is the ratio of the weight of water absorbed by the sample to the weight of dry sample. The swelling ratio reflects the up-taken water content, and correlates inversely with the crosslinking density. That is, the more crosslinking, the less water can in general be taken up. The solid content was calculated as the ratio of weight of dry sample to the weight of wet sample, and the final collagen concentration was calculated as dry weight of collagen to final volume of the gel (Figure A.1).

The results show that as the collagen to homopolymer ratio increases, the swelling ratio and final collagen concentration increases, and the total solid content decreases. This indicates that as the ratio of collagen to polymer increased, crosslinking is lowered. Since the amount of polymer was constant and only the proportion of collagen was

increased, we deduce that the final collagen concentration increased and the solid content decreased.

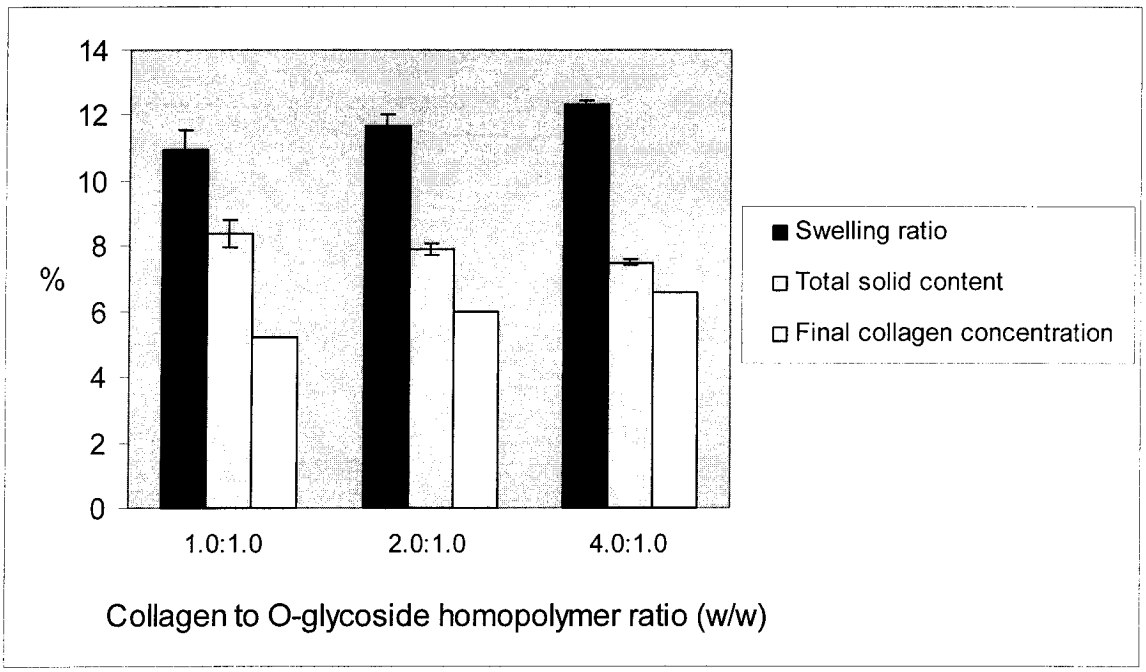

Figure A.1 Swelling properties of the collagen-homopolymer hydrogels.

A.4. Hydrogel Mechanical Properties

Mechanical properties of the hydrogels were investigated to quantify the strength and flexibility of the collagen composites (Figure A.2). Three physical properties were measured: (1) modulus, (2) stress, and (3) strain. Samples of 12 mm x 500μm in size were swelled in PBS overnight at 4°C. Nylon sutures were then installed at opposite sides, with a distance of 8 mm between them. Extension was then applied at a rate of 10 mm/min. The maximum stress at rupture (gram-force) reflects the strength of the gel, while maximum elongation or strain at rupture (mm) reflects its flexibility. The modulus was calculated from the ratio of stress to strain (gram-force/mm).

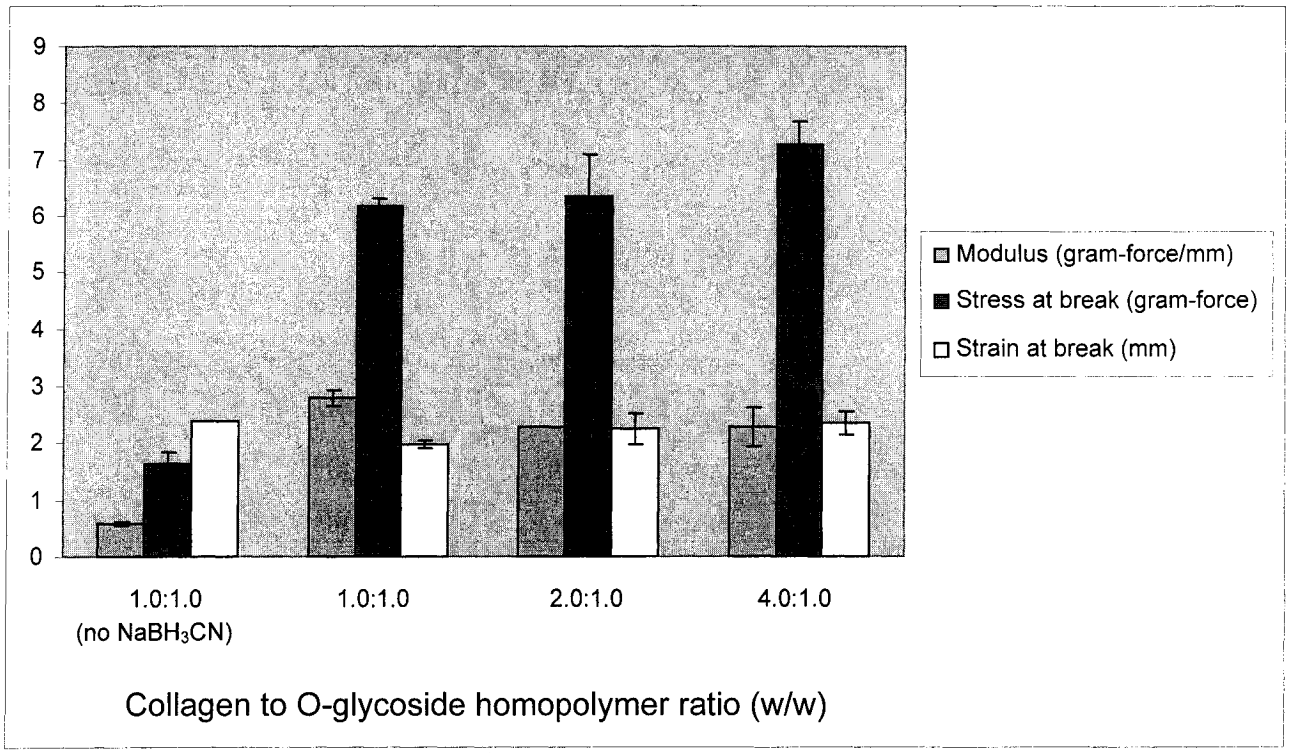

Figure A.2 Mechanical properties of the collagen-homopolymer hydrogels.

Gels prepared from collagen and homopolymer *without* addition of the reducing agent were very weak. This confirms that reduction of the imine (formed by reaction of the lysine amino group with the free aldehyde of the reducing sugar) to an amine is necessary in order to obtain a permanently crosslinked, strong collagen composite. Figure A.2 also indicates that the gels containing more collagen were stronger. In comparison to the hydrogels, the human cornea is orders of magnitude stronger (bulk modulus 13.12 gram-force/mm; maximum stress 97.01 gram-force; maximum strain 9.15 mm). However, since the hydrogels are flexible and strong enough to withstand the pull of the suture, they are good materials for cornea equivalents.

A.5. Hydrogel Biocompatibility

Preliminary biocompatibility testing was performed by in vitro growth of human corneal epithelial cells though the crosslinked collagen gel. The microscope images were taken after 3 days (Figure A.3). The number of cell counted before they became confluent confirmed that the cells are growing and dividing during the 3 days (Table A.2). The ingrowth of cells indicates that the gels appear biocompatible under these conditions. [2-4]

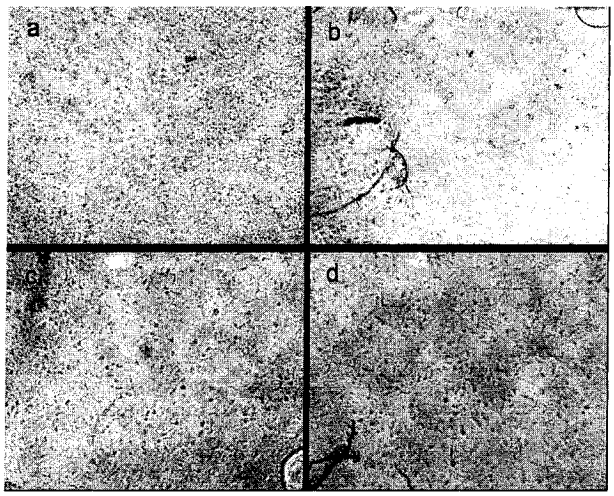

Figure A.3 In vitro growth of human corneal epithelial cells (from an established cell line) through hydrogels with collagen/homopolymer ratio: a. 1:1 (without $NaCNBH_3$); b. 1:1; c. 2:1; d. 4:1.

Table A.2 Biocompatibility of the collagen-homopolymer hydrogels.

Collagen to O-glycoside homopolymer ratio	Days of cell growth	Percentage of confluent	Biocompatibility
1:1 (without $NaCNBH_3$)	3	50	Biocompatible
1:1	3	70	Biocompatible
2:1	3	50	Biocompatible
4:1	3	50	Biocompatible

A.6. Conclusions

The O-glycoside homopolymer synthesized by tandem ROMP-hydrogenation method successfully crosslinked collagen. The polymer demonstrated its utility in support of the collagen matrix of the artificial cornea. The slowly reacting O-glycoside crosslinking moieties of the homopolymer allow time to control the crosslinking reaction, therefore the resulting hydrogels are crosslinked evenly, in contrast to other materials fabricated using more reactive crosslinking agents. Mechanical testing indicated that gels, made from collagen and the polymer, were relatively strong and flexible. Their porosity and water absorbance was investigated by swelling analysis. Preliminary studies of biocompatibility show non-toxicity to human corneal epithelial cells during a 3 day culture period.

A.7. References

1) Tipler, P. A. *Physics for Scientists and Engineers*; 4th ed.; W. H. Freeman and Company: New York, 1999; Vol. 2, Electricity and Magnetism, Light.

2) Griffith, M.; Osborne, R.; Munger, R.; Xiong, X.; Doillon, C. J.; Laycock, N. L. C.; Hakim, M.; Song, Y.; Watsky, M. A. *Science* 1999, *286*, 2169.

3) Li, F.; Carlsson, D.; Lohmann, C.; Suuronen, E.; Vascotto, S.; Kobuch, K.; Sherdown, H.; Munger, R.; Nakamura, M.; Griffith, M. *PNAS* 2003, *100*, 15346.

4) Suuronen, E. J.; Nakamura, M.; Watsky, M. A.; Stys, P. K.; Muller, L. J.; Munger, R.; Shinozaki, N.; M., G. *The FASEB Journal* 2004, *18*, 170.